TAMPEREEN TEKNILLINEN YLIOPISTO
TAMPERE UNIVERSITY OF TECHNOLOGY

MART KROON

A COMPARATIVE IN VITRO STUDY OF CELL GROWTH ON TEXTILE SCAFFOLDS FOR TISSUE ENGINEERING APPLICATIONS

Master of Science thesis

Examiner:
Professor Minna Kellomäki
Supervisor:
Doctoral Student Elina Talvitie
Examiner and topic approved by the Faculty Council of the Faculty of Engineering Sciences on 29 March 2017.

ABSTRACT

MART KROON: A comparative *in vitro* study of cell growth on textile scaffolds for tissue engineering applications
Tampere University of technology
Master of Science Thesis, 74 pages, 14 Appendix pages
March 2017
Master's Degree Programme in Materials Science and Engineering
Major: Polymers and Biomaterials
Examiner: Professor Minna Kellomäki

Keywords: polylactide, biotextiles, tissue engineering, scaffolds, cell culture

Biotextiles are fibrous structures created from synthetic or natural materials, which are used as biodegradable temporary scaffolds in tissue engineering. The function of such cell-seeded devices is to heal or replace damaged organs or tissues. Biocompatibility and retention of mechanical properties in the relatively hostile environment is required from the fiber materials. Porosity, pore sizes and pore shapes affect cell coverage and distribution on the scaffolds. Textile manufacturing techniques provide a vast variety of available structures in both small and large scale production.

The aim of this thesis was to compare cell viability and distribution on textile scaffolds. For this purpose melt spinning method was used to process poly-L/D-lactide 96/4 (PLDLA 96/4) fibers. A 36-week hydrolytic degradation experiment was conducted for the gamma irradiated fibers to evaluate retention of mechanical properties and changes in crystallinity and thermal properties. Tensile testing method was used for mechanical properties and differential scanning calorimetry (DSC) for the two last mentioned. The fibers were used to manufacture braided, knitted and woven fabrics. Heat sealing and compression at elevated temperature was used to prepare multi-layered scaffolds with approximately 1 mm thickness. Recovery after heat treatment and swelling in cell culture medium was evaluated for the scaffolds. Human urothelial cells (hUCs) and human foreskin fibroblasts (hFFs) were used in the cell culture experiment. Live/Dead analysis and crystal violet staining were used to assess cell viability and distribution.

Tensile strength of the PLDLA 96/4 fibers decreased during degradation as did strain at maximum load. Crystallinity increased with a few percent. Glass transition temperature decreased, as was predicted based on previous studies. Unexpectedly, the melting temperature showed a slight increase during degradation. In the recovery and swelling experiments, unwanted changes were not observed. The cell culture experiment demonstrated good biocompatibility for the fibers. After 2 weeks of incubation, the less porous braided and woven scaffolds had the most attached hUC and hFF cells. The large pores of knitted scaffolds remained mostly cell free for both cell types throughout the experiment.

The experiments conducted for this thesis demonstrated that PLDLA 96/4 fiber bundles can be processed into biodegradable braided, knitted and woven textile scaffolds. These structures support viability of cells in vitro. The number of attached cells was the largest in braided and woven structures that had significantly smaller pores in comparison to knitted scaffolds.

TIIVISTELMÄ

MART KROON: Solujen kasvun vertailu tekstiili-skaffoldeilla *in vitro* kudosteknologisiin sovelluksiin
Tampereen teknillinen yliopisto
Diplomityö, 74 sivua, 14 liitesivua
Maaliskuu 2017
Materiaalitekniikan diplomi-insinöörin tutkinto-ohjelma
Pääaine: Polymeerit ja biomateriaalit
Tarkastaja: professori Minna Kellomäki

Avainsanat: polylaktidi, biotekstiilit, kudosteknologia, skaffoldit, soluviljely

Kudosteknologian biotekstiilit ovat luonnollisista tai synteettisistä kuiduista valmistettuja biohajoavia tukirakenteita eli skaffoldeja. Näitä solujen kanssa implantoitavia rakenteita on tarkoitus käyttää kudosten tai kokonaisten elinten korjaamisessa. Kuiduilta vaaditaan bioyhteensopivuuden lisäksi mekaanisten ominaisuuksien riittävää säilymistä kehon vaativissa olosuhteissa. Rakenteen huokoisuus, huokosten koko ja huokosten muoto vaikuttavat solujen levittymiseen. Tekstiilien valmistusmenetelmillä voidaan valmistaa monipuolisesti erilaisia rakenteita, joiden ominaisuudet vaihtelevat laajalti.

Diplomityön tavoitteena oli vertailla solujen elinkykyisyyttä ja levittäytymistä tekstiiliskaffoldeilla. Tätä varten poly-L/D-laktidi 96/4:stä (PLDLA 96/4) valmistettiin kuitufilamentteja sulakehruu-menetelmällä. Muutoksia gammasäteilyllä steriloitujen kuitujen mekaanisissa ominaisuuksissa, kiteisyydessä ja termisissä ominaisuuksissa hydrolyyttisen hajoamisen aikana seurattiin 36-viikkoisella kokeella. Kuiduista valmistettiin punottuja, neulottuja ja kudottuja tekstiilejä, joita käytettiin 1 mm paksuisten skaffoldien valmistuksessa. Rakenteiden mittapysyvyyttä lämpökäsittelyn jälkeen ja ravinnenesteen upotettuna seurattiin kahden viikon kestoisten kokeiden avulla. Soluviljelykokeissa käytettiin ihmisen uroteelisoluja (hUCs) ja ihmisen esinahan fibroblasteja (hFFs). Live/Dead-analyysia ja kristallivioletti-värjäystä käytettiin elinvoimaisuuden ja levittäytymisen arvioimisessa.

PLDLA 96/4 kuitujen vetolujuus ja myötymä suurimman rasituksen aikana laskivat hajoamisen seurauksena. Kiteisyys kasvoi muutamalla prosentilla. Kuten aikaisempien tutkimusten perusteella oli odotettua, lasisiirtymä-lämpötila laski hajoamisen seurauksena. Sulamislämpötilan lievä kasvu ei vastannut aikaisempien kokeiden tuloksia. Palautumis- ja turvotuskokeissa havaitut mittamuutokset eivät olleet merkittäviä. Soluviljelykoe osoitti polylaktidi-kuitujen olevan bioyhteensopivia molempien solutyyppien kanssa. Kahden viikon inkuboinnin jälkeen punotuilla ja kudotuilla skaffoldeilla oli eniten soluja kiinnittyneenä. Erityisesti fibroblastit suosivat kuoppia harjanteiden sijaan rakenteissa. Neulosten suuret huokoset pysyivät lähes kokonaan soluttomina koko viljelyjakson ajan.

Kokeet osoittivat PLDLA 96/4 kuitukimppujen soveltuvan biohajoavien punottujen, neulottujen ja kudottujen skaffoldien valmistukseen. Skaffoldit tukevat hUC- ja hFF-solujen kasvua *in vitro*. Suurimmat solumäärät havaittiin punotuissa ja kudotuissa skaffoldeissa, joissa huokosten koko oli selvästi neuloksia pienempi.

PREFACE

This study was a collaboration between the Biomaterials Science and Tissue Engineering Group of Tampere University of Technology and the Adult Stem Cell Group of the Institute of Biosciences and Medical Technology (BioMediTech) at the University of Tampere.

First, I would like to thank Professor Minna Kellomäki for providing me the opportunity to have such an interesting Master's thesis project, for inspecting the thesis and for professional comments. I would also like to thank my supervisor, doctoral student Elina Talvitie for guiding me through the project and giving valuable comments along the way. Doctoral student Inari Lyyra has given professional assistance in several stages of the project and been of great support, for which I am very thankful. Janne Koivisto, I am thankful for your comments on aseptic working technique, amongst many other topics. I am very grateful to Docent Susanna Miettinen for providing the facilities for the cell culture experiment and allowing me to work with their group. In addition, laboratory technician Anna-Maija Honkala deserves great words of gratitude for her work and guidance in the cell culture experiment.

I cannot thank enough everyone I have had pleasure to work with in the research groups, fellow students working on their own thesis projects, my family, friends and especially Heidi support and encouragement.

Tampere, 7.11.2017

Mart Kroon

CONTENTS

TERMS AND DEFINITIONS

Θ	Braid angle
°C	Celsius degree
°	Degree of arc
Ø	Diameter
σ	Tensile stress
A	Surface area
BioMediTech	Institute of Biosciences and Medical Technology
BMSC	Bone Marrow Stem Cell
$CaCl_2$	Calcium chloride
CAD	Computer Assisted Design
CAM	Calcein acetoxymethyl ester
CO_2	Carbon dioxide
DMEM/F-12	Dulbecco's Modified Eagle Medium: Nutrient Mixture F-12
DPBS	Dulbecco's Phosphate-Buffered Saline
DSC	Differential scanning calorimetry
E	Young's modulus
ECM	Extracellular matrix
ESC	Embryonic stem cell
EthD-1	Ethidium homodimer-1
F	Force
GMP	Good manufacturing practices
GPa	Gigapascal
GPC	Gel permeation chromatography
H_2O	Water
HBSS	Hank's Balanced Salt Solution
hFF	Human fibroblast
$H_{melting}$	Melting enthalpy
hUC	Human urothelial cell
iPSC	Induced pluripotent stem cell
kGy	Kilogray
MPa	Megapascal
MSC	Mesenchymal Stem Cell
M_w	Molecular weight
N	Newton
NaPBS	Phosphate-buffered saline solution
P(DTD DD)	poly(desaminotyrosyl-tyrosine dodecyl dodecanedioate)
P(LA-CL)	Polycaprolactone-co-lactide
PA	Polyamide
PBS	Polybutylene succinate
PCL	Polycaprolactone
PDS	Polydioxanone
PE	Polyethylene
PEA	Poly(esther amide)
PEEK	Polyether ether ketone
PEG	Polyethylene glycol
PES	Polyester
PET	Polyethylene terephthalate

PGA	Polyglycolide
PHA	Polyhydroxyalkanoates
PLA	Polylactide
PLDLA	Poly-L/D-lactide
PLDLA 96/4	Poly-L/D-lactide with 96 wt% D-lactide and 4 wt% L-lactide
PLGA	Poly(lactide-co-glycolide)
PP	Polypropylene
PS	Polystyrene
PS1	Photo Stitch 1 software
PS2	Photo Stitch 2 software
PTFE	Polytetrafluoroethylene
PVA	Polyvinyl alcohol
PVDF	Polyvinylidene fluoride
rpm	Revolutions per minute
TE	Tissue engineering
T_g	Glass transition temperature
T_m	Melting temperature
TUT	Tampere University of Technology
UTS	Ultimate Tensile Strength
wt%	Percentage by mass
X_c	Degree of crystallinity

1. INTRODUCTION

Biotextiles are described as non-viable, permanent or temporary, fibrous textile structures created from synthetic or natural materials, which are used as medical devices inside or outside the body. The function of such textiles is to improve the health, medical condition, comfort and wellness of the patient by prevention, treatment or diagnosis of an injury or disease. In addition, biotextiles are in contact with circulating blood or body fluids. Therefore, they need to function in a relatively hostile biological environment. This distinguishes biotextiles from most other medical textiles. [1] When a biotextile is seeded with living cells, it is considered a tissue engineering (TE) construct. For these constructs, it is often desirable to use biodegradable polymers [1] that are replaced over time with regenerating native tissue when implanted [1; 2].

Implantable textile structures are routinely used in surgery to direct, supplement or replace the functions of living tissues. Examples include sutures, vascular grafts, ligament and tendon prostheses, heart valves and joint replacements. Using biomaterials alone can be successful, but infection, failure and rejection of implants remains an issue. The field of tissue engineering challenges this issue by combining biomaterials and mammalian cells to create living synthetic tissue constructs [3] to increase the biocompatibility of the implants.

Woven, knitted, braided and embroidered fabrics are usually made from filament or staple fiber yarns and non-wovens from the fibers or directly from a polymer. The properties of the fabrics depend on the properties of the yarns or fibers and the geometry of the structure, for non-wovens also on binder properties and bonding method. [4] Because there are numerous combinations of different materials and structures, the properties of the fabrics vary on a broad range. Therefore, it is possible to design textiles that mimic structural and mechanical properties of various biological tissues. [5] To enhance chemical compatibility, the fibers or textile structures may also be surface modified to improve host-biomaterial interactions. [6] Mechanical properties of textiles are usually anisotropic, with exception of some non-wovens. Characteristic properties include high in-plane stiffness and low bending resistance. [5] To meet the requirements of different applications, the required characteristics need to be understood and the parameters influencing the performance must be known. Traditional textile forming methods such as braiding, knitting and weaving allow production of structures with minimal batch-to-batch variation even at large scale production. This makes textiles an interesting group of materials, when considering commercializing a product.

In this work, textile scaffolds were manufactured from melt spun poly(LD-lactide) 96/4 (PLDLA 96/4) fibers using three different methods: (i) braiding, (ii) knitting and (iii) weaving. Changes in mechanical and thermal properties during hydrolytic degradation of the fibers were assessed using tensile testing and differential scanning calorimetry (DSC) tests. Cell viability and distribution on these structures was studied using human foreskin fibroblasts (hFF) and human urothelial cells (hUC) with live/dead analysis and crystal violet staining. The aim was to compare the distribution of cells between the three textile types used in the scaffolds. The scaffolds varied in pore sizes and in fiber arrangement.

THEORETICAL BACKGROUND

2. TEXTILES IN TISSUE ENGINEERING

Based on 188 research articles [Appendix A] with full online access from Tampere University of Technology (TUT), cell growth in braided, embroidered, knitted, woven and non-woven textile structures has been a subject of interest for past 20 years. The data includes research articles where cell growth on textile structures has been studied *in vitro*, *in vivo* or both. However, in some references that is not the main topic of the research. Electrospinning as a method is excluded from the non-wovens, but it should be noted that during this research, more electrospinning articles in the field of tissue engineering were found than for the other textile methods combined. The exclusion was because of practical reasons, to decrease the number of articles to process. In addition, not all electrospun structures can be considered to be non-woven textiles. The thesis focuses on more traditional textiles. Figure 1 presents the number of articles released in five-year periods since the year 1996. The most articles per year were published in the years 2010, 2006 and 2005 with 22, 20 and 19 articles. It is necessary to speculate here, that limited access to recently released articles probably decreases the amount of articles included here from last few years. The same may apply as well to older articles initially not published online. This should be considered when inspecting chart in Figure 1.

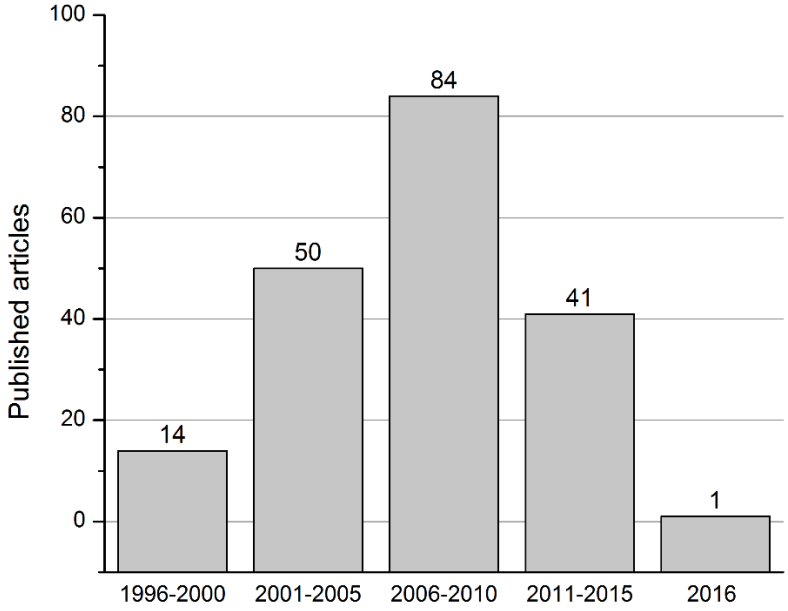

Figure 1. *Number of research articles published during time period. [Appendix A].*

In most of the research articles in Figure 1, only one type of textile structure was used. 7 articles describe use the of two types of textiles [7-13]. Ramakrishna mentioned in 2001 investigating hepatocyte attachment on braided, knitted and woven fabrics in their preliminary research [3], but a comprehensive comparative research of cell growth on textile structures manufactured with several different methods is still to be conducted.

2.1 Tissue engineering

To find a solution to chronic donor organ shortage, tissue engineering constructs are being researched. TE has been described as a field of research where artificial tissue and organs are fabricated, but this description is too broad. TE constructs differ from artificial organs such as mechanical hearts by combining living cells and biomaterials to mimic mammalian extracellular matrix (ECM). [14] Besides treating human patients, the constructs could also be used to replace animal models in research areas such as drug development.

2.2 Structures

According to the same 188 articles in Appendix A mentioned earlier, non-wovens, followed by the knits and braids, are the most researched textile structures in tissue engineering (Figure 2) in respect of cell growth. Using non-wovens is attractive for research because manufacturing scaffolds does not necessarily require expensive and complicated machinery. Having a mould, fibers and a binder [15] or only a bundle of fibers arranged by hand [16] can be sufficient depending on the purpose. Therefore, for example new materials, coatings, treatments and different cell types, and their combinations can be investigated with smaller investments. On the other hand, if considering production on larger scale, the orientation and density of the fibers is more difficult to control in non-wovens in comparison to the other methods such as braiding, knitting or weaving. This means also less control over pore sizes and shapes.

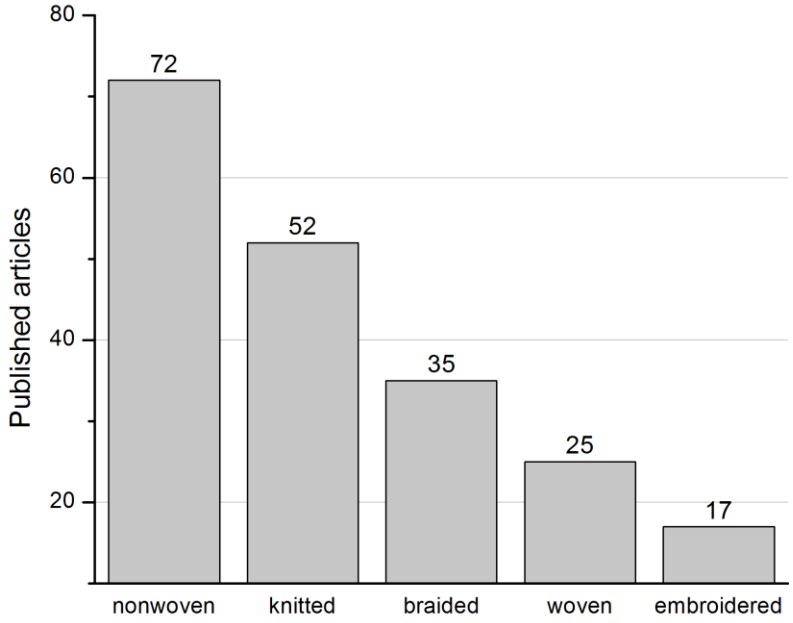

Figure 2. *The most used manufacturing techniques for textiles in TE. [Appendix A]*

The suitable type of textile structure for an application is often determined by the requirements set by the intended application. For example, knits and braids may be more suitable

for applications requiring high tensile strength such as regeneration of tendons or ligaments. On the other hand, non-woven meshes with low mechanical strength may be suitable to fill soft tissue or low load bearing cartilage and bone defects. Different textiles can also be used to produce hybrid structures such as presented in articles from Hegewald et al. [10], Farè et al. [9] and Iwai et al. [8], which all have layers manufactured with different techniques.

2.2.1 Non-woven

Non-woven fabrics are made by entangling loose fibers or directly from polymers. Entangling methods include carding, hydroentangling, needle-felting, chemical bonding and thermal bonding. Entangled fibers may be in either staple or continuous form. Manufacturing directly from polymers usually takes place by melt blowing, spun bonding or electrospinning. [4; 17] Figure 3 presents an example of a needle-felted scaffold that was manufactured from melt spun poly(ester amide) (PEA) fibers to investigate the suitability of the material for tissue engineering applications [18].

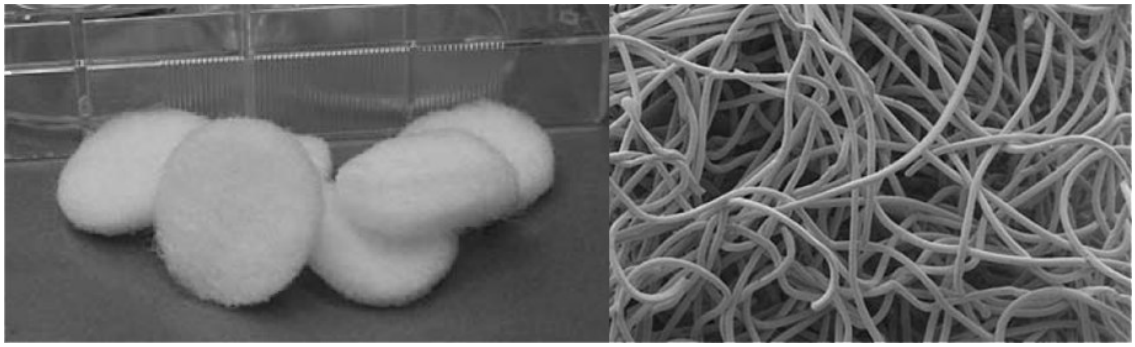

Figure 3. *Needle-felted non-woven PEA scaffolds. Modified from [18].*

The properties of non-woven fabrics depend on the fibers, arrangement of the fibers and bonding method. From tissue engineering aspect, micro- and nanofiber non-woven scaffolds are nearly ideal for growing tissues due to their resemblance to native ECM, high surface-to-volume ratio and highly porous interconnected pore network, all important for cell attachment and proliferation. [4] As disadvantages, non-wovens often do not recover after extension [4] and the scaffolds structure can be difficult to control and reproduce accurately on microscopic level in the manufacturing process.

2.2.2 Knitted

Knitting is a technique where continuous series of loops of yarns are intermeshed using hooks or needles. A needle or hook is used to catch a yarn and to draw it through a previously formed loop to create a new loop. Knitted fabrics are categorized as weft or warp knits. In the first-mentioned, loops are formed transversely and in the latter vertically, into rows and columns respectively (Figure 4). A warp knitting machine uses a running

sheet of yarns, similar to a weaving loom. In comparison, weft knits can be produced faster, more economically and can be accomplished with a single spool of yarn. [4]

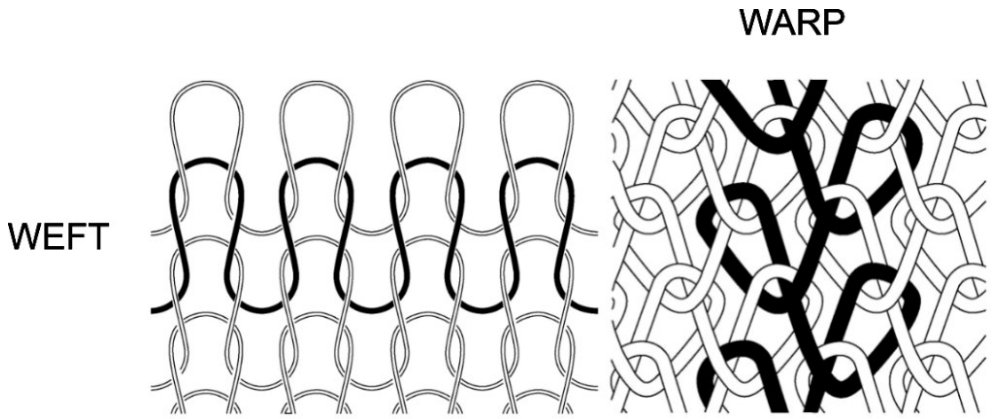

Figure 4. *Schematic illustrations of the structures of weft-knitted fabric (left) and warp-knitted fabric (right). Modified from [19, p. 70].*

Knits as a class are more flexible, compliant and conformable than for example woven fabrics. The simplest weft knits are very extensible and dimensionally unstable, but these properties can be improved by adding yarns into the knit to interlock the loops. Warp knits in general are more interlocked, dimensionally stable and do not unravel as easily when cut. [4] The pore size of the fabric can be adjusted by changing the loop size, yarn diameter and filament count of the yarn, but it still tends to be higher than in other types of fabrics.

2.2.3 Braided

Braids are manufactured by crossing at least three yarns diagonally, so that the yarns are alternating over and under each other (Figure 5). The method is similar to weaving, except the yarns are in different angles. Braided structures may be flat, tubular or tubular with a core. As the yarns are taken from individual spools, it is possible to use a variety of different yarns simultaneously in a braid. For the core, any solid material with high length to diameter ratio may be used as long as its diameter does not exceed limits set by the machinery. For example, different yarns, tubes or rods of can be used. Tubular braids are produced by braiding over a mandrel, which is later removed. [4]

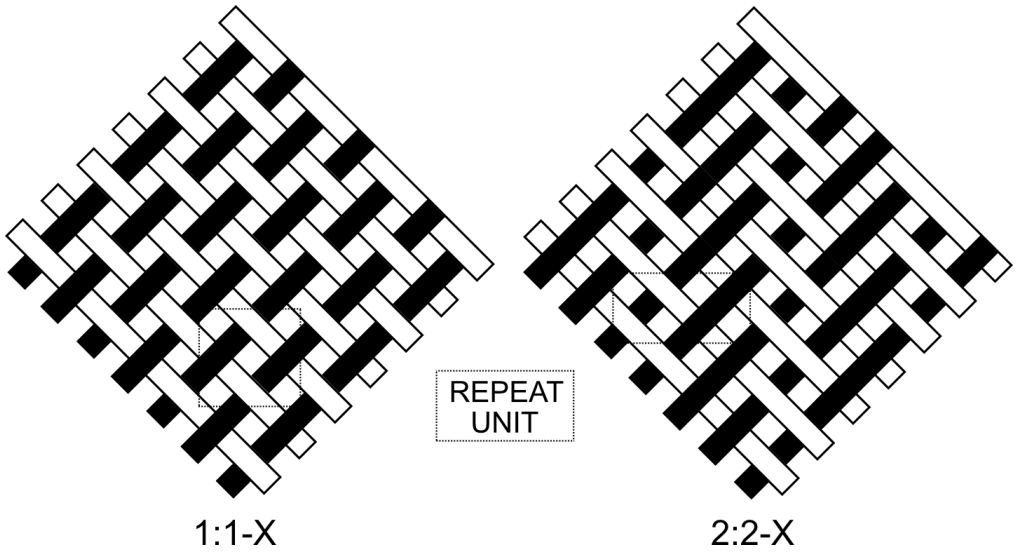

Figure 5. *1/1 braided structure (left) and 2/2 braided structure (right). X = number of yarns fed simultaneously.*

Pick spacing, braid angle and the constituent yarns determine the mechanical properties and porosity of the braids. The tensile behavior of common biaxial braids can be divided into two steps as shown in Figure 6. Under tensile load in the first step the yarns slide against each other until maximum geometrical deformation is reached. During elongation, the braid angle decreases as the yarns position more towards the direction of braid axis. In the second step, tensile behavior depends on the tensile properties of the yarns. In this case, the Young's modulus (E) is lower in the first step. [4; 20] This simplified two-step behavior does not always apply to braids that have initially yarns in the braid axis direction, such as some triaxial braids or braids with a core yarn. In such cases, the modulus of the additional yarns can be higher than the braid would otherwise have in step 1, which results the yarn being the dominant factor when tensile stress is first applied. Like wovens and weft-knits, braids tend to unravel when cut.

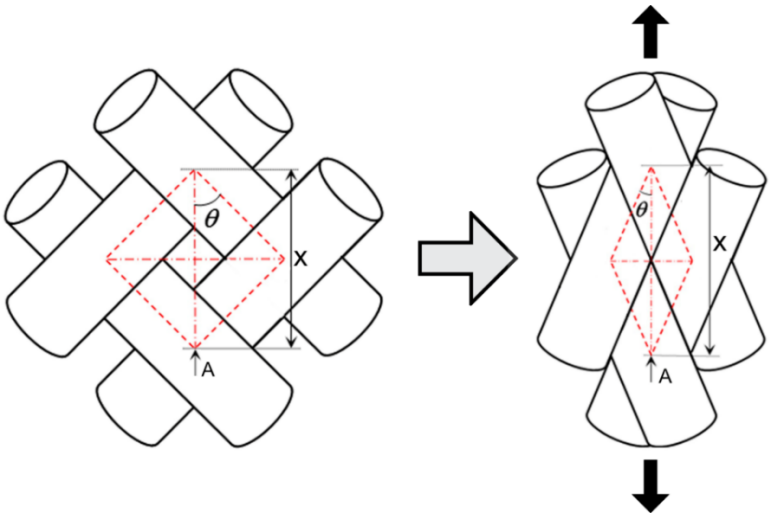

Figure 6. *Behavior of a braid under tensile stress. Θ=braid angle, X=pick spacing and A=braid axis. Modified from [20].*

Most common use of braids in clinical applications is as sutures. While in tissue engineering porosity is required property from implantable structures, in case of sutures it is seen as an increased risk to harbor contaminants. [4] Due to highly tailorable tensile strength and pore size, braids are of especially interesting structures for ligament and tendon tissue engineering. [21]

2.2.4 Woven

Woven fabrics are made on a loom where cross-threads, called the weft, are inserted to interlace with a transverse sheet of yarns called the warp. The simplest biaxial woven structure is known as a plain weave. It has the weft yarns alternating over and under the warp yarns as shown in Figure 7. [4] Hundreds of biaxial structures with different interlacings can be manufactured depending on the properties of the loom in use. The biaxial woven fabrics where the warp and the weft are perpendicular to each other are the most common, but multiaxis weaves and three-dimensional structures are also possible to manufacture. [22]

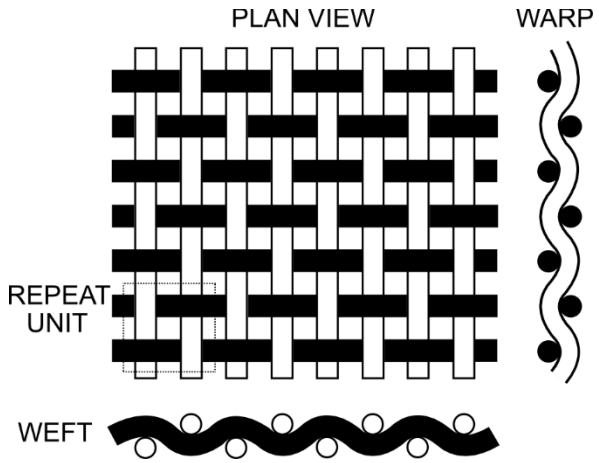

Figure 7. *Schematic illustration of the structure of a plain weave fabric.*

Biaxial woven fabrics are considered to be dimensionally stable and to have low extensibility, though this can be modified to some extent by incorporating elastomeric yarns. By controlling warp and weft density, yarn diameter and yarn type, fabric porosity can vary from zero to a high value. [4] Warp and weft densities are affected by the type of yarns used and the pressure applied by the beater. Affecting yarn properties include cross-sectional diameter, filament count and stiffness. A concern with woven fabrics is that they tend to unravel at the edges when cut [4]. There are methods, such as sewing or melting the edges, to avoid this behavior.

2.2.5 Embroidered

Embroidery is a method where yarn is stitched onto a base fabric with a needle in a controlled process. The base fabric may or may not be removed after stitching. Advantages

of embroideries are high variability in possible designs and controlled adjustment of mechanical properties to meet the requirements of the application. With electronically controlled machinery, computer assisted designs (CAD) can be manufactured (Figure 8). The method allows rapid prototyping of laboratory samples for research in small scale with minimal material usage. In addition, it is easy to upscale the process to large scale production if desired. [5; 23; 24] Example of an embroidered implant is presented in Figure 8, which shows a poly(caprolactone-co-lactide) (P(LA-CL)) scaffold designed for calvarial bone defect treatment in rabbits by Rentsch, C. et al. The CAD-design was embroidered on a water-soluble polyvinyl alcohol (PVA) base fabric, which was later removed. The scaffold consists of two parts that were sewn together after embroidery. [25]

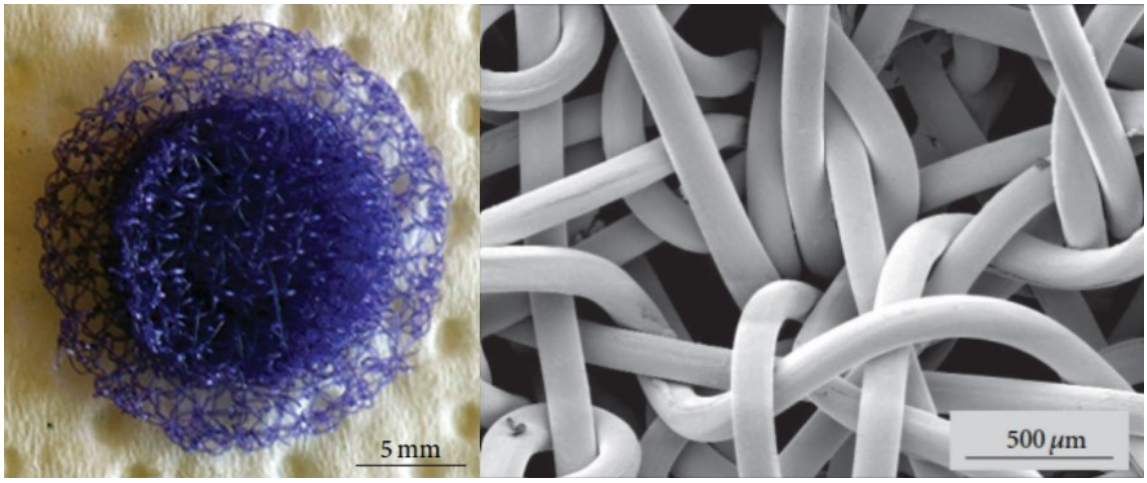

Figure 8. *Embroidered P(LA-CL) scaffold [25].*

Unlike braided, knitted and woven fabrics, embroidered fabrics do not necessarily consist of repeated units or have a defined fabric formation direction. The yarns can be arranged in any direction on a flat surface and even rounded patterns can be created. Adding yarns on the top of each other results in a three-dimensional structure. The smallest structural unit in embroidered textiles is a stitch. These stitches can vary in length, density, direction and type of locking. If desired, groups of periodically arranged stitches can form a repeated pattern. By utilizing the color change feature on embroidery machines, several types of yarns can be used simultaneously. This allows, for example, reinforcing the embroideries with high tensile strength yarns or using both multi- and monofilament yarns with variable cross-sectional diameters. These freedoms in design allow the manufacturing of textiles with well-controlled properties mimicking the anisotropic properties of mammalian tissues. [5; 24]

2.3 Fiber materials

The 188 research articles in Appendix A describe the use of 33 different fiber materials for manufacturing textile structures. Five most commonly used materials are presented in Figure 9. From these materials silk stands out as the only natural polymer, while the others

are synthetic or natural derived. Interestingly, one of the materials, poly(lactide-co-glycolide) (PLGA), is a copolymer of two other materials polyglycolide (PGA) and polylactide (PLA). This increases the significance of PGA and PLA as fiber materials. All five materials are biodegradable polymers with a wide range of degradation rates varying from months to years. [26; 27] A list consisting all of the 33 fiber materials used can be found in Appendix B. The wide range of materials shows how versatile selection of materials is available to be processed into biotextiles. For example, some less expected material selections include bioglass [28], carbon nanotubes [29] and titanium [30]. In principle, anything solid with a high length to thickness ratio can be used as the weft of woven fabrics or arranged into non-woven structures. For braiding, embroidery and knitting, in general, more strict restrictions apply.

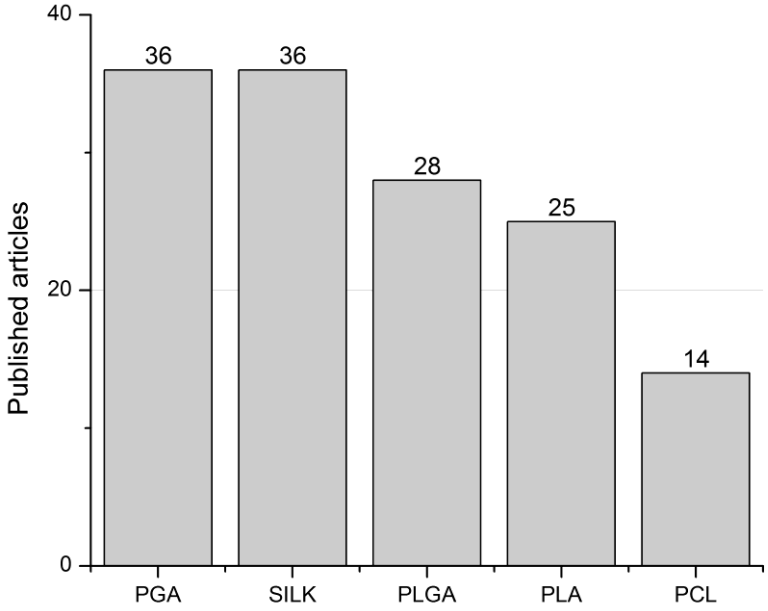

Figure 9. *The most used fiber materials for TE textiles [Appendix A].*

All fiber materials used in textile based TE constructs need to be biocompatible with the host tissue and need to have sufficient properties to be processed into yarns and fabrics. In addition, bioactivity is also often desired for the implant to perform as desired. There are several physical fiber attributes to consider: size and shape, tensile properties, bending properties, thermal properties, surface energetics and moisture properties. [4] Biocompatibility and bioactivity are discussed in more detail in subsection 2.4.1 on page 18.

For tissue engineering purpose, a small fiber diameter is usually considered an advantage, but at the same time, the processing of very thin fibers into textiles may be more challenging. Stiffness is important for both processing and application. During processing, the yarns must bend into desired forms such as loops in knits. In implants, flexibility can be crucial for conformability and intimacy of contact. Thermal properties affect especially

processing, but also for the stability of material when in use. For cells to successfully attach and proliferate on biomaterial surface, the surfaces must be wetted. Therefore, it is an advantage for the biomaterial to be hydrophilic, which results in spreading of aqueous fluids on the surface instead of beading. [4] For hydrolytically degrading biomaterials, reaction to aqueous fluids is an important factor, because it affects the degradation kinetics.

2.3.1 PGA

Polyglycolide, a thermoplastic linear aliphatic poly(α-ester), was used as a biodegradable Dexon® suture as early as 1969. Since then it has been used in tissue engineering scaffolds because of its degradation properties, mechanical properties and cell viability on the scaffolds. PGA is hydrophilic and 45–55 % crystalline. Because of its highly crystalline structure, it has excellent mechanical properties and low solubility in organic solvents. [26] The glass transition temperature ranges between 35–40 ºC and melting temperature from 220 ºC to 230 ºC. Due to its fiber forming capability by melt extrusion, it is suitable for textiles. The fibers are stiff, but can be processed into yarns. The stiffness can be reduced by copolymerizing glycolide monomers with other monomers such as ε-caprolactone. [26; 31] PGA has been shown to have elastic modulus from 7.0 GPa to 12.5 GPa, elongation of 15–30 % at break and high tensile strength of 890 MPa at break [31-33].

High molecular weight (M_w) PGA is synthesized via catalyzed ring-opening polymerization of cyclic diesters of glycolide as shown in Figure 10 below. The process yields material with high M_w polymer chains and 1–3 % of residual monomers. [31] It is possible to synthesize low M_w PGA via condensation method, but the obtained brittle polymer cannot be processed into fibers. [34]

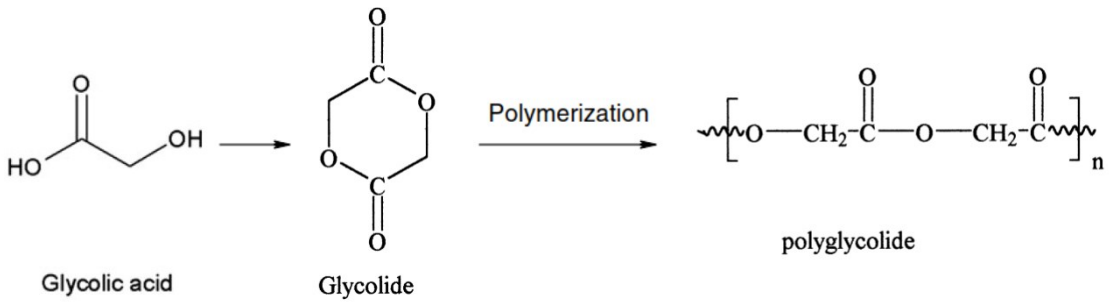

Figure 10. *Polyglycolide synthesis from glycolide monomer via ring-opening polymerization. Modified from [31; 35].*

PGA degrades through hydrolysis where water molecules break the ester bonds in the polymer backbone. Because of hydrophilicity of the material, it undergoes bulk degradation. The polymer loses its strength, often suddenly, in 1–2 months and loses its mass in 6–12 months. The polymer degrades into glycolide, which at high concentration may lower the pH of the tissue and cause inflammation. Glycolide is further broken down into

glycine to be either excreted into urine or to be converted into CO_2 and H_2O in the citric acid cycle. [32] The acidic degradation products and high degradation rate may be considered as disadvantages in tissue engineering applications. [26]

2.3.2 PLA

Similarly to PGA, polylactide (PLA) is also a thermoplastic linear aliphatic poly(α-ester) that undergoes hydrolytical biodegradation. The two polymers are structurally similar, differing in addition of pendant methyl group in PLA. The group lowers the melting temperature (T_m), increases hydrophobicity and decreases degradation rate by reducing the ester bond scission. Lactic acid or 2-hydroxypropionic acid monomers exist in two isomeric forms, L- and D-lactic acid, making it a chiral molecule. Only L-lactic acid occurs in nature, in mammals specifically. Polymerization of either one alone results in semi-crystalline polymers. [26; 31; 36] However, the polymerization of a mixture of these two monomers leads to formation of amorphous polymers if the polymer contains more than approximately 15 % of the D-isomer [37]. The glass transition temperature (T_g) of PLLA and PDLA is at 55–65 ºC and T_m around 180 ºC. PLLA is approximately 37 % crystalline, depending on the polymers M_w and processing conditions. It has good tensile strength of 30–70 MPa at break, high modulus of 4.8 GPa and low elongation of 6–18 % at break. [26; 33; 36] Poly(LD-lactide) (PLDLA) is amorphous, as stated above, and has T_g of 55–60 ºC. It has lower modulus than PLLA, around 1.9 GPa. [26]

Synthesis of PLA is also similar to the synthesis of PGA. It is possible to synthesize PLA directly from L- and D-lactid acid monomers via polycondensation method, but the produced polymer has low M_w and poor mechanical properties. The preferred method is to first produce cyclic dimers, lactides, from which PLA is synthesized using ring opening polymerization (Figure 11). Because lactid acids exist in two stereoisomeric forms, the lacide dimers can be arranged into three different dimers: L,L-lactide, D,D-lactide or L,D-lactide. [38]

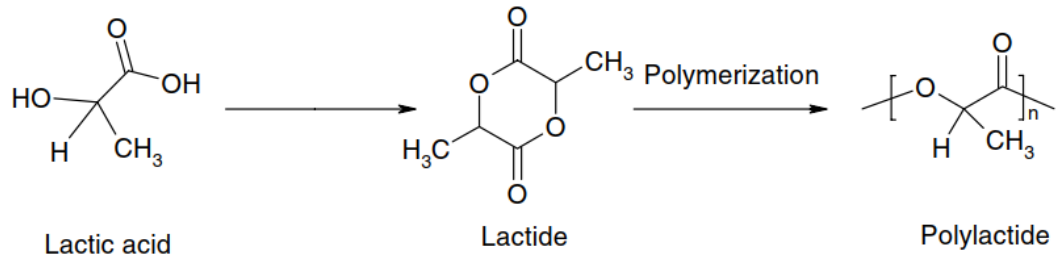

Figure 11. *Polylactide synthesis via ring opening polymerization [38].*

PLA undergoes hydrolytic bulk degradation. Scission takes place at the ester groups of the polymer backbone breaking the polymer chain eventually into lactic acid, which is metabolically converted to water and carbon dioxide. Hydrolysis of PLA is autocatalysed by increased presence of carboxylic chain ends. The degradation rate is affected by such

factors as molar weight and distribution, swelling of the matrix, morphology, stereochemistry, crystallinity and chain mobility. In semi-crystalline structure, hydrolysis preferably takes place at the less densely packed amorphous region as the structure is easier for water to penetrate. For this reason, amorphous PLDLA degrades at higher rate than crystalline PLLA, which is reported not being completely resorbed *in vivo* even after 5.7 years. PLDLA experiences loss of strength in 1–2 months and loss of mass in 6–12 months. During hydrolysis molecular weight and distribution, surface morpohology, mechanical properties, crystallinity and other properties are affected. [31; 32; 38; 39]

2.3.3 PLGA

Poly(lactide-co-glycolide) (PLGA) is copolymerized from glycolic acid and L- or DL-lactic acid to tailor material properties of either constituent polymer. High M_w PLGA can be obtained via ring-opening polymerization method as presented in Figure 12. Copolymers in wide range of monomer ratios have been researched for controlled drug release applications and medical devices such as sutures and tissue engineering scaffolds. [31; 40]

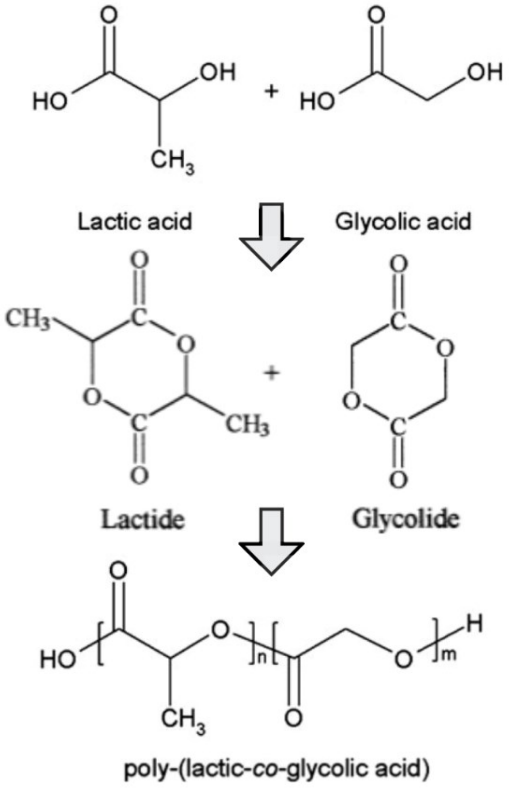

Figure 12. *PLGA copolymer synthesis. Modified from [31; 35].*

Because PLA and PGA have different susceptibility to hydrolysis, the degradation rate of PLGA can be modified by adjusting the copolymer ratio. This property makes it an appropriate biomaterial for temporary medical applications. The dependence is not linear as

can be seen in Figure 13. The highest degradation rate of 1–2 months is achieved with 50:50 copolymer ratio. Slower rates have been attained with 75:25 and 85:15 ratios, 4–5 months and 5–6 months respectively. [31; 40] PLGAs with higher lactic acid content are more hydrophobic, which leads to longer degradation time [41]. In addition to copolymer ratio, the degradation rate is affected by multiple factors including molecular weight and size and shape of the object. The degradation method of PLGA is bulk erosion via hydrolysis of the ester bonds. [26] Similarly to the homopolymers PLA and PGA, the degradation products of PLGA are metabolized by the body.

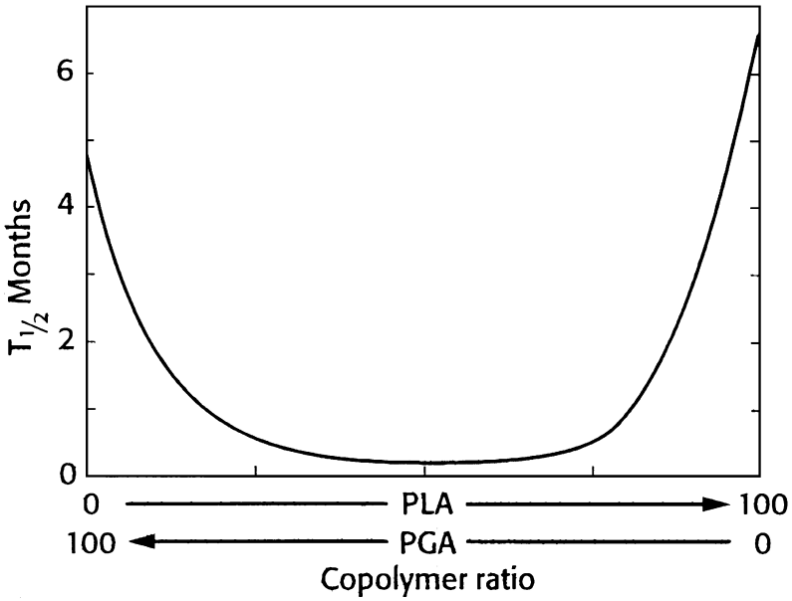

Figure 13. *Half-life of PLLA and PGA homo- and copolymers in vivo [31; 42].*

As PLA and PGA independently, PLGA is also a thermoplastic polyester. Depending on the polymer ratio, it exists in both amorphous and semi-crystalline forms. When the L-lactide is used, having 25–70 % glycolide results in amorphous structure. With DL-lactide, 0–70 % of glycolide elicits the same result. [31; 40] The T_g of PLGA is generally considered to be higher than 37 ºC, but it has been experimentally shown to vary in the range of 28–49 ºC [43]. The T_m for semicrystalline PLGA is in the range of approximately 120–220 ºC [44]. The elastic modulus of PLGA is around 2 GPa and elongation from 3 % to 10 % [33; 35].

2.3.4 PCL

Poly(ε-caprolactone) or polycaprolactone (PCL) is a semicrystalline linear aliphatic polyester consisting of five methylene groups linked by an ester group as shown in Figure 14. It has low tensile strength of 5-29 MPa and elastic modulus of 0.4 GPa, however the elongation at break is high, 300–800 %. [26; 33; 40]. PCL has low melting point of 55–60º C and glass transition temperature of -60 ºC. This in combination with good solubility

in many organic solvents and the ability to form miscible blends with a wide range of polymers, makes PCL highly processible. [26] Copolymerization and blending can be used to tailor the mechanical and degradation properties of the polymer.

High M_w PCL is obtained by the alcohol initiated ring-opening polymerization of ε-caprolactone as presented in Figure 14. Other methods, such as ROP of 2-methylene-1,3-dioxepane has been investigated, but the first mentioned remains the most significant method. [26; 40] As a result of polymerization, a hydrolysable ester linkage is formed [36].

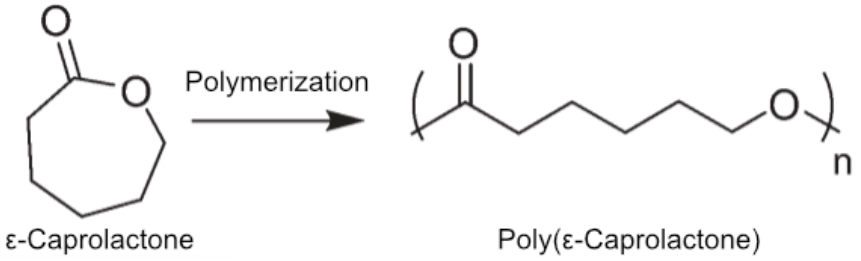

Figure 14. *Ring-opening polymerization of PCL. Modified from [40].*

PCL degrades by bulk or surface hydrolysis of ester linkages in the polymer backbone. Due to hydrophobicity and crystallinity, it takes PCL from 2 to 4 years to degrade. The rate can be increased by copolymerizing PCL with for example PGA or PLA. [36; 45] The degradation product, caproic acid is metabolized via the citric acid cycle [36; 40; 45]. Long degradation time, drug permeability and biocompatibility make PCL a suitable matrix material for long-term drug and vaccine delivery devices. [26]

2.3.5 Silk

Silks are classified as natural protein based polymers. The two main sources for silk are spiders and silkworms. The attractiveness of silks for TE comes from its good mechanical properties and biocompatibility. Silk fibers have high elasticity and tensile strength. [36; 46] The elastic modulus is found to be in the range of 5–17 GPa, ultimate tensile strength at 500–972 MPa and strain at break at 4–20 % [46]. To enhance biocompatibility, modification of the fibers is sometimes necessary. For example, the glue-like sericin protein coating is often removed from silkworm silk fibers. The primary structure of silk is a repeated sequence of proteins whose molecular weight is approximately 25 000–500 000 g/mol. The high mechanical strength comes from the secondary structure, oriented β-sheet crystals within the fibers. The fibers are connected with hydrogen bonds. Chemical structure of silk protein chain is shown in Figure 15. Silks are glycine rich. The second and third most common amino acids in the sequence are serine and alanine, but many others exist as well. [36; 46]

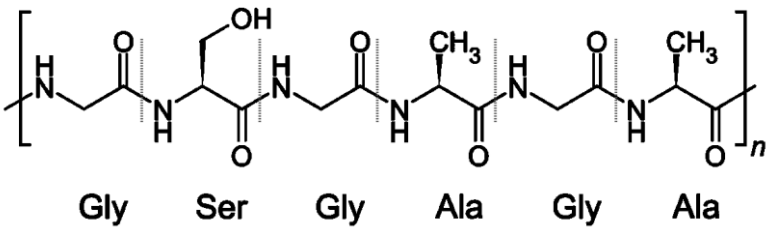

Figure 15. *Chemical structure of silk. Modified from [47].*

Silk degrades slowly proteolytically by proteases such as chymotrypsin. *In vitro* studies have shown the scission to take place at the less-crystalline regions of the proteins, resulting in smaller peptides that can be phagocytosed and metabolized. *In vivo,* the fibers lose their tensile strength in approximately 1 year and degrade beyond recognition within 2 years. The degradation rate depends on implantation site, mechanical forces, type of silk and cross-sectional diameter of the fiber. [46]

2.4 Preclinical studies

Before a tissue engineering construct can enter clinical trials on humans, it has to go through rigorous preclinical research to ensure patient safety and to demonstrate efficacy of the design. In the first stage, materials are characterized for adequate attributes such as mechanical properties, degradation behavior, effect of sterilization and biocompatibility. This is mostly done *in vitro*, but also *ex vivo* when possible. If the material does not pass the first stage, it does not enter the second stage of investigation. The second stage consists of *in vivo* biocompatibility and performance studies in animal models. [48] Initially small animal models are used to study tissue-biomaterial interactions in non-functional conditions. If successful, experiments succeed with functional tests in larger animal models more similar to humans. [48; 49] Data obtained from 188 published research articles in Appendix A, shows that most of these studies include *in vitro* methods as shown in Figure 16. Also worth noticing is the complete absence of *ex vivo* experiments. The types of cells and animals used in these studies are discussed in more detail in subsection 2.4.2, along with cell culturing conditions.

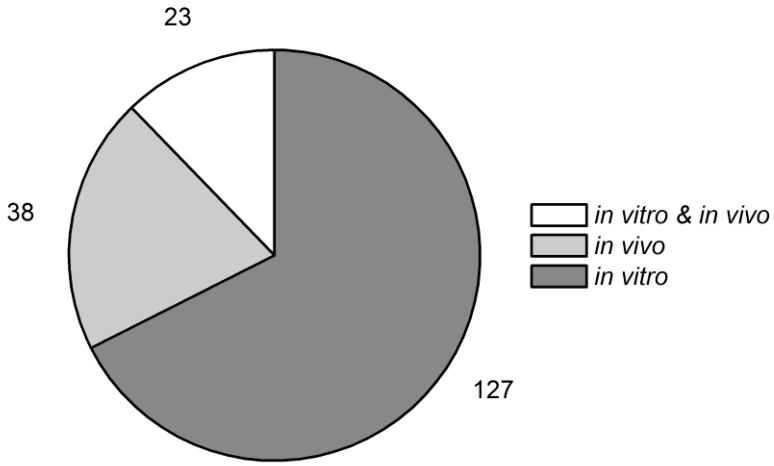

Figure 16. *In vivo and in vitro methods used with biotextiles in TE research [Appendix A].*

Main advantages for using *in vitro* methods over *in* vivo for biocompatibility screening are reasonable cost, requirements for facilities and equipment, processing time for multiple material candidates and absence of live animals. Still, *in vivo* studies in suitable animal models are necessary before an implantable tissue engineering construct can be considered for clinical trials. Testing on different species means that the results from animal models are not directly comparable to humans. Therefore choosing an appropriate animal is very important. The need for use of animal models must be thoroughly considered and if used, planned responsibly to avoid unnecessary animal experimentation. [48]

2.4.1 Biocompatibility

Biological and synthetic materials have some very different characteristic properties. For example, tissues contain cells and are able to regenerate or heal. [48] Tissue engineering constructs aim to diminish these differences. To achieve this, biomaterials used in these constructs must be compatible with the host tissue.

When a foreign body is inserted into the human body, complex defense mechanisms are activated. This is how the body protects itself from numerous threats. Implanted biomaterials and tissue engineering constructs must be designed to be accepted by the immune system. In case of biodegradable materials, also the degradation products must be considered. Otherwise, the implants are treated as threats and will not be able to fulfil their therapeutic purposes. This acceptance of foreign bodies by the host is referred to as biocompatibility. [14]

Biocompatibility can be tested by simulating the host environment in several stages. At first the material is tested *in vitro* with live cells and tissues, then *ex vivo* if possible,

followed by animal models before clinical trials on humans. [48] Evaluation is performed in this order because of ethical, financial and practical reasons.

Bioactivity describes an interaction between a biomaterial and the surrounding tissue that elicits a specific response. The activity can be based on either biological recognition or material transformation. In the first-mentioned, the biomaterial may be incorporated for example with growth factors to transfer information from the biomaterial to the surrounding cells. In the latter, a material transforms from one state or shape to another when introduced to the host tissue as a reaction to for example temperature or pH level. Transformations can be utilized to release substances such as growth factors or antibiotics. Bioactivity can be used for many purposes, including promoting of cell adhesion and proliferation, enhancing vascularization and preventing blood coagulation or infection. [50]

2.4.2 Cell cultures and animal models

Based on research articles in Appendix A, most common cells grown on biotextiles *in vitro* can be grouped under differentiated cells. In addition, numerous studies have been conducted using stem cells and a few studies using tumor cells. Both animal and human cells have been widely used, as both are relatively easy to obtain. Most cells in these studies were studied *in vitro*, but some were implanted with a scaffold into an animal model. In some experiments, the cells were grown on the scaffolds *in vitro* before implantation. Visual presentation of these statistics is presented in Figure 17. When viewing the chart, it should be taken into account that one research article may contribute to more than one category.

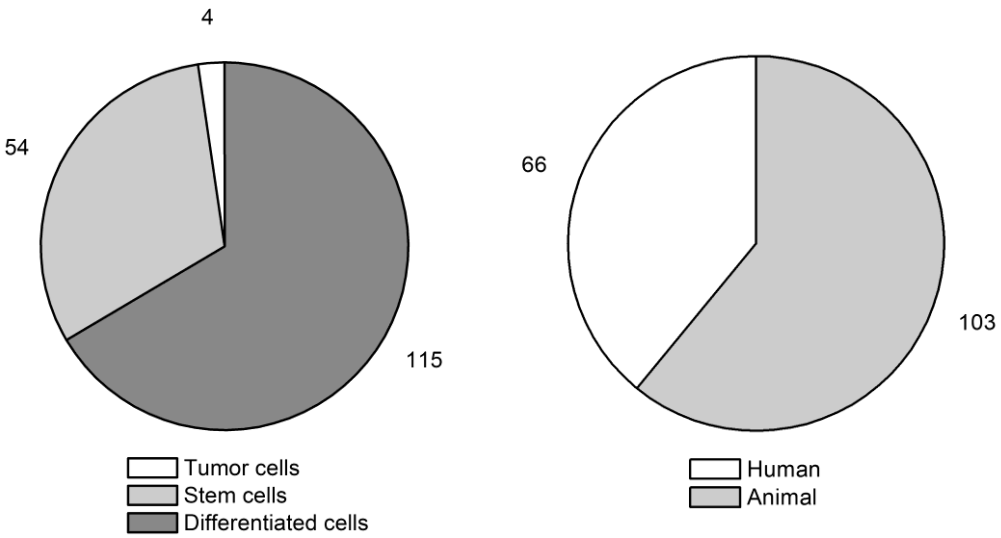

Figure 17. *Cell types (left) and cell sources (right) used with biotextiles in TE research. [Appendix A]*

50 studies in Appendix A that used differentiated cells used fibroblasts. The next most common cell type, used in 22 studies, were cartilage cells such as chondrocytes, temporomandibular joint disc cells and annulus fibrosus cells. Endothelial cells and ligament or tendon cells were used in 14 and 10 studies respectively. Other differentiated cell types were used by less than 10 studies. Mesenchymal stem cells (MSCs) were the most common stem cell type used. Embryonic stem cells (ESCs) and induced pluripotent stem cells (iPSCs) were used in only 2 studies. From the MSCs bone marrow stem cells (BMSCs) were used in 43 studies making them stand out as the most commonly used type of stem cells. BMSCs were followed by adipose stem cells with 7 studies, neural stem cells with 2 and amniotic fluid stem cells with 1 study. The few tumor cells that were used in experiments were astrocytomas, neuroblastomas, carcinoma cells and melanoma cells.

The selection of a cell type is based on intended application, availability, cost and purpose of the study. For example, if the goal of the study is to investigate biocompatibility of a material without any specific application in mind, possibly the most affordable and easily obtained cells can be used. In general, different cell types and sources are used as presented in Figure 18. Commercial cell lines are suitable for the initial stages of research because they are relatively inexpensive, easy to culture and have reproducible phenotypes. Later, isolated animal cells are used in small and large animal studies. Before clinical trials, human primary cells are used with large animal models. In clinical trials on humans, only autologous cells are used. Use of stem cells, often BMSCs, is common. [14] Figure 18 shows changes in cell sourcing as tissue engineering research progresses.

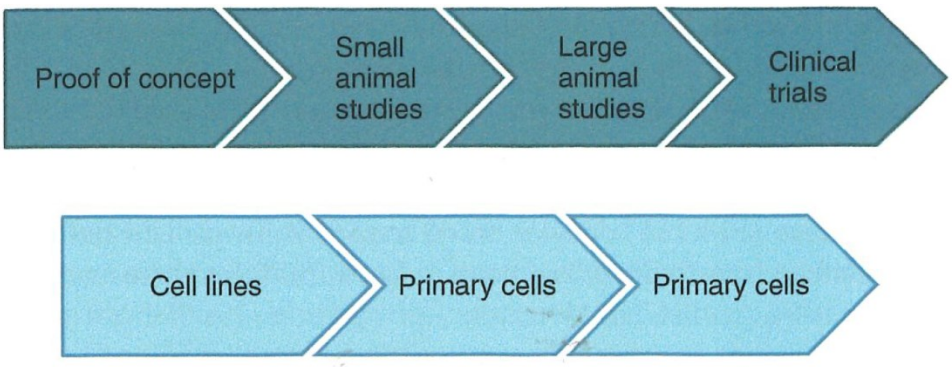

Figure 18. *Cell sourcing in tissue engineering research [14, p. 55].*

Cells are cultured *in vitro* in static, dynamic or bioreactor conditions. Static condition is the most straightforward and the most common method (Figure 19) where the cells are not conditioned to any added stimulation. The definitions of dynamic and bioreactor cell culturing conditions are partially intersecting. Sometimes all dynamic culturing conditions are referred to as bioreactors, but to differentiate the more complex setups from the less complex they are treated separately here. In dynamic conditions, flow of culture medium is added to the system using devices such as spinner flasks [51; 52] or roller bottles. With bioreactors, *in vivo* conditions are simulated during *in vitro* cell culturing, flow of

culture medium being one of the possible controlled parameters. Other common parameters are for example mechanical stimulus, pH and nutrient levels. In tissue engineering, bioreactors are often custom built or customizable systems for cell culturing and proliferation and for providing controllable and stabile physiological conditions for artificial tissue formation, development and maturation. [14]

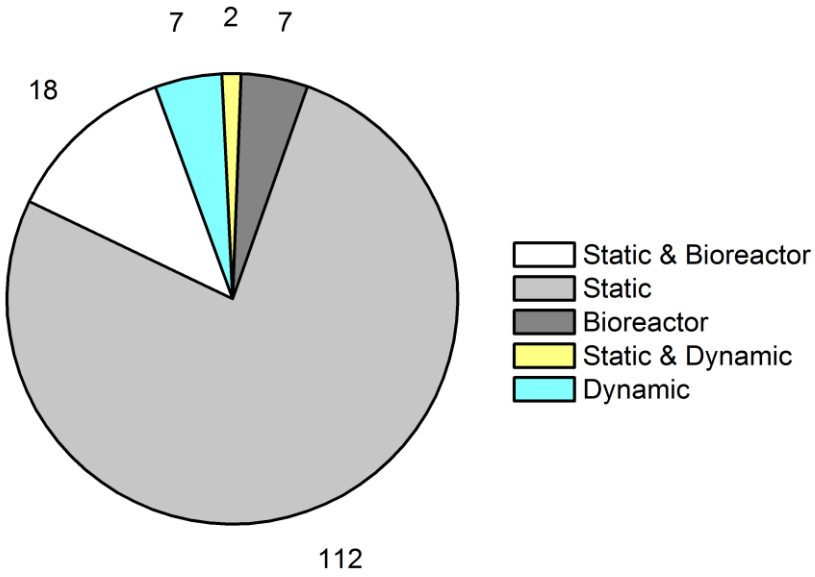

Figure 19. *Cell culturing conditions used with biotextiles in TE research [Appendix A].*

Different animal models used in research articles of Appendix A are presented in Figure 20. The data supports the progress from small animal models to large animal models in tissue engineering research shown previously in Figure 18. Total of 48 research articles describe the use of small animal models and 17 articles of large animals. Worth noticing is the absence of primates, the anatomically and physiologically closest animal models to humans. Working with primates is a rare privilege for researchers.

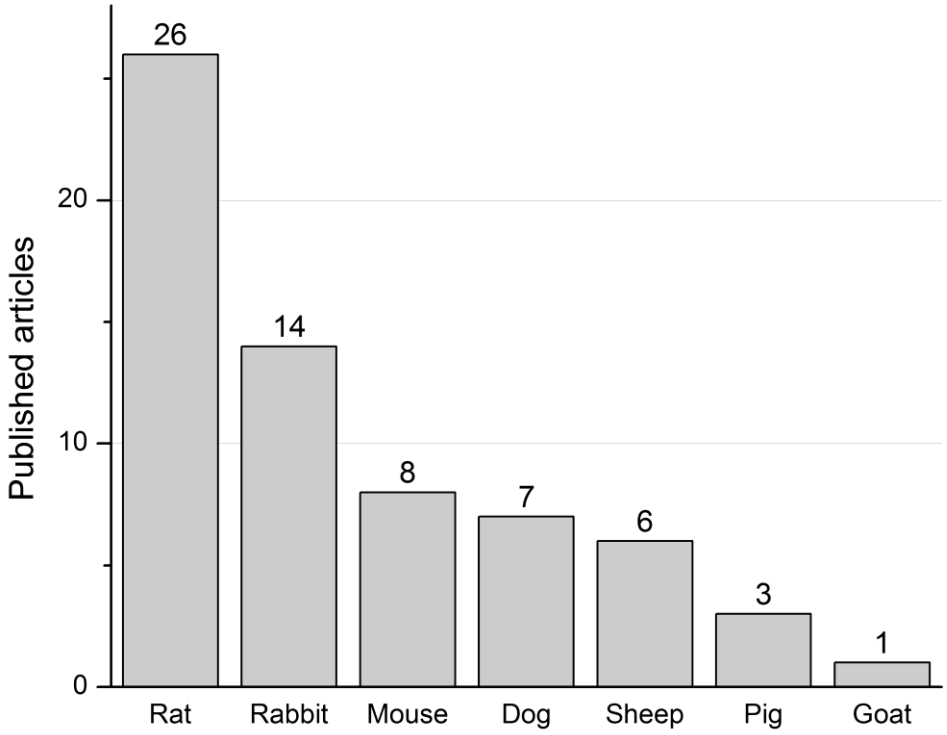

Figure 20. *Different animal models used with biotextiles in TE research [Appendix A].*

The path from preclinical studies to clinical trials is complex. It involves an enormous amount of choices to be made with materials, equipment, animals and methods used both in *in vitro* and *in vivo*. In addition, there is ethical factors to consider as well when working with animal models. Detailed planning and constant evaluation of progress are necessities for a tissue engineering research project to be successful. [53]

2.5 Clinical applications

When looking at data collected from 188 published research articles in Appendix A, it is apparent that textiles have been most researched for applications requiring good mechanical properties (Figure 21). Artificial tendons and ligaments are subjected to tensile stress, bones to compression and cartilage to shear and compression. For each application, the types of textiles used in the research are also shown in Figure 21. The data contains experiments from different stages of research, both *in vitro* and *in vivo*. This explains why 20 articles mention using non-wovens in research for tendon or ligament applications that require high tensile strength. For example, the non-wovens may have been used for early stage static cell culture tests for biocompatibility of a material. In that case, the tensile properties of the textile are not relevant. Another value standing out is the large amount of 21 research articles utilizing non-wovens for cartilage tissue engineering applications. It is also worth noticing that embroideries have been used almost only in bone tissue engineering. The possibility to manufacture three dimensional scaffolds with controlled dimensions is desirable for filling bone defects.

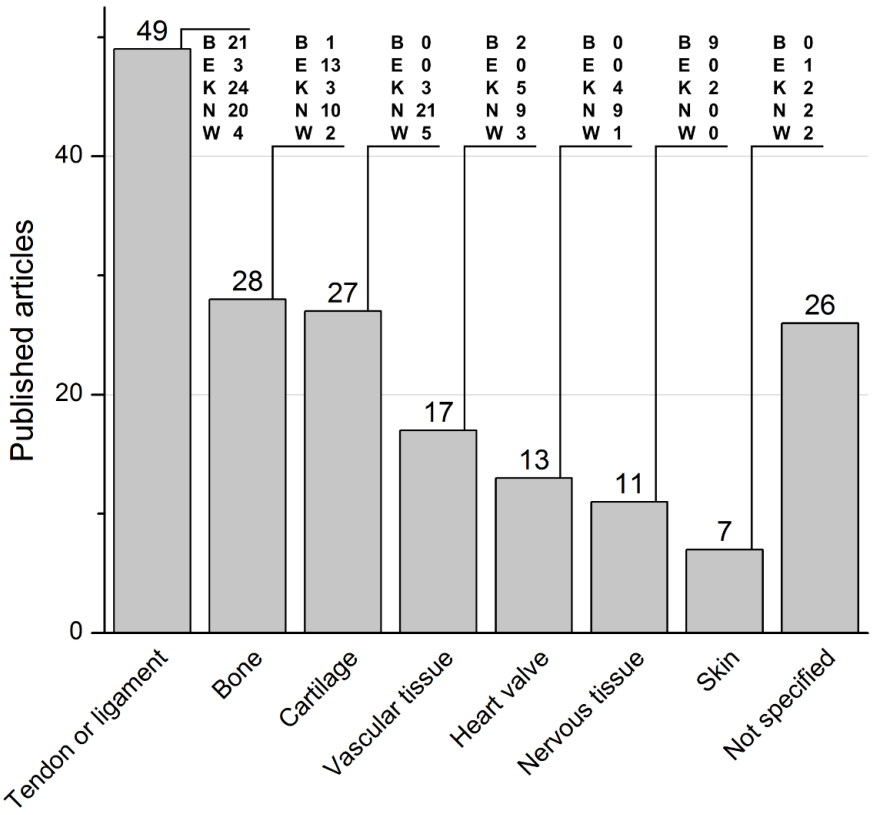

Figure 21. *The most common intended tissue engineering applications and types of textiles used for each. B=braided, E=embroidered, K=knitted, N=non-woven and W=woven. [Appendix A]*

Biotextiles are promising materials for tissue engineering applications. The versatility of the manufacturing techniques allows processing structures with a wide range of properties to address mechanical requirements and to provide a hospitable environment for cells. The main challenge remains to combine modern manufacturing techniques, biomaterials and advances in biological research to process tissues or organs, preferably in a seamless automated process. Extensive research must be conducted to develop products that have mechanical and biological properties that are comparable to live organs and tissues. Besides regenerative medicine, tissue engineered biotextiles could be utilized as *in vitro* disease models and drug testing. [3; 54]

EXPERIMENTAL PART

3. PRELIMINARY EXPERIMENTS

The aim of the preliminary experiments was to learn about the possibilities and limitations of the available equipment. For example, requirements for mechanical properties of the fibers and range of possible pore sizes in textiles were of interest. Fiber properties such as tensile strength and stiffness affect its ability to be processed into textile structures. Acquired information guided in choosing a suitable fiber and designing the manufacturing and testing process for the scaffolds. Stages of the preliminary experiments are shown in Figure 22.

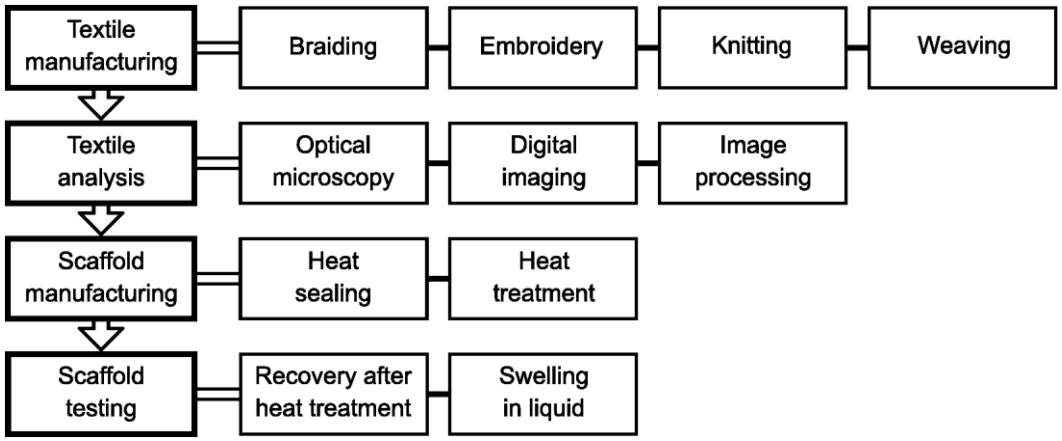

Figure 22. *Workflow of the preliminary experiments.*

Some of the stages are described in more detail, accompanied by illustrations in the materials and methods chapter. This way more emphasis is put on the chapter which covers manufacturing of the scaffolds for cell culturing.

3.1 Textile manufacturing

Four types of fibers were used in the preliminary experiments. The selection was based on ready availability at TUT where all of the fibers were previously produced. To evaluate requirements of fiber properties for textile manufacturing, it was advantageous to have fibers made of several different materials and in varying cross-sectional diameters to compare. Information on the fibers can be found in Table 1. From the fibers shown, fibers F3 and F4 have similar properties. The latter was introduced to the study because the fiber F3 inhibited curliness, which can lead to unwanted entanglement during processing.

Table 1. *Properties of the fibers used in the preliminary experiments.*

Name	Material	Cross-sectional diameter (µm)	Cross-sectional shape	Filaments
F1	PLA/PEG 95/5	106	round	4
F2	PBS/PLA 75/25	104	round	4
F3	PLDLA 96/4	56	star	4
F4	PLDLA 96/4	65	star	4

Knitted, woven, braided and embroidered textiles were manufactured using the fibers in Table 1. The processes and results are discussed in the next subsections.

3.1.1 Knitting

Single jersey knits were manufactured with circular knitting machine ELHA R-1S by Textilmaschinenfabrik Harry Lucas GmbH (Neumünster, Germany). A cylinder with diameter of 0.5 inches was used. To observe variation in the loop size, the fabrics were knitted with both 9 (every other) and 19 (all) needles using two needle lifting heights. Other controllable variables included machine speed, yarn tension, fabric withdrawal tension and feed position of the yarn. These do not affect the loop size, but need to be adjusted to successfully operate the machine.

Knitting settings and properties of the knits are combined to Table 2. The measurements to determine the loop size were taken from the middle of the 4-ply yarn bundle. Course and wale densities were calculated with measurements taken with a common office ruler with 1 mm accuracy.

Table 2. *Circular knitting machine settings and textile properties from the preliminary study. N = 3 for the loop lengths and pore sizes.*

Name	Fiber	Needles	Needle lifting height (mm)	Loop length (mm)	Pore size (mm^2)	Courses /cm	Wales /cm
K1-F1-9N-H	F1	9	HIGH	9	1.18	4	6
K2-F2-9N-H	F2	9	HIGH	8	0.87	5	6
K3-F3-9N-H	F3	9	HIGH	8	0.92	4	7
K4-F1-9N-L	F1	9	LOW	8	0.65	4	7
K5-F2-9N-L	F2	9	LOW	8	1.14	5	6
K6-F3-9N-L	F3	9	LOW	7	0.87	5	6
K7-F2-19N-H	F2	19	HIGH	8	0.87	4	6
K8-F3-19N-H	F3	19	HIGH	6	0.39	5	11
K9-F3-19N-L	F3	19	LOW	6	0.29	6	11

Knitting fiber F1 with 9 needles was problematic on both needle lifting heights. The needles were not able to catch the yarn, which resulted in holes in the knit. The yarn seemed not to be pliable enough and thus F1 was not chosen to be knitted with full set of 19 needles. In comparison, fiber F2 was easier to knit with 9 needles. When switched to 19 needles, the F2 was very problematic to knit having similar issues as F1 with 9 needles. F3 was successfully knitted with 19 needles on both needle lifting heights. The loop size with F3 was visibly smaller with 19 needles than with 9 needles. On 19 needles, lowering the needle lifting height did not have much effect on the loop size. Only the course density increased by one course per centimeter. These findings show that the densest single jersey knit with the smallest loop size can be manufactured from fibers with the smallest cross-sectional diameter when using a full set of needles at low lifting height. However, the loops and pores were still quite large even at their smallest. The width of the loops was in the range of hundreds of micrometers.

3.1.2 Weaving

4-ply F2 and F4 yarns were used to manufacture approximately 10 mm wide strips of plain weave woven fabric using a tabletop hand loom by Brio AB (Malmö, Sweden). The fabrics will be referred to as W1-F2 and W2-F4. For this process, F3 was substituted with similar yarn F4 due to the curliness of F3. F1 was left out from the study after it was shown previously to be unsuitable for knitting.

Warp and weft densities for the woven fabrics are presented in table 3. W2-F4 had small less dense areas where the weft density was as low as 40 yarns/cm. With an optical microscope no pores were clearly visible in any of the fabrics. Transparency of the fibers makes confirming the existence of small pores with diameters up to dozens of micrometers difficult from the images. Both yarns had sufficient mechanical properties for weaving. Neither of the fibers here had a significant advantage over the other in the weaving process.

Table 3. *Properties of woven fabrics manufactured in the preliminary experiments.*

Name	Yarn	Warp density (yarns/cm)	Weft density (yarns/cm)
W1-F2	F2	20	33
W2-F4	F4	20	125

In addition, weaving by adding metal filaments to alternate with F2 or F4 was experimented with. The aim was to create larger pores into the structure after removing the metal filaments. The weaving was not successful. The wefts were not oriented straight as the metal filaments did bend in an unwanted way when pressed with the beater. The structure did not resemble a traditional weave any more. Also especially in combination with

F4, the fibers did slide over the metal filaments. The metal filaments had cross-sectional diameters of 0.3 mm and 0.5 mm.

3.1.3 Braiding

A modified late 19th century braiding machine was used to manufacture eight braids from yarns F2 and F4. The machine can be used with 12 or 24 spools. For this preliminary experiment, 24 spools were used as it creates more dense braid. To reduce mechanical stress per filament, the filament count of F4 was increased to 8. Some of the samples were braided over a 2.75 mm plastic mandrel that was later removed. Two braiding positions, which affect the braid angle, were used. Lower position produces a braid with lower braid angle. The braid angle is the angle between the longitudinal axis of the braid and the yarn. For all samples regular 2:2-1 pattern was used. Braid properties are combined to Table 4.

Table 4. *Braiding machine settings and braid properties from the preliminary experiments. N = 3 for braid angle.*

Name	Fiber	Filament count	Braid angle Θ (°)	Braiding position	Mandrel (Yes/No)	Smallest pore (mm^2)	Largest pore (mm^2)
B1-F2-H	F2	4	38	High	No	0.004	0.024
B2-F2-H-M	F2	4	39	High	Yes	0.217	0.489
B3-F2-L-M	F2	4	42	Low	Yes	0.008	0.062
B4-F2-L	F2	4	42	Low	No	0	0
B5-F4-H	F4	8	36	High	No	0	0
B6-F4-H-M	F4	8	41	High	Yes	0.106	0.363
B7-F4-L-M	F4	8	40	Low	Yes	0	0
B8-F4-L	F4	8	42	Low	No	0	0

Braids using fiber F2 showed great amount of variation in pore size. The measured pores are located between the yarns. In some braids, there were also small pores between the fibers. Braiding with yarn F4 resulted in dense structures with no visible pores under microscope, except in braid B6 where the structure was loose in comparison. Using the mandrel increased the pore sizes in the structures with both yarns. If accompanied with high braiding position, the structures tended to be too loose to maintain their shape when handled after removing the mandrel. Both fibers had sufficient mechanical properties for braiding.

To use the fibers with the braiding machine the fibers were first wound onto special wooden bobbins made for the braiding machine. A custom built winding line was assembled for this purpose. The yarn winding process will be described in more detail in the materials and methods chapter of the experimental part.

3.1.4 Embroidery

A sewing and embroidery machine Innov-is 955 by Brother Industries Ltd (Nagoya, Japan) was used to create stitched patterns on a plain weave cotton fabric. Embroidery patterns were created in PE-Design Plus software and uploaded to the embroidery machine. The software has two wizards for creating patterns: Photo Stitch 1 (PS1) and Photo Stitch 2 (PS2). For both wizards, a monochrome square was used as the initial image. Settings from the wizards and yarn specifications are combined to Table 5. In the PS1 and PS2 settings, the far ends of line interval and density values were used. The run pitch value was the lowest possible. Higher density and line interval values result in more detailed stitching. Run pitch specifies the length of one stich. All samples were embroidered using a size 75/11 needle.

Table 5. *Embroidery settings from Brother® PE-Design Plus software and yarns used in the process. Top thread is on a spool and bottom thread on a bobbin.*

Photo Stitch 1			
Name	**Yarn (spool/bobbin)**	**Coarse/Fine**	**Run pitch (mm)**
E1-CC-C-PS1	Cotton/Cotton	Coarse	2
E2-CC-F-PS1	Cotton/Cotton	Fine	2
E7-F2C-C-PS1	F4/Cotton	Coarse	2
E8-F4C-F-PS1	F4/Cotton	Fine	2
E9-F2C-C-PS1	F2/Cotton	Coarse	2
E10-F2C-F-PS1	F2/Cotton	Fine	2
E11-F2F2-C-PS1	F2/F2	Coarse	2
E12-F2F2-F-PS1	F2/F2	Fine	2
Photo Stitch 2			
Name	**Yarn (spool/bobbin)**	**density (lines/mm)**	**Line inerval**
E3-CC-H-L-PS2	cotton/cotton	2.5	5
E4-CC-H-H-PS2	cotton/cotton	5	5
E5-CC-L-L-PS2	cotton/cotton	2.5	2.5
E6-CC-L-H-PS2	cotton/cotton	5	2.5

Samples E1-E6 were embroidered using common cotton embroidery yarns. To distinguish the top thread from the white base fabric, a black yarn was used. From these samples, it was easy to see how changing the settings in the wizards affected the end results. Embroids that were created using PS1 had the top thread covering the base fabric more evenly in comparison to ones created with PS2. In addition, the difference between coarse and fine density settings in PS1 was easy to see by naked eye. This lead only the PS1 to be used with following experiments with yarns F2 and F4 as it was more suitable for the intented purpose.

Fiber F4 did not have high enough mechanical properties. It was cut almost immediately after beginning the embroidery process and the samples E7 and E8 were not finished. F2 endured moderately better. Manufacturing sample E9 with cotton bottom thread was completed without top thread being cut. E10 was completed as well but the top thread was cut once and entangled to the machines parts several times. In samples E11 and E12, fiber F2 was used for both top and bottom threads, but entanglement continued to be a problem. Upon inspection with an optical microscope the samples embroidered with F2 and F4 had a lot of loose and randomly oriented filaments unlike in samples E1–6. The structure resembled more a non-woven fabric than a controlled stitching. The yarns F2 and F4 were not suitable for embroidery because of the entangling loose filaments and insufficient mechanical properties. The embroidery machine was not suitable for processing yarns with multiple loose filaments or low tensile strength. The method was therefore chosen not to be used for manufacturing scaffolds for the cell culture study.

3.2 Microscopic imaging and image processing

Image processing and analysis software ImageJ by National Institutes of Health (Rockville, United States) was used to determine several structural attributes from digital images taken with a digital camera BUC4-500C by BestScope (Beijing, China) attached to an optical microscope 475110–9904 by Zeiss (Oberkochen ,Germany). Imaging software ISCapture by Tucsen (Fuzhou, China) was used to take the images. From all textile types, pore size was measured. In addition, course and wale densities were measured from knits, warp and weft densities from woven fabrics and braid angle from braids. For each textile type, the measurements were taken from fabrics after manufacturing and from scaffolds after heat treatment. For both, one sample was examined from each textile type.

3.3 Scaffold manufacturing

To achieve more three-dimensional structures, knitted, braided and woven fabrics were processed into multi-layered scaffolds. For clarification, a tubular fabric was considered to have two layers. For each fabric, pieces of approximately 2 cm in length were arranged on top of each other and the ends melted together with an impulse sealer Magneta 621-M52 by Audion (Weesp, The Netherlands). This was not possible for the braids that were manufactured without the mandrel as they weren't wide and pliable enough to be arranged as described. In other knitted and braided fabrics, up to few millimeters wide gap was left within the tube. The woven scaffolds had smaller, but visible gaps as well between the layers. The gaps were removed by heat treating the scaffolds between steel plates under a weight. It was also of interest to approximate the number of layers necessary to manufacture a scaffold with a specific thickness as the scaffolds for cell cultruring were desired to have similar thicknesses.

To determine suitable temperature for heat treatment, scaffolds with 1 to 8 layers were kept at 60 ºC, 70 ºC, 80 ºC and 100 ºC for 15 minutes between steel plates. For compression, a 400 g steel plate was added. In addition, adding 0.5–1.0 mm thick steel frames around the samples was experimented with. These frames prevented excess compression of the samples allowing to include more layers while minimizing changes in structure. After heating, the fabrics were cooled between the plates under the weight at room temperature for five minutes before visual inspection.

70–80 ºC was found to be a suitable temperature range for the heat treatment as the layers stayed compressed together, but did not melt. Woven scaffolds did not require the use of frames, but for knits and braids with 4 or more layers it seemed to have some advantage. Also, it was evident that a less dense structure led to larger changes in the structures of knits and braids. This was not layer count dependant.

3.4 Recovery after heat treatment and compression

The cell culturing would take place at least several weeks after manufacturing the scaffolds, therefore it was necessary to investigate how the scaffolds behaved after the heat treatment. The scaffolds should stay in their compressed state to avoid large gaps between the layers. One knitted fabric, two woven fabrics and four braids were chosen for this experiment. Scaffolds prepared from these fabrics preserved their original characteristic structure trough the heat treatment process on at least satisfactory level.

The scaffolds were kept at 80 ºC for 15 minutes between steel plates under a 400 g weight and allowed to cool at room temperature for 5 minutes before they were removed from between the plates. Five scaffolds were prepared from each fabric. The length, width and thickness of the scaffolds was measured with a digital caliper before the heat treatment and at 0 h, 1 h, 20 h and 7 d after the treatment. Visual inspection of the structure was done immediately after the heat treatment. Comments can be found in Table 6. From the scaffolds, braid B6 experienced greatest structural changes. The yarns had moved in relation to each other and the structure did not look like a typical braid. Other braids had some loose loops at the edges, but the center areas were mostly as before heat treatment. The knit and the woven fabrics held their initial structure very well.

Table 6. *Fabrics used in the recovery experiment, layer count for each fabric and comments on appearance after heat treatment.*

Sample	Layers	Comments
B2-F2-H-M	6	Appearance mostly good, but also includes areas where the braid has lost its characteristic structure.
B3-F2-L-M	4	Attached from the ends to the surface with a tape to keep upright. After compression layers were misaligned.
B6-F4-H-M	8	Charasteristic structure lost in processing.
B7-F4-L-M	4	Appearance good at the center, poor at the edges.
K9-F3-19N-L	8	Appearance very good.
W1-F2	3	Layers tightly packed, but not fused. Appearance very good.
W2-F4	4	Layers tightly packed, but not fused. Appearance very good.

From Figure 23 can be seen that none of the scaffolds exhibited significant changes in their dimensions after the heat treatment. For each sample, measurements taken at 0 h, 1 h, 20 h and 7 d were compared to the dimensions prior to the heat treatment. The graph presents average percentages for each sample type.

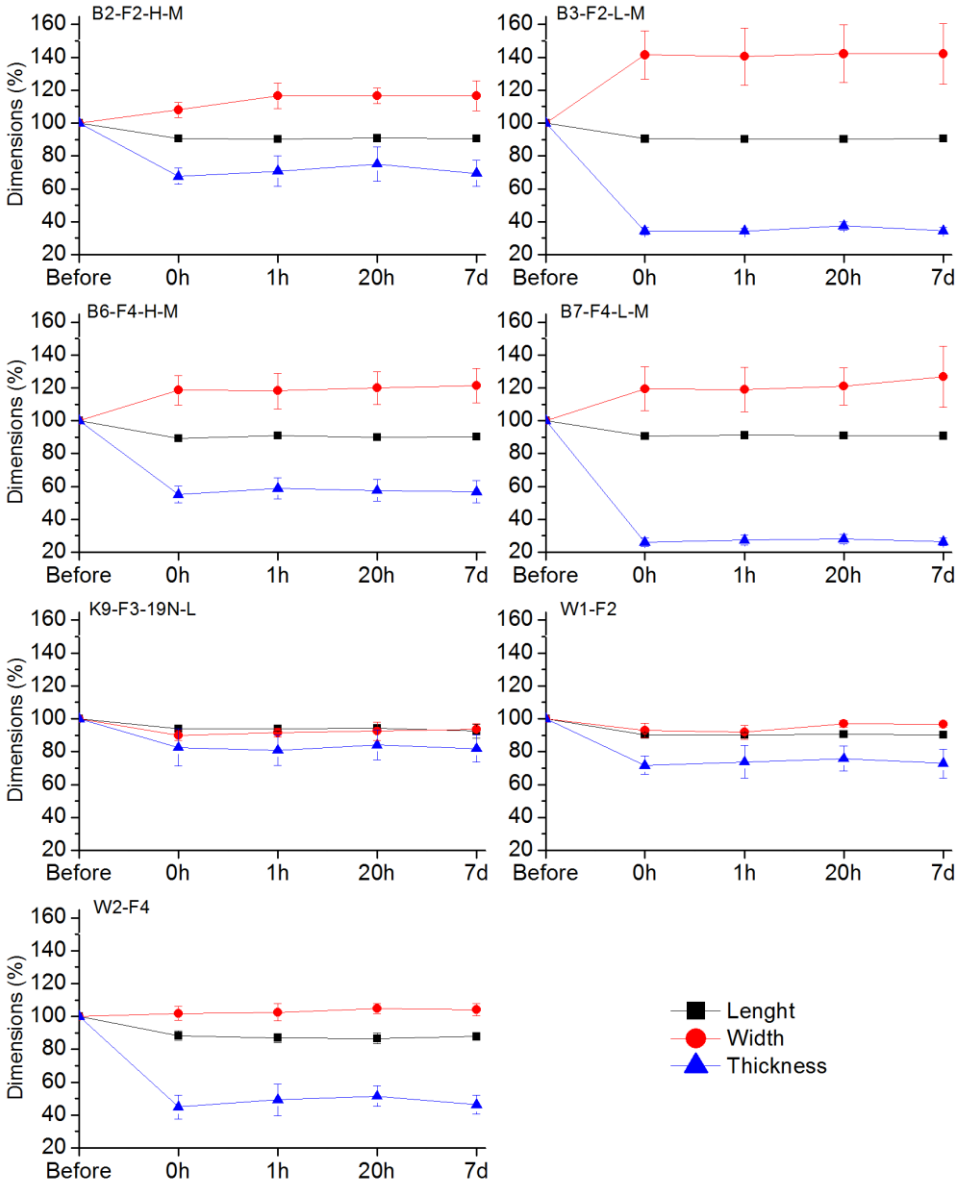

Figure 23. *Relative changes in length, width and thickness after heat treatment of braided, knitted and woven scaffolds. (n=5).*

Both visual inspection and measurements indicated that it was possible to use heat treatment under compression method on all three textile types. The braids were the most susceptible to exhibit unwanted structural changes. However, good results with sample B6 showed that the typical structure of the braid could be preserved.

3.5 Swelling in liquid

As the scaffolds would be kept in a cell culture medium during the cell culture studies, it was necessary to study if the liquid environment caused unwanted behavior, such as excess swelling or floating. Swelling could affect the flatness of the structure and cause the scaffolds to fall on their side, which would disturb micrography.

Braided, knitted and woven samples were kept in a sodium phosphate-buffered saline solution (NaPBS) in an incubator at 37 °C for a week. Length, width and thickness were measured with a caliper at 0 h, 1 h, 2 h, 4 h, 21 h and 7 d. Five samples were tested of each scaffold type. For each sample, all measurements were compared to the dimensions prior to adding the solution. Figure 24 presents average percentages for each sample type.

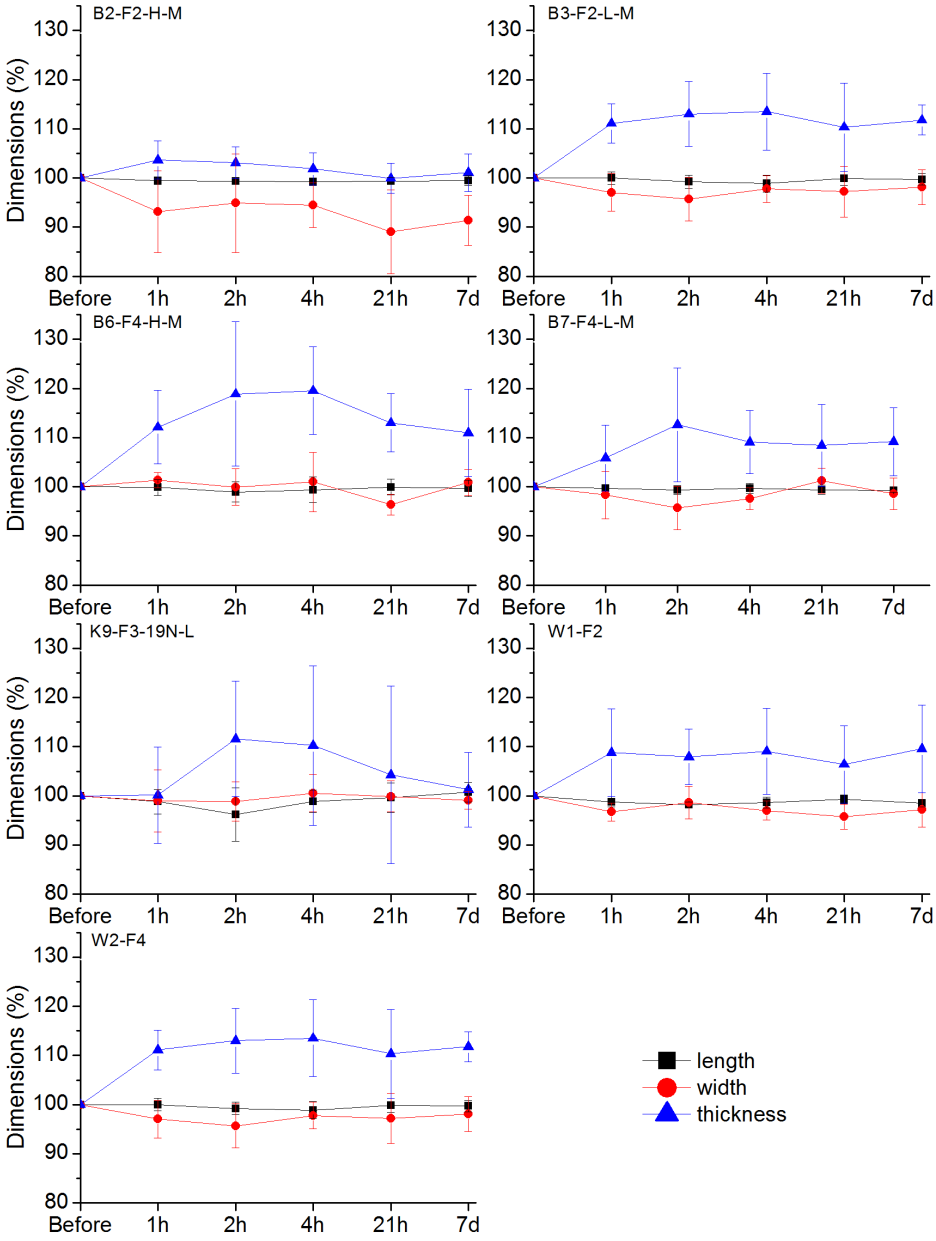

Figure 24. *Relative changes of braided, knitted and woven scaffolds during swelling experiment. n = 5.*

All of the scaffolds floated on the surface when the liquid was added because air was trapped inside the scaffolds. To remove the air, the scaffolds were tapped with blunt ended forceps while submerged. This was repeated at each time point until the scaffolds stayed under surface. Only a few scaffolds needed this at 21 h. All of the scaffolds were submerged at 7 d. In addition, an observation was made where air was trapped into the

seamed end of a sample. Because of this, the sample was not flat on the bottom of the bottle. One end was touching the bottom and other was floating a few millimeters above the bottom.

The changes in length, width and thickness were very small. A difference could be also due to measuring from a slightly different part of the scaffold. As a conclusion, the changes were not significant as they were not visible to naked eye.

4. MATERIALS AND METHODS

The main experimental part of the thesis begun with melt spinning PLDLA 96/4 fibers. A 36-week hydrolytic degradation study was conducted simultaneously with other stages shown in Figure 25. Three types of textile scaffolds were manufactured to be used in the cell culture study.

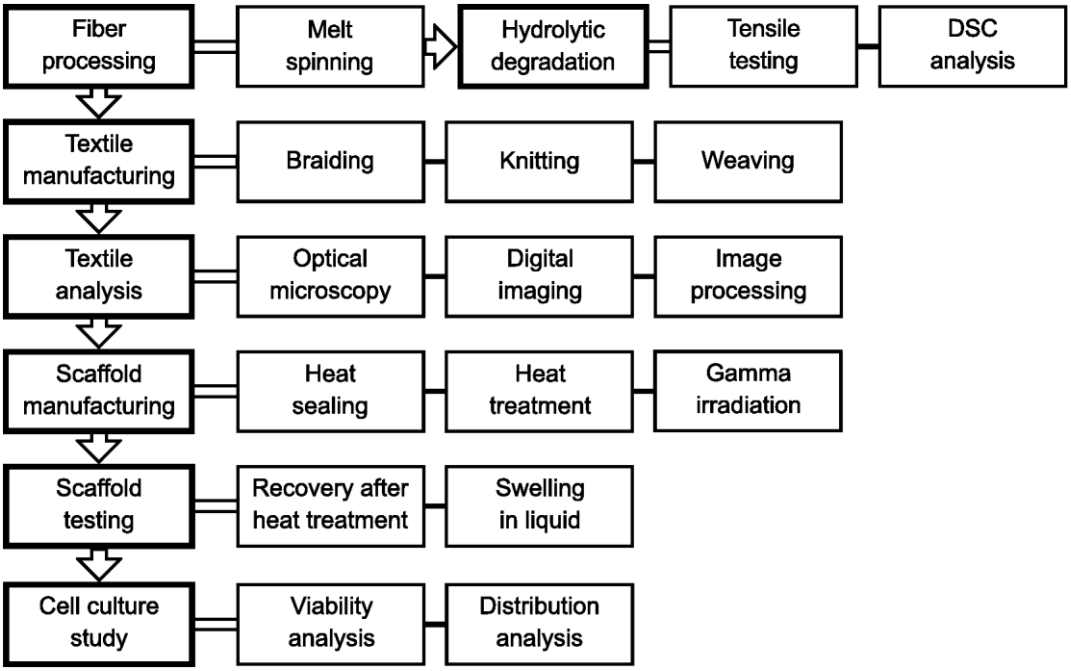

Figure 25. *Workflow of the main experimental part of the thesis.*

Materials and methods used in the different manufacturing and testing stages and in the cell culture study will be presented in the following sections. The design of the main experimental part of the thesis is based on the preliminary experiments. Only hydrolytic degradation study, gamma irradiation process and cell culture study were not included in the preliminary part.

4.1 Fiber processing

Melt spinning method was used to manufacture polymer fibers. The information of the used material and basis for materials selection is presented in the next section, which is followed by a description of the fiber manufacturing process. Details of the production line and processing parameters are given.

4.1.1 Material

Good manufacturing practice (GMP) grade PLDLA copolymer Purasorb® PLD 9620 with 96/4 molar ratio of L- and D-lactides by Corbion Purac Biomaterials (Gorinchem, The Netherlands) was used in this study to manufacture continuous fibers with a melt spinning method. Material data is combined to Table 7.

Table 7. *PLDLA 96/4 material information [55].*

Tradename	Purasorb® PLD 9620
L/D molar ratio (%)	96/4
Inherent viscosity (dL/g)	1.92
Form	Granule
Batch	1405002058
Manufacturer	Corbion Purac Biomaterials

Preliminary experiments showed PLDLA 96/4 to be suitable for manufacturing textiles and it was of interest to compare results from these experiments to results from previous unpublished experiments with the same polymer. Fibers F3 and F4 that were used in the preliminary experiments were manufactured from a different batch of the same polymer.

4.1.2 Melt spinning

The melt spinning line (Figure 26) consisted of a K-SFS-24 gravimetric feeder by Coperion K-Tron (Stuttgart, Germany), a Gimac TR 12/24 GM single screw micro extruder by Gimac di Maccagnan Giorgio (Milano, Italy), five draw panels by Fourné Maschinenbau GmbH (Alfter, Germany) and a RPC.HS filament winder by Comoli (Paruzzaro, Italy). Technical details of the extruder can be found in Table 8.

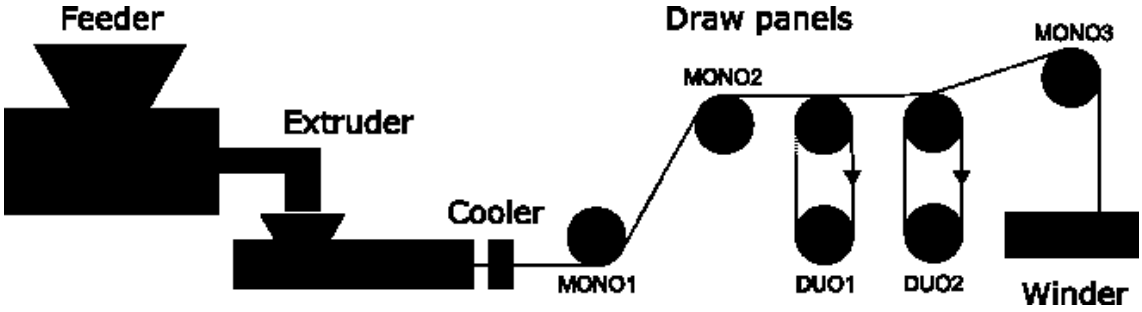

Figure 26. *Illustration of the melt spinning line used to manufacture PLDLA 96/4 fibers from granules to form a 4-ply multifilament yarn.*

Table 8. *Technical details of Gimac TR 12/24 GM single screw micro extruder.*

Extruder	Gimac TR 12/24 GM
Screw diameter (mm)	12
Screw Length/Diameter ratio	24/1
Number of heating zones	6
Melt temperature sensor	Heating Zone 5
Pressure sensor	Heating Zone 5
Die	4 x Ø 0.4 mm (round)

In the process, polymer granules were inserted to the feeder, which dispensed the granules to the extruder at a constant rate of 150 g/h. Nitrogen gas was pumped into the hoppers of both the feeder and the extruder to replace atmospheric oxygen. The polymer was melted in the extruder at elevated temperature and was forced through a die with four round holes 0.4 mm in diameter each. The extruder was cooled with a FL1203 recirculating water cooler by Julabo GmbH (Seelbach, Germany), which was set to operate at 10 °C. After extrusion, the fiber was cooled by airflow. The godets on draw panels MONO2, DUO1 and DUO2 were heated to temperatures presented in Table 9. Table 10 presents information on drawing velocities and number of rounds the fiber makes around a godet or a pair of godets. Cross-sectional diameters of the fibers were measured with a digital micrometer. Air humidity was at 20 % during processing.

Table 9. *Temperature settings for PLDLA 96/4 extrusion.*

Heating zone	Temperature setting (°C)
1	182
2	187
3	192
4	203
5	214
6	237

Table 10. *Fiber drawing parameters for melt spinning process of PLDLA 96/4.*

Draw panel	Godet temperature (°C)	Drawing velocity (m/min)	Number of rounds
MONO1	-	70	1
MONO2	70	72	5
DUO1	85	130	6
DUO2	90	220	10
MONO3	-	222	1
Winder	-	225	-

Prior to melt spinning the polymer granules were dried in a VD-series vacuum drying oven by WTC Binder GmbH (Tuttlingen, Germany). The uncapped bottles with the polymer were kept in the vacuum over night at room temperature, which was followed by 16h at 100 °C. After heating, the granules were allowed to cool to room temperature in the vacuum and kept there until extrusion.

4.2 Textile manufacturing

Three types of textiles were manufactured from the PLDLA 96/4 fibers. The manufacturing methods were braiding, knitting and weaving. For each method fibers were used as non-twisted bundles, yarns. 8-ply yarn was used for braiding to reduce mechanical stress experienced by a single fiber. For other methods 4-ply yarn was used. Each manufacturing method is described in following subsections.

Microscopic imaging and image processing methods were used to determine properties of textiles before processing using devices and methods previously described in section 3.2. Briefly, from all textile types, pore size was measured. In addition, course/wale densities were measured from knits and warp/weft densities from woven fabrics. Braid angle was determined from braids.

4.2.1 Braiding

A modified late 19th century braiding machine was used to manufacture a tubular braid. For braiding, 4-ply PLDLA 96/4 yarn was wound from two spools to a single bobbin to double the filament count to 8 using a custom yarn winding line (Figure 27). In the process, the winder pulled the yarn from two spools onto a bobbin. A series of yarn guides were used to allow the winder to pull the yarn from the spools as smoothly as possible. In the winder, a carriage section distributed the yarn evenly on the bobbin with a steady back and forth motion. The winder was set to wind the yarn at a velocity of approximately 0.4 m/s.

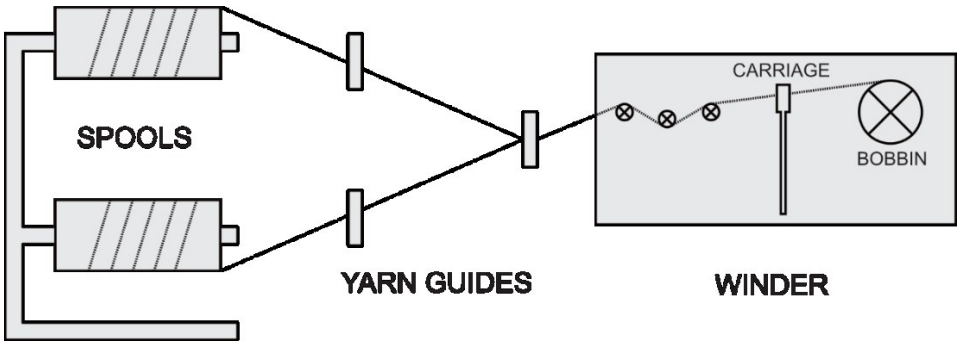

Figure 27. *A simplified illustration of the yarn winding line.*

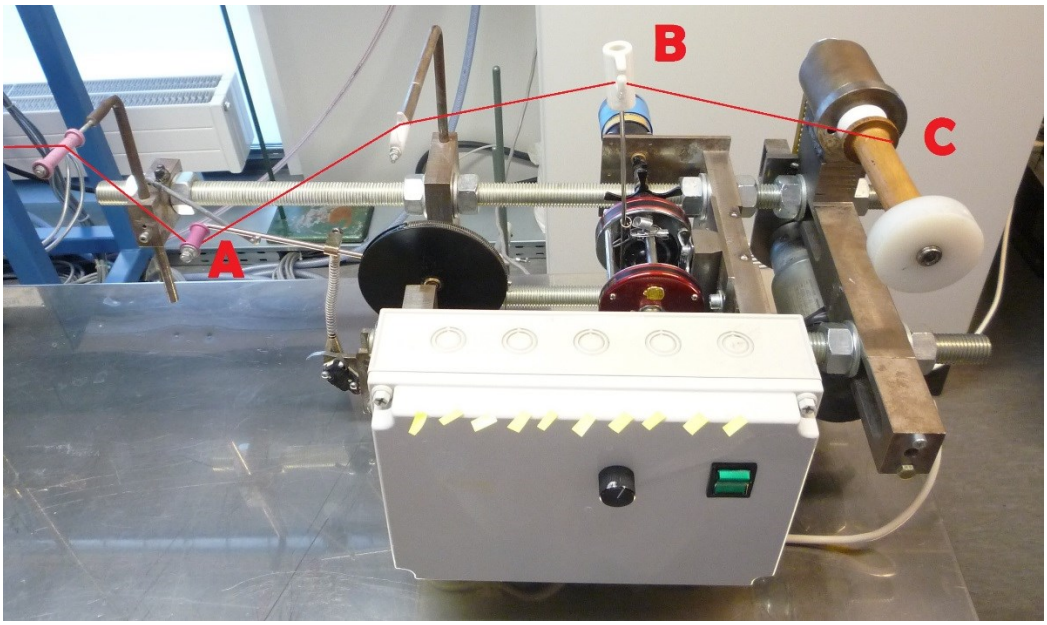

Figure 28. *Yarn winding machine. The path of the yarn is highlighted in red. A=velocity control lever, B=carriage and C=bobbin.*

A 2:2-1 braid was manufactured using a full set of 24 bobbins. The yarns were braided over a flexible hollow plastic mandrel with a diameter of 2.75 mm, which was later removed. The braiding position (see Figure 29) was kept at the level of the lower yarn guide by adjusting the tension of the winder manually. Lower position results in higher braiding angle. To accompany the simplified illustration a photograph of the machine is included (Figure 30).

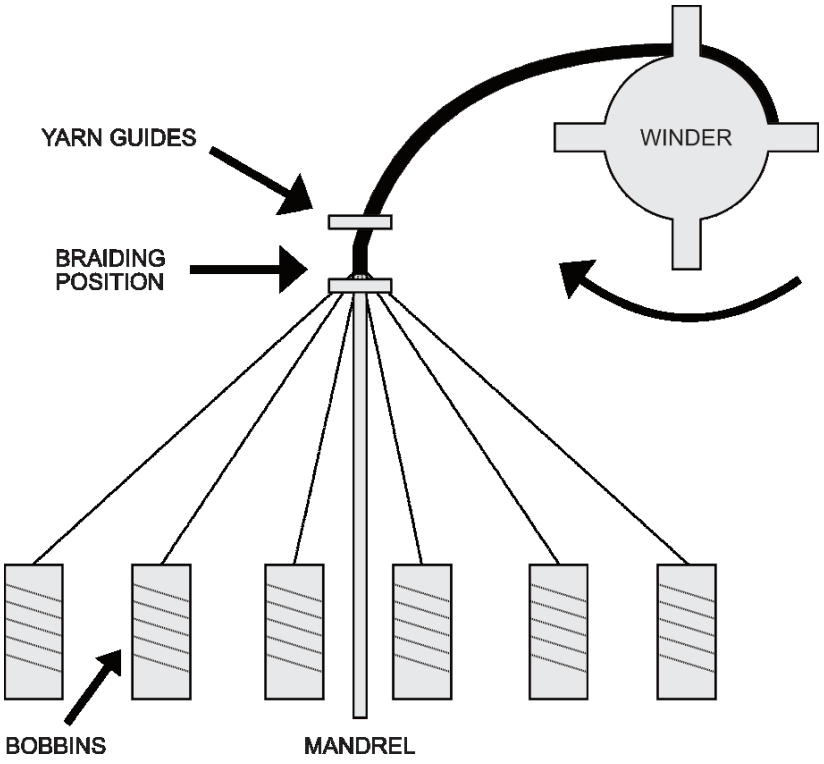

Figure 29. *A simplified illustration of the braiding machine.*

Figure 30. *Braiding machine. Lower yarn guide in pink.*

After braiding, the braid was washed in Etax Aa 99.5 % ethanol by Altia Oyj (Helsinki, Finland) in an M12 ultrasonic cleaner by FinnSonic (Lahti, Finland) 2 times to remove machine lubricants and other unwanted substances. Each washing cycle lasted for 2 minutes and the ethanol was changed between cycles. The braid was dried in a fume hood overnight and stored in a vacuum drying oven at room temperature until used to prepare the scaffolds.

4.2.2 Knitting

A tubular single jersey knit was knitted from 4-ply PLDLA 96/4 yarn using an ELHA R-1S circular knitting machine by Textilmaschinenfabrik Harry Lucas GmbH shown in Figure 31. A full set of 19 latch needles was used in the ½ inch cylinder. In addition to needle count and cylinder size, adjustable parameters were fabric withdrawal tension, needle lifting height, yarn tension and knitting speed. The two latter parameters did not have numerical values and the first-mentioned is a unitless parameter. Information on the machine and the used parameters are collected to Table 11.

Figure 31. *ELHA R-1S circular knitting machine.*

Table 11. *Machine and processing parameters for knitting.*

Parameter	Value
Cylinder	½"
Needle count	19 of 19
Needle lifting height	24.4–24.6 mm
Yarn tension	Low
Knitting speed	Low
Fabric withdrawal tension	4.0–4.1

To form a knit, the yarn is drawn from the spool by the motion of the needles. It is guided through yarn guides and a brake that is used to adjust the yarn tension. This is followed by a feed area where the yarn is set to be grabbed by the hook of a needle to form a loop to the knit. The circular knit is then drawn away from the needles with a fabric withdrawal mechanism, a nip roller. By controlling the rolling speed of the roller, the tension of the fabric between the needles and the roller is adjusted. Tension is needed to pull the fabric away from the needles to allow a new row of loops to form. See Figure 32 for an illustration of the knitting process.

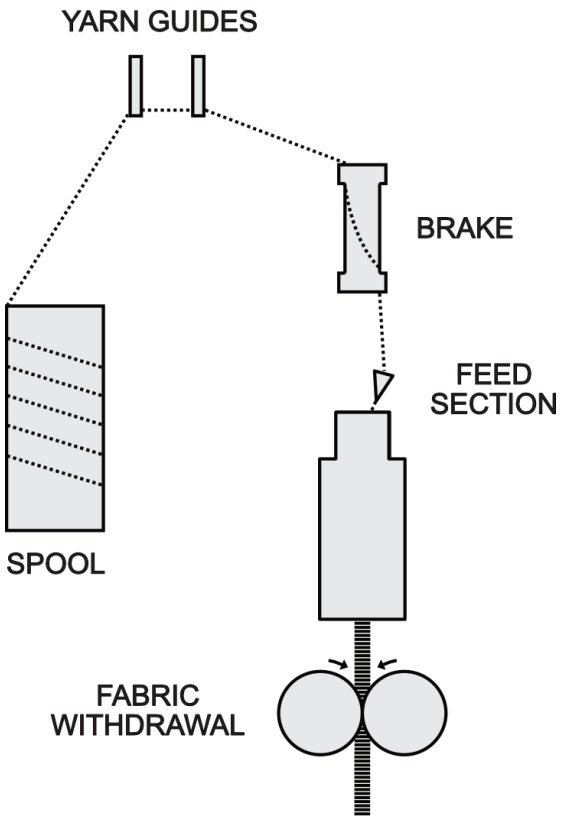

Figure 32. *A simplified illustration of the circular knit manufacturing process.*

The knit was washed in ethanol while treated with ultrasound as previously described in subsection 4.2.1. Lubricant used in the needle mechanism is in contact with the knit and therefore needs to be removed by washing.

4.2.3 Weaving

Plain weave fabric was manufactured by using a modified tabletop handloom by Brio AB shown in Figure 33. The original reeds of the beater were replaced with reeds that had higher slit density. By doing this, a higher warp yarn density was achieved. For both the warp and the weft, 4-ply PLDLA 96/4 yarn was used. To produce a fabric with a width of approximately 1 cm, 20 yarns were used in the warp.

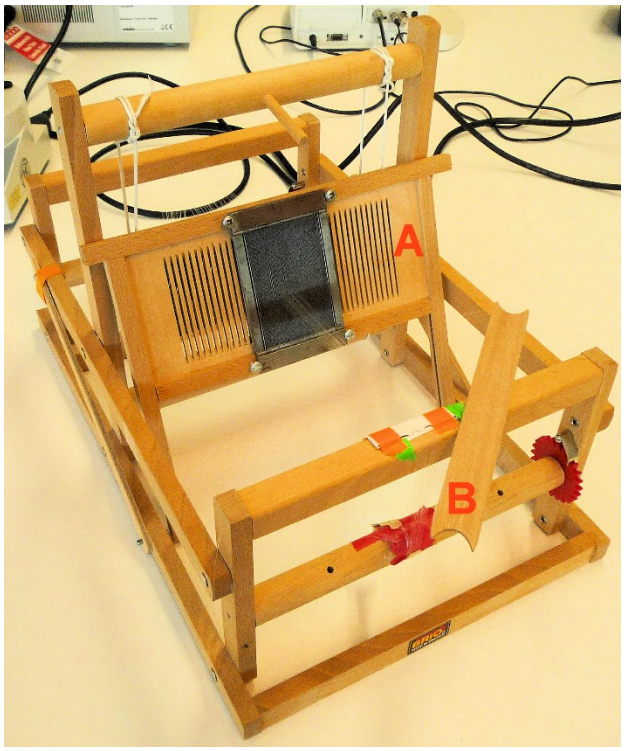

Figure 33. *Modified tabletop handloom and a shuttle for inserting the weft yarns. A=beater with modified reeds and B=shuttle.*

For weaving, approximately 100–150 cm of yarn was collected around the shuttle. A knot was made to both ends of the yarn to prevent it from unraveling. With the shuttle, the weft yarn was guided through the warp and secured to its place with the beater. After changing the position of the heddles, the shuttle was taken back to the other side through the warp. The yarn was again secured to its place with the beater. This was repeated until enough fabric was created.

The fabric was washed in ethanol while treated with ultrasound as previously described in subsection 4.2.1. Unlike in braiding and knitting processes, lubricants were not used on the loom. However, the fabric was washed to remove for example dust gathered from the air.

4.3 Scaffold manufacturing

To perform recovery, swelling and cell culture studies, multilayered scaffolds were manufactured from the previously braided, knitted and woven fabrics. The number of layers for each textile type was chosen so that all the final scaffolds would be approximately 1 mm in thickness. To be able to fit the scaffolds into cell culture wells, the scaffolds were not to exceed 15 mm in any direction. For each scaffold, the layers were first heat sealed together from the ends prior to heat treatment under compression.

4.3.1 Layer arrangement and heat sealing

Magneta 621-M52 impulse sealer by Audion was used to melt the PLDLA 96/4 fabrics to prevent unraveling of the fabrics and to join the layers. As mentioned earlier, tubular fabrics are considered to have two layers in one cross-section. To achieve approximately 1 mm thick scaffolds, each fabric type was arranged to have different amount of layers (Table 12). The process (Figure 34) consisted of three main stages: (1) The fabric was divided into sections and cut, (2) the sections were arranged on top of each other and (3) the multilayered structure was heat sealed from the ends. At the third stage, the structure was held between forceps for sealing. The Figure 34 shows the process for knitted scaffolds. Braided and woven fabrics were treated in similar manner except the layer count and therefore the amount of sections differed. In some cases, not all of the sections were joined from the ends before seaming at stage 3. Especially with braided scaffolds it was sometimes necessary to separate the sections to arrange them accurately on top of each other for stage 3. This was because of high thickness to width ratio.

Table 12. *PLDLA 96/4 textile scaffolds were prepared by heat treatment.*

Textile type	Scaffolds manufactured	Notation	Layer count
Braided	20	B1–B20	6
Knitted	24	K1–K24	8
Woven	21	W1–W21	3

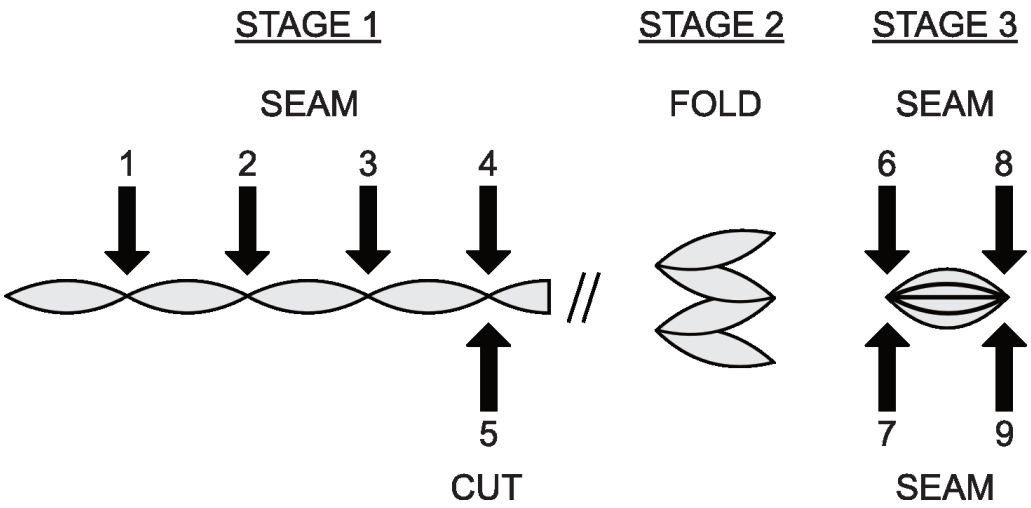

Figure 34. *Preparing the PLDLA 96/4 textile fabrics into multilayered structures consisted of three main stages.*

The same heating and cooling parameter values (Table 13) were used for all textile types. With these settings it was necessary to use the sealer on the both sides of the structure at stage 3 of the process to melt the ends firmly together.

Table 13. *Impulse sealer settings used in preparing PLDLA 96/4 textile scaffolds.*

Parameter	Value
Heating	6–7
Cooling	6

Heat treatment under compression for the structures was done immediately after seaming. The process is presented in the following subsection.

4.3.2 Heat treatment under compression

The textile scaffolds were heat treated in a laboratory drying oven at 70 °C for 15 minutes and allowed to cool at room temperature for 5 minutes before removing the samples from the setup. For the treatment, the scaffolds were placed on a steel plate and a 0.5 mm thick steel frame was added around the scaffolds. Compression was created by adding a 592 g steel plate on the top of the assembly as shown in Figure 35.

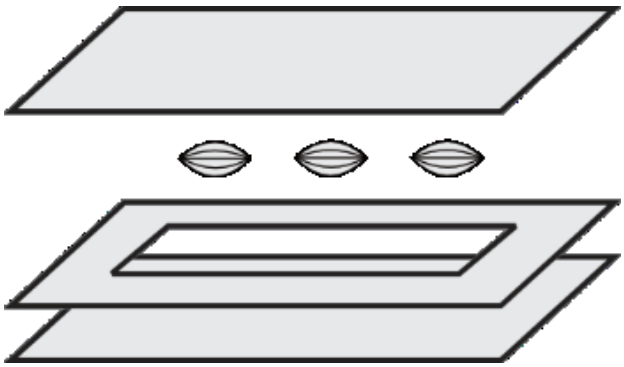

Figure 35. *PLDLA 96/4 scaffolds were heat treated under compression. A 0.5 mm frame surrounded the samples to prevent excess compression.*

A polytetrafluoroethylene (PTFE) adhesive tape was used on one end of braided scaffolds to maintain correct position. Because of the high thickness to width ratio of the braids, they were subjective to fall on their side. Minimum contact was made with the tape to the scaffolds. Covering only the melted seam at the end of the scaffold was enough.

4.4 Gamma irradiation

The scaffolds for cell culture, recovery and swelling tests and fibers for *in vitro* hydrolytic degradation study were sterilized with gamma-irradiation. A dose of ≥25 kGy was given at BBF Sterilisationsservice GmbH (Kernen, Germany). Gamma irradiation indicator labels were used to confirm received dose. For sterilization, the samples were packed into plastic pouches, which were inserted to metallic zip lock bags. The latter were packed into a cardboard box to be sent out for irradiation. All other scaffolds were heat treated prior to irradiation except B17–B20, K16–K19 and W16–W19 which were to be used on

recovery and swelling studies. Before the scaffolds were packaged to be gamma irradiated, they were washed in 99.5 % ethanol as previously as described previously in subsection 4.2.1.

4.5 Recovery of the scaffolds after heat treatment

To study if the scaffolds maintained their compressed state after the heat treatment textile scaffolds were heat treated under compression and the dimensions were measured during a 1-week period. Four gamma irradiated scaffolds were tested from each textile type. Heat treatment procedure was the same as described earlier in subsection 4.3.2. After the treatment, the samples were stored in closed plastic bottles at room temperature to be used in swelling experiment. Length, width and thickness were measured with a digital caliper before the heat treatment, immediately after and at 4 h, 1 d and 7 d time points. Measurements from the latter four were compared to ones taken before the treatment and percentual changes were calculated.

4.6 Swelling of the scaffolds in cell culture medium

A swelling study was conducted for textile scaffolds. The same scaffolds were previously used in the recovery study. Scaffolds were kept submerged in Dulbecco's Modified Eagle Medium: Nutrient Mixture F-12 (DMEM/F-12) by Thermo Fisher Scientific (Waltham, United States) in an incubator (unknown model) by Termaks AS (Bergen, Norway) at 37 °C for 1 week period. Each scaffold was stored in an individual closed plastic bottle. Length, width and thickness of all scaffolds was measured with a digital caliper before the scaffolds were inserted to the medium. The samples were inspected for contamination every 24 h and contaminated samples were removed and measured. At 7 days also non-contaminated samples were measured and discarded. Change of color from pink to yellow in the culture medium indicated contamination.

When the scaffolds were inserted into the medium, there was air trapped inside the scaffolds. This air was removed by tapping the bottoms of the bottles against the work surface of a KR-140 laminar flow cabinet by Kojair Tech Oy (Tampere, Finland).

To avoid contamination, the scaffolds were first washed in 99.5 % ethanol as previously as described previously in subsection 4.2.1. Inserting the scaffolds into the cell culture medium and later measurements were done as aseptically as possible in a laminar flow cabinet. The laminar cabinet was located in a laboratory, which was not designed for aseptic working.

4.7 Hydrolytic degradation of the fibers

A hydrolysis study was conducted for the gamma irradiated PLDLA 96/4 fibers to determine *in vitro* degradation properties of the fibers. Time points for the 36-week series are

shown in Table 14. Tensile testing and differential scanning calorimetry methods were used to determine mechanical properties, thermal properties and crystallinity of the polymer fibers.

Table 14. *Time points for in vitro hydrolytic degradation study of the PLDLA 96/4 fibers. Y=YES.*

Method	Timepoints (week)													
	0 DRY	0 WET	1	2	3	4	8	12	16	20	24	28	32	36
Tensile	Y	Y	Y	Y	Y	Y	Y	Y	Y	Y	Y	Y	Y	Y
DSC	Y	-	Y	-	-	-	Y	-	Y	-	Y	Y	-	Y

For tensile testing, 4-ply fiber bundles were cut into 25 cm sections and tied from one end. 8 bundles were prepared for each time point. DSC samples were prepared from 2.5 m sections of the 4-ply bundle, one section for each time point. The samples were sterilized with gamma irradiation as described earlier.

The fibers for weeks 1–36 were placed in closed 35 ml test tubes filled with sodium phosphate-buffered saline solution (NaPBS) and kept in a static incubator at 37 °C. A test tube containing only NaPBS was included as a control. Composition of the solution is presented in Table 15.

Table 15. *Sodium phosphate-buffered saline solution composition.*

Reagent	Amount (g/l)	Concentration (mol/l)
Na_2HPO_4	3.54	0.0249
$NaH_2PO_4*H_2O$	0.76	0.0055
NaCl	5.90	0.1009

The solutions pH was 7.35–7.45. The solution was changed every two weeks. For monitoring, pH was measured from the control and 5 other test tubes before changing the solution. For pH measurements, a SevenMulti pH-meter by Mettler-Toledo (Columbus, United States) was used. When the fibers were first inserted to the solution and every time the solution was changed, the test tubes were turned upside down a couple of times the next day to remove air bubbles from the surfaces of the fibers. Samples for week 0 were stored in sealed plastic pouches at room temperature until used.

4.7.1 Mechanical properties

An Instron 4411 material testing machine by Instron (Norwood, United States) was used to conduct tensile testing for the PLDLA 96/4 fibers. Testing parameters are listed in Table 16. For each week, 6 parallel samples were tested, leaving 2 spare samples for every time point.

Table 16. *The parameters used in tensile testing of the PLDLA 96/4 fibers.*

Parameter	Value
Load cell	500 N
Gauge length	50 mm
Crosshead speed	30 mm/min
Temperature	room

The tensile strength of the 4-ply yarn was calculated using equation (1):

$$\sigma = \frac{F}{A}\,, \tag{1}$$

where σ denotes tensile strength or stress (N/mm^2 = MPa), F is tensile load (N) and A is cross sectional area (mm^2) of the specimen. The cross-sectional diameters of the fibers were measured with a digital micrometer at 0, 1, 2 and 3 week time points. The diameters were used to calculate cross-sectional areas for the fibers. To calculate the total cross-sectional area of the 4-ply yarn, the areas of the individual fibers were summed together. Measurements from the first 3 weeks were used to calculate an average cross-sectional area to be used from week 4 onward in the calculations.

Before tensile testing, the samples were taken from the static incubator to room temperature a few hours before the measurements. Immediately before testing, each sample was taken from the buffer solution, rinsed with distilled water and measured with a micrometer when necessary. At week 0, the wet samples were placed in buffer solution 1 h before testing and also rinsed immediately before the testing. The dry samples were tested as they were removed from the sealed plastic pouches used for gamma irradiation.

4.7.2 Thermal properties

A Q1000 differential scanning calorimeter by TAinstruments (New Castle, United States) was used to determine the crystallinity (X_c), melting temperature (T_m) and glass transition temperature (T_g) of sterilized PLDLA 96/4 fibers at time points shown in Table 14 in section 4.7. The fiber was rolled into 5 mg (± 3 mg) balls to fit into standard aluminum sample pans. Encapsulating press was used to close the pans. The test method included two heating cycles from 0 to 200 °C at the rate of 20 °C/min. X_c was calculated using equation (2):

$$\frac{\Delta H_{melting}}{93.7\ J/g} \times 100\,\%\ , \tag{2}$$

where $\Delta H_{melting}$ is melting enthalpy obtained from the melting peak in the DSC thermogram and 93.7 J/g is melting enthalpy value for 100 % crystalline PLLA. Two parallel samples were used.

DSC samples were removed from the test tubes at set time points and washed with distilled water. After washing the samples were dried in a fume hood overnight and stored in vacuum for several days before packing into sealed plastic pouches. Samples from the first six time points were analyzed together and the samples from the last time point separately.

4.8 In vitro cell culture study

The *in vitro* cell culture study was conducted in the Adult Stem Cell Research group laboratories at the Institute of Biosciences and Medical Technology (BioMediTech), University of Tampere. Two types of cryopreserved human cells were used in the study, human urothelial cells (hUC) and human foreskin fibroblasts (hFF). The isolation of hUCs from patients was performed as previously described by Sartoneva et al. in 2011 [56]. hUCs from passage 5 were used in this study. The hFFs, passage 14, were from CCD-1112Sk CRL-2429 cell line by ATTC (Manassas, United States).

Cryopreserved cells were taken from nitrogen gas phase storage and thawed in a 37 °C water bath. Dimethyl sulfoxide as used as a cryoprotectant in the freezing solution. Immediately after thawing the cells were suspended into cell culture medium, centrifuged 5 min at 1000 rpm, again suspended into cell culture medium and transferred into T75 cell culture flasks by Nunc (Roskilde, Denmark). The cells were incubated in humidified atmosphere at 37 °C with 5 % CO_2 in Forma Steri-Cycle i160 CO_2 incubator by Thermo Fisher Scientific for 48 h. The hUCs were passaged by washing the cells in each bottle with 5 ml of Gibco Hank's Balanced Salt Solution (HBSS) by Thermo Fisher Scientific and detaching the cells with 3 ml of Gibco TrypLE Select enzymes by Thermo Fisher Scientific. The hFFs were passaged similarly, except Dulbecco's Phosphate Buffered Saline by Lonza (Verviers, Belgium) was used for washing instead of HBSS. The cells were incubated with the enzymes for 5–10 min. 5 ml of sterile filtrated 10 % Human Serum in HBSS was used to inactivate the enzymes in each flask. The suspensions were collected into two bottles, one for each cell type and centrifuged at 1000 rpm for 5 min. The formed cell pellets were suspended in cell culture mediums. Epilife Calcium-free cell culture medium base by Life Technologies (Carlsbad, United States) supplemented with penicillin and streptomycin antibiotics by Lonza, 1 % EpiLife Defined Growth Supplement by Life Technologies and 0.1 % 0.06 M $CaCl_2$ by Life Technologies was used for hUCs. DMEM/F-12 medium base by Thermo Fisher Scientific supplemented with 5 % human serum, 1 % penicillin and streptomycin antibiotics and 1 % GlutaMAX L-glutamine by Thermo Fisher Scientific for the hFFs. A Bürker chamber was used to count the cells.

Pre-wetted scaffolds were inserted into Nunclon delta 24 well multidishes by Nunc. 2 parallel samples were used from each fabric type for both cell types. 50 µl of cell suspension was pipetted on the top of each scaffold 2 hours before adding 1 ml of cell culture medium to each well, supplemented Epilife for hUCs and supplemented DMEM/F-12 for

hFFs. This seeding procedure allowed the cells to attach better to the scaffolds before the mediums were added. 50 µl of cell suspension corresponds to 40 703 hUCs cells and 50 000 hFFs. The cells were incubated at 37 °C with 5 % CO_2. The mediums were changed every 3–4 days. Cell viability and distribution was qualitatively analyzed and micrographs were taken after 1, 4, 7 and 14 days of cell culture.

4.8.1 Pre-wetting of the scaffolds

The textile scaffolds were pre-wetted in cell culture medium 48 h before seeding to increase hydrophilicity of the biomaterial. Scaffolds were assorted to 50 ml falcon tubes by type of scaffold. 10 ml of medium was added to each tube. Trapped air was removed from the scaffolds by tapping the tubes against a table until the scaffolds remained submerged. The tubes were stored in an incubator at 37 °C until the cell seeding.

4.8.2 Cell viability and distribution

Cell viability and distribution on the surfaces of the scaffolds was qualitatively assessed after 1, 4, 7 and 14 days of cell culture. On days 1, 7 and 14 Live/Dead staining was used and on day 4 crystal violet staining. Micrographs were taken for evaluation. Total of 24 samples were used, 2 parallel samples from each fabric type for both cell types.

For Live/Dead staining a LIVE/DEAD Viability/Cytotoxicity Kit for mammalian cells by Invitrogen Molecular Probes (Eugene, United States) was used. Two probes are used in this method, calcein acetoxymethyl ester (CAM) to produce green fluorescence and ethidium homodimer-1 (EthD-1) for red fluorescence. Cell culture medium was removed from the wells and 1 ml of DPBS (Dulbecco's Phosphate-Buffered Saline) was added to wash the scaffolds. A working solution containing 0.036 µM EthD-1 and 0.5 µM CAM in DPBS was prepared and used to replace the DPBS in the wells. The seeded scaffolds in the working solution were dark incubated at room temperature on a slow tilt shaker for 30 min. Working solution was removed and replaced with DPBS. Scaffolds were transferred to clean wells containing 1 ml DPBS each for viewing and imaging. Images were taken with an IX51 fluorescence microscope by Olympus (Tokyo, Japan) and DP30BW camera by Olympus. Live cells were shown in green and dead cells in red.

For crystal violet staining, the cell culture medium was removed from the wells and replaced with DPBS to wash the scaffolds. A fixing solution was prepared by diluting glutaraldehyde to 5 % using DPBS. The fixing solution was pipetted into the wells after removing DPBS and incubated for 30 min to fix the live cells. After the fixing solution was removed, the scaffolds were washed twice with type II water. 0.1 % crystal violet dye was filtrated through paper and added to the wells after washing to be incubated for 20 min. The scaffolds were gently washed with type II water until no dye was visible in the water and allowed to dry. For micrography, the scaffolds were transferred to clean

wells. Two microscopes and cameras were used to take images: (*i*) Axio Vert.A1 microscope, AxioCam MRc5 camera and Zen Blue Edition software, all by Zeiss and (*ii*) 475110 – 9904 microscope by Zeiss, BUC4-500C camera by BestScope and ISCapture software by Tucsen.

5. RESULTS AND DISCUSSION

The results and discussion chapter is divided into three sections. The first section presents the fiber and scaffold properties along with the results from the recovery after heat treatment and the swelling in cell culture medium studies. The second section covers the hydrolytic degradation studies including tensile testing and DSC analysis. In the last section, the results from the *in vitro* cell culture study with hUCs and hFFs are presented.

5.1 Textile scaffolds

Experiments were performed to study the scaffolds behavior during heat processing and cell culture study. General properties of the fibers, textiles and scaffolds are presented in the following subsections.

5.1.1 Fiber and textile properties

The melt spun 4-filament PLDLA 96/4 fibers used in the scaffolds had an average diameter of 44 µm, when individual measurements ranged from 33 µm to 52 µm (n = 40). The cross-sectional shape of the fibers was round. General properties of the textiles used in the scaffolds can be found in Table 17. The textiles used in scaffold manufacturing are shown in Figure 36.

Table 17. *Properties of textiles used for PLDLA 96/4 scaffolds.*

Textile type	Filament count	Min. pore size (mm^2)	Max. Pore size (mm^2)	Ave. pore size (mm^2)	Braid angle (°)
Braided	8	0.001	0.027	0.014	37
Knitted	4	0.164	0.539	0.352	N/A
Woven	4	0	0	0	N/A

Textile type	Loop length (mm)	Courses/cm	Wales/cm	Warp density (yarns/cm)	Weft density (yarns/cm)
Braided	N/A	N/A	N/A	N/A	N/A
Knitted	6	5	12	N/A	N/A
Woven	N/A	N/A	N/A	22	116

A great difference was seen between the pore sizes of the textiles. The woven fabrics were so dense that no pores was clearly visible when observing with a microscope. Transparency of the fibers and shadows made it impossible to confirm if there where were very small pores present. Pores in the knitted fabric were easily visible to the naked eye, as

were the largest pores in the braided structures. As can be seen in Figure 36, the loops in the knits were vastly larger than in other textile types.

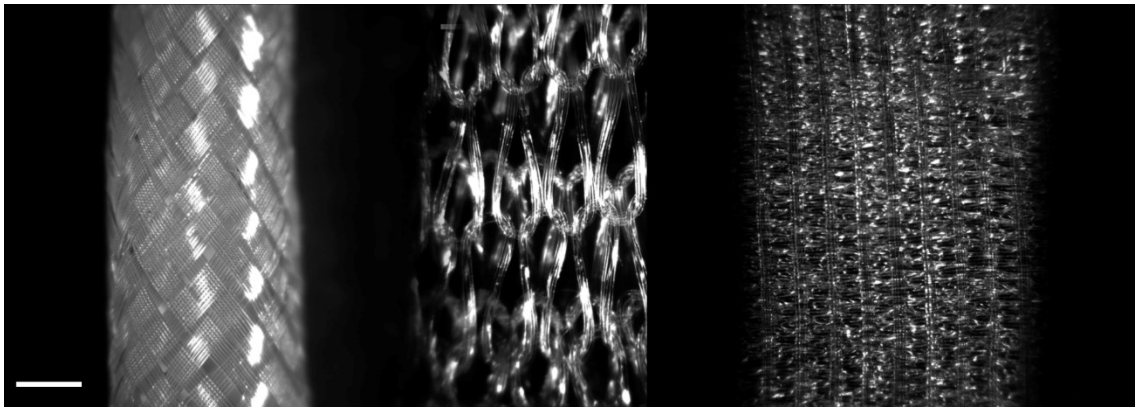

Figure 36. *From left to right: braided, knitted and woven PLDLA 96/4 textiles before processing. Knitted and woven structures are not shown in their complete width. Scale bar 1 mm.*

From these three manufacturing methods and associated devices, braiding provided the most control over the pore size, while weaving provided practically no control. The knits were manufactured with the smallest loop size possible, but the difference in pore sizes between the textile types remained large. The pore size in the braids was chosen to be between the pore sizes of the knits and the woven fabrics. It would have been desirable to manufacture structures with more uniform pore sizes for this study. The combination of this yarn and the used manufacturing devices limited the possibilities in this regard.

5.1.2 Recovery after heat treatment and compression

The recovery study showed that all scaffold types remained very well in their compressed state after the heat treatment and compression as can be seen in Figure 37. After the heat treatment and compression, the greatest change was observed in thickness of the scaffolds. The changes in length and width remained within a few percent range.

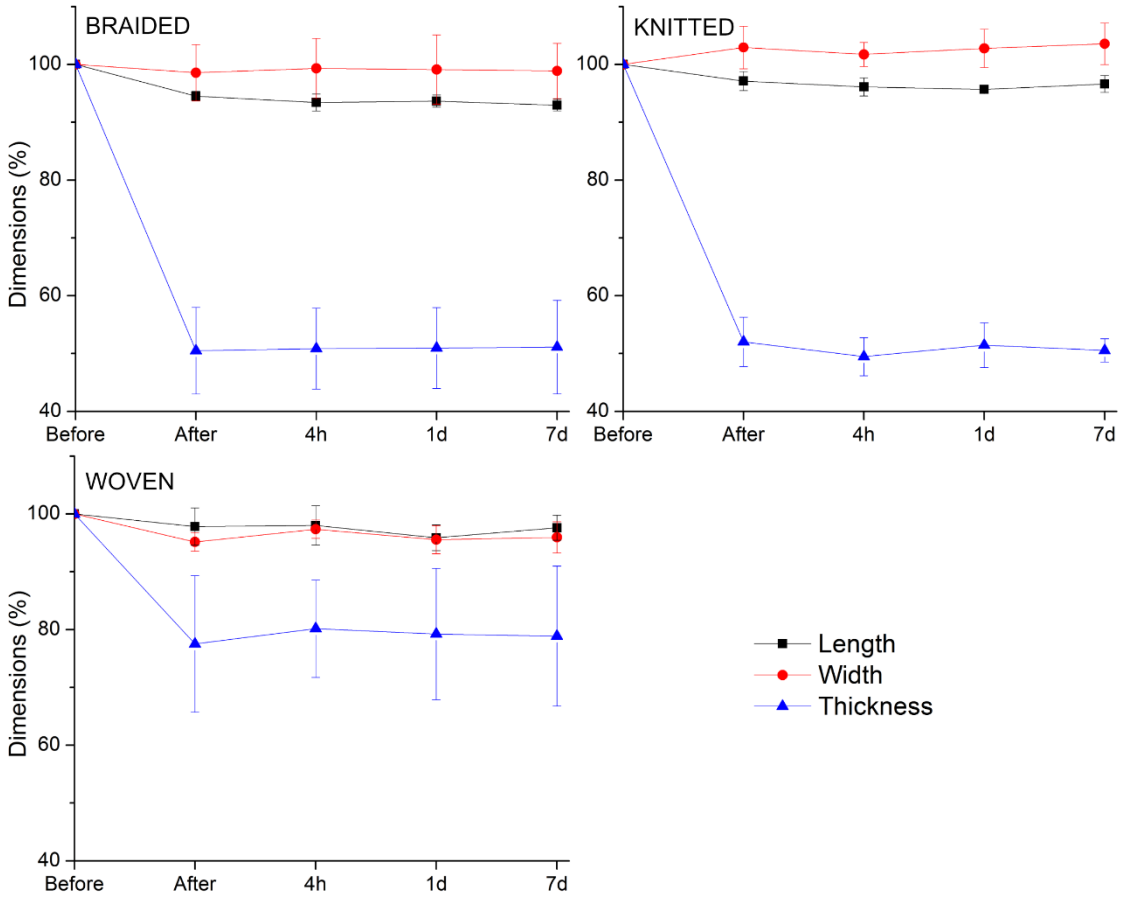

Figure 37. *Recovery of PLDLA 96/4 scaffolds after heat treatment. N = 4.*

The results suggested that the dimensions of the scaffolds would not change significantly between the heat treatment process and the cell culture study. For the separately manufactured cell culture scaffolds the time between the heat treatment and cell seeding was 6 weeks. During this period, the scaffolds were gamma irradiated.

5.1.3 Swelling in cell culture medium

Figure 38 shows the woven scaffolds to experience the least changes in dimensions. The values stayed very close to the initial measurements throughout the 1-week experiment. In braided and knitted scaffolds, the changes were larger, especially in thickness. The less dense structure of the braided and knitted scaffolds allows the cell culture medium to penetrate more easily and in larger volumes. Still, the change was barely visible to the naked eye and was not significant for cell culture purpose.

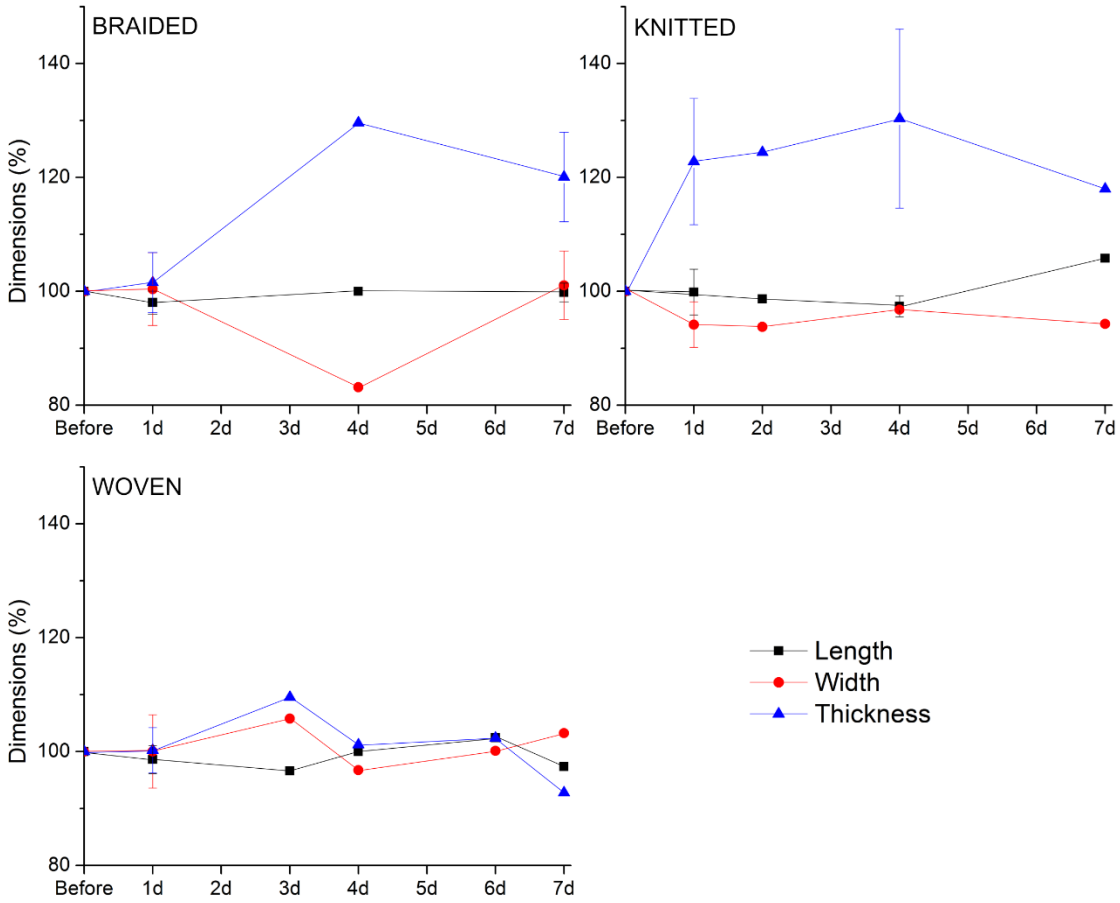

Figure 38. *Swelling of PLDLA 96/4 scaffolds in DMEM/F-12 cell culture medium after heat treatment. N = 4.*

As stated in the materials and methods section, contaminated scaffolds were removed on the day of observation and measured. For this reason, some time points contain measurements from only one sample and therefore do not have standard deviation error bars present in Figure 38. After 2 days one knitted scaffold was removed, after 3 days one woven scaffold, after 4 days one braided, two knitted and one woven scaffold and after 5 days one woven scaffold. Having more parallel samples would have provided more accurate prediction on future behavior, but this study provided enough confidence that swelling would not be an issue during the cell culture study.

5.2 Hydrolytic degradation study of the fibers

A 36-week hydrolytic degradation study was performed for the PLDLA 96/4 fibers. Changes in mechanical properties were studied using a tensile testing method. DSC analysis was performed to measure changes in crystallinity and in thermal properties such as glass transition and melting temperatures. The results are presented and discussed in the following subsections. Determining molecular weight of the samples at each time point would have been desirable, but was not possible due to a malfunctioning gel permeation

chromatography (GPC) device. The molecular weights of polymer chains affect both mechanical and thermal properties of the samples.

5.2.1 Thermal properties

DSC analysis provides information on degradation of the polymer fibers, because decrease in molecular weight is often related to decrease in glass transition and melting temperatures. Unexpectedly, the melting temperature was increased by 2 °C during the 36-week incubation period. In previous studies with irradiated PLDLA 96/4 fibers Ellä et al. reported a decrease of 0.6 °C after 20 weeks [57] and Lyyra a decrease of 0.5 °C after 36 weeks [58]. As is illustrated in Figure 39, the overall changes in the melting temperature were very small. The results from DSC analysis can be found in Appendix C.

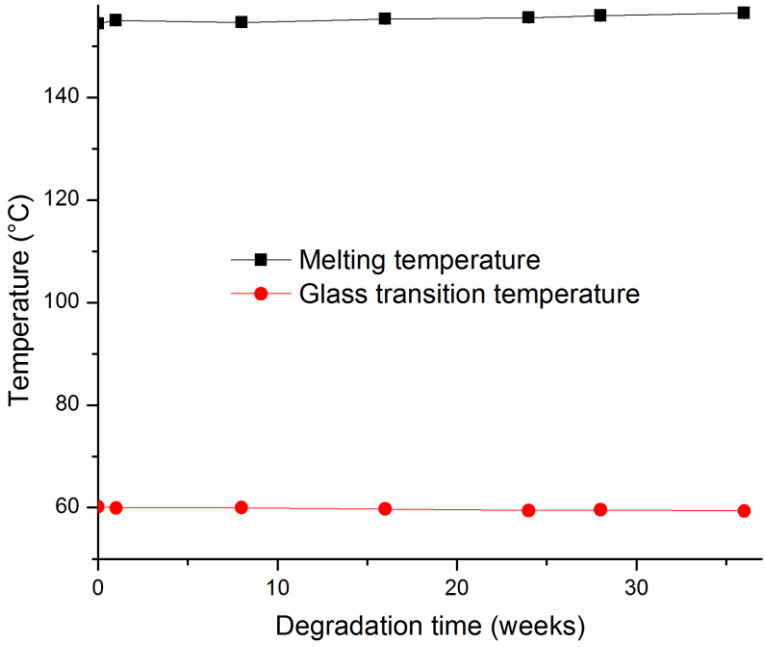

Figure 39. *Glass transition and melting temperatures of irradiated PLDLA 96/4 fibers undergoing hydrolytic degradation. (n = 2)*

The glass transition temperatures slightly decreased during the 36-week incubation period, by 0.9 °C (Figure 39). This corresponds well to results from previous studies. Ellä et al. reported a decrease of 1.6 °C after 20 weeks [57] and Lyyra a decrease of 4.9 °C after 36 weeks [58]. It takes less energy for the materials to change from glassy to rubbery state when the molecular weight of the polymer has decreased. In this regard, the material behaved as expected.

The crystallinity of the PLDLA 96/4 fibers increased from 42.4 % to 44.1 % during the 36-week incubation (Figure 40). The value peaked at 24 weeks reaching 46.0 % if the results from week 28 are dismissed as unreliable. At week 28, measurements from both parallel samples differed a great amount from other measurements. Ellä et al. and Lyyra both reported increased crystallinities in their studies. Ellä et al. 8 % after 20 weeks [57]

and Lyyra 1.9 % after 36 weeks [58]. The initial crystallinity was 37 % in the first mentioned and 41.0 % in the latter.

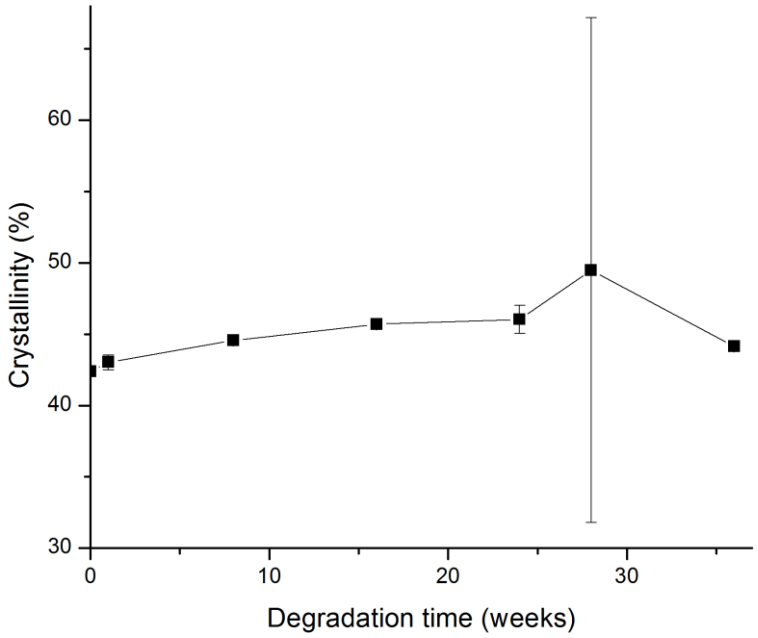

Figure 40. *Crystallinity of irradiated PLDLA 96/4 fibers undergoing hydrolytic degradation. (n = 2)*

Thermograms in Figures 41 and 42 are provided to give more information on changes in thermal properties of the fibers during the hydrolytic degradation study. For both Figures, samples with typical thermogram shapes were chosen from weeks 0, 16 and 36. The melting endotherms in Figure 41 at approximately 155 °C do not change significantly in size or shape during the study. The peaks remain large and narrow. This corresponds well to the small changes in the crystallinity of the fibers. A greater increase in crystallinity would result in melting peaks covering a larger surface area. Thermograms from the first heating cycle were used to measure all melting temperatures and crystallinities of the samples.

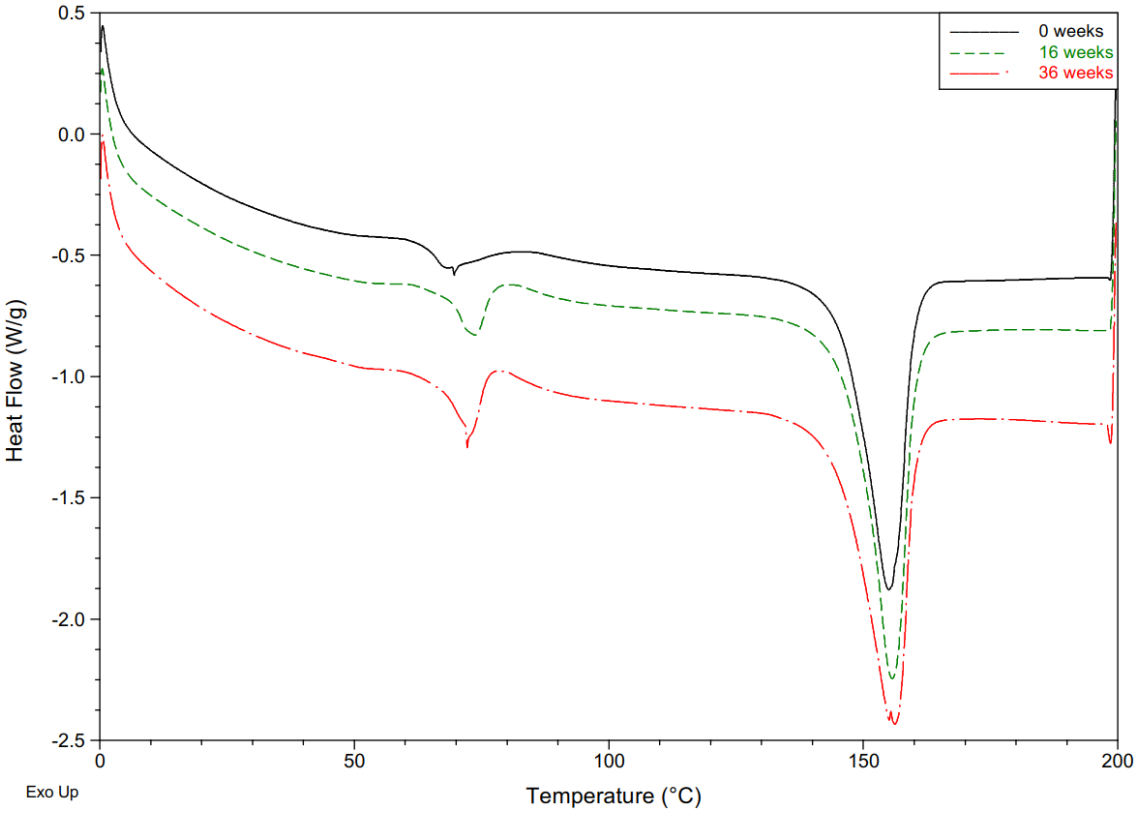

Figure 41. *DSC thermograms from the first heating cycle of irradiated PLDLA 96/4 fibers undergoing hydrolytic degradation.*

Thermograms from the second heating cycle were used to measure the glass transition temperatures of the fibers. Figure 42 shows the shapes of the curves at glass transition to get slightly steeper during the degradation. The size of the peaks also decreases, but both changes are very small. Between 100 °C and 165 °C cold crystallization exotherm can be observed, which is followed by melting peak indicating melting of these crystals. The cooling rate during the analysis is too high to allow crystals to be formed after the first heating cycle. The amorphous structure organizes into crystal structure upon heating during the second cycle and melts subsequently after more energy is applied.

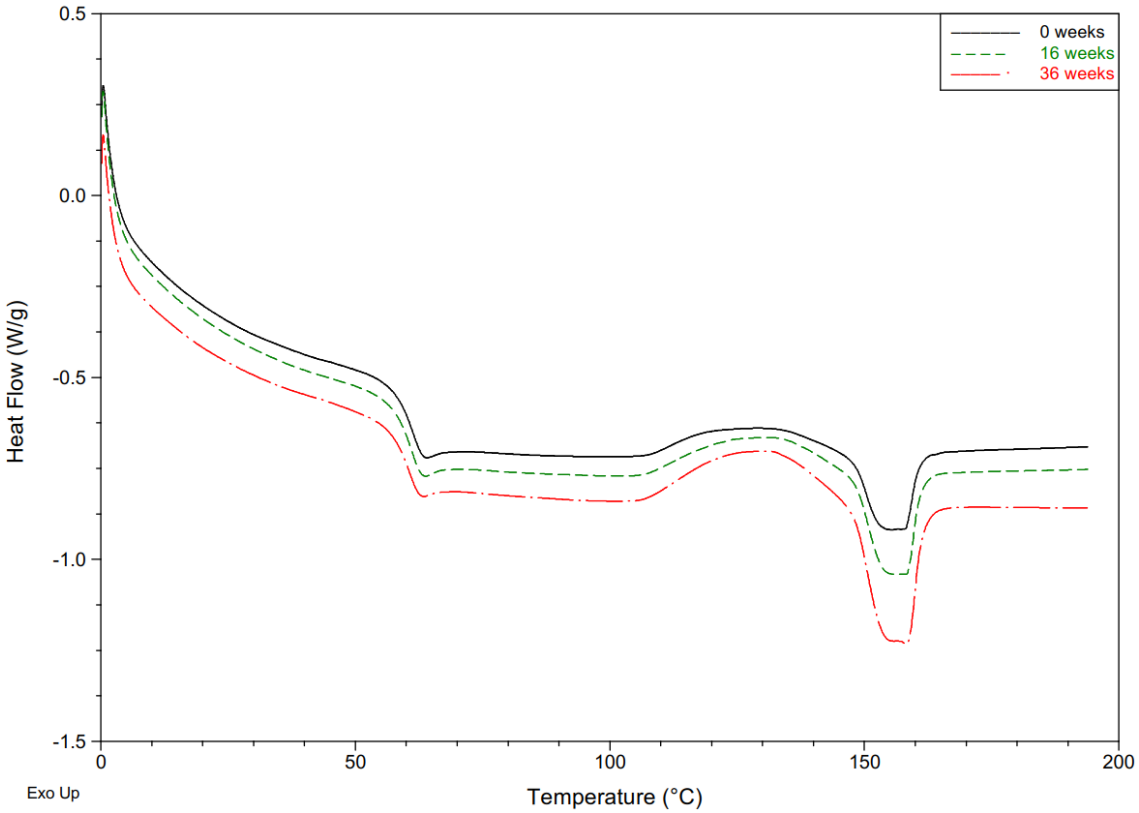

Figure 42. *DSC thermograms from the second heating cycle of irradiated PLDLA 96/4 fibers undergoing hydrolytic degradation.*

The results from DSC analysis are similar to results from previous studies. The slightly upwards trend of melting temperatures during degradation is not a concern, as the difference in comparison to the referenced studies is in range of a few degrees at most. Valuable information on crystallinity was obtained to supplement the results from tensile testing presented in the following subsection.

5.2.2 Mechanical properties

Tensile testing method was used to measure tensile strength and strain at maximum load of the PLDLA 96/4 fibers at each time point of the hydrolytic degradation study. Relative ultimate tensile strength (UTS) is presented in Figure 43 and relative strain at maximum load in Figure 44. The absolute values of the mechanical properties can be found in Appendix D.

The tensile strength is a valuable tool for material performance evaluation as it is related to the cross-sectional area of the sample. During the 36-week hydrolysis study, the average tensile strength decreased to 67 % (201 MPa) of the initial value (299 MPa). Hydrolytic scission of the polymer chains leads to decrease in molecular weight of the polymer, which lowers the mechanical properties. The strength decreased rapidly 20 % during the first 4 weeks of the study. After 20 weeks, the fibers had retained 79 % (235 MPa) of their initial strength, which is higher than 65 % and 66 % reported previously by Ellä et al. [57]

and Lyyra [58]. The results from these studies are not directly comparable, because of differences in processing parameters and raw material properties such as initial molecular weight. Paakinaho et al. have shown the processing temperatures to affect the lactide monomer content of melt-processed PLDLA 96/4. The presence of lactide monomers is a result of thermal degradation of polylactide during extrusion. Degradation rate of the polymer increases with the monomer concentration. [59] The fibers were intact and easy to handle after 36 weeks. The study gives an insight to degradation rate of the fibers, but could still have had continued. In the study by Lyyra, the irradiated fibers did not withstand handling after 28 weeks of hydrolytic degradation as the tensile strength had decreased to 82 % of the initial value [58].

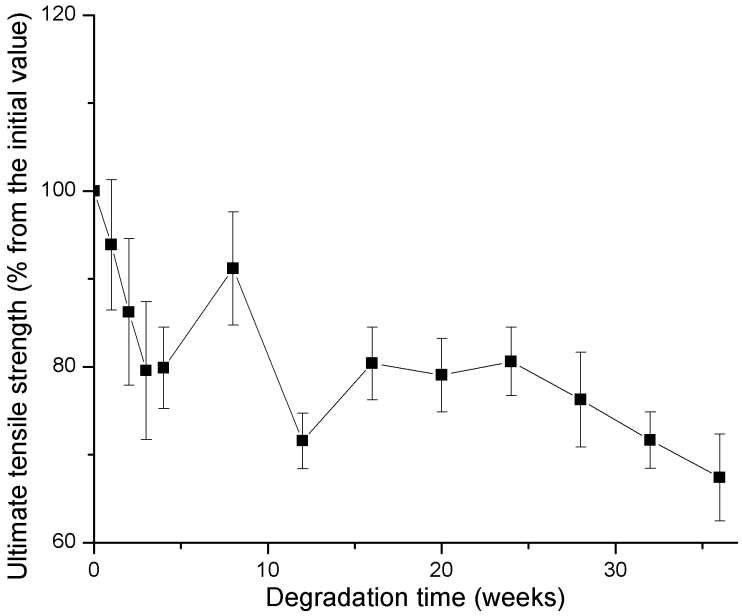

Figure 43. *Ultimate tensile strength retention of irradiated PLDLA 96/4 fibers undergoing hydrolytic degradation. (n = 5–6)*

The relative strain results in Figure 44 show the fibers to have a small degree of upward trend until week 20, after which the strain values begin to decrease. In the study by Ellä et al., a similar trend was seen during the first 20 weeks of hydrolytic degradation [57]. Lyyra demonstrated the strain values to remain close to the initial value until 16 weeks after which a rapid decrease was observed [58]. After 36 weeks, the average strain value had decreased to 91 % of the initial value. The increase of crystallinity observed in the DSC analysis decreases the strain values of the fibers. The changes in the strain at maximum load did not change significantly during the study. This proposes that the study could have had continued beyond 36 weeks as was already suggested when discussing the tensile strength results. It is necessary notice the large standard deviation values in the results, which leads to questioning the reliability of the results.

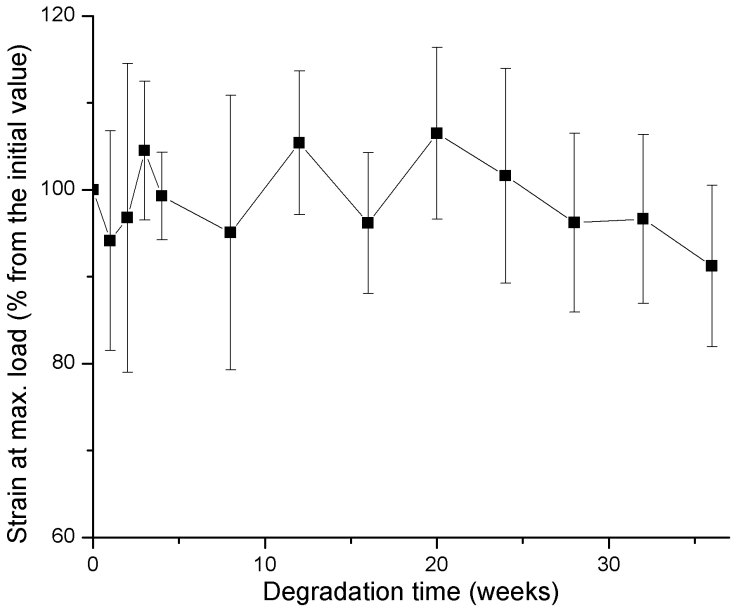

Figure 44. *Changes in strain at maximum load of irradiated PLDLA 96/4 fibers undergoing hydrolytic degradation. (n = 5–6)*

Though the samples were handled with a careful manner, the results can be affected by user- and device-related errors. The first mentioned includes not having the sample fibers at uniform tension between the clamps or having the samples not applied precisely in the tensile testing direction. The fiber bundles had entangled to various degrees in the test tubes. It is possible to cause mechanical stress to the fibers when separating the bundles for testing. Slipping of the fiber between the clamps may occur during testing, which is an example of a device-related error. Because of not double checking the test program settings before each test, in the last three time points an incorrect crosshead speed value 10 000 mm/s was used. Lower speed may lead to increased strain values and decreased strength values [60].

5.3 In vitro cell culture studies

The viability and distribution of hUCs and hFFs on PLDLA 96/4 textile scaffolds was studied using Live/Dead and crystal violet staining methods. In Live/Dead images live cells are shown in green and dead cells in red. Images taken from crystal violet stained cells show live cells in violet. Throughout the experiment, a large amount of live cells was seen spread on bottoms of the wells. Both sides of the scaffolds were inspected at each time point and images taken from the top surfaces where the cells were initially seeded.

5.3.1 Cell viability and distribution in vitro

Figure 45 shows that all PLDLA 96/4 textile scaffold types supported hUC viability. On day 1, very few cells were found attached to the scaffolds. On day 7, the amount of attached cells had significantly increased on all scaffold types. Only the knitted scaffolds did not experience clear increase in the amount of attached hUCs between days 7 and 14. Red glow and small dots were present in some images, such as woven scaffold on day 14 in Figure 45. One confirmed dead cell was found on a braid on day 1.

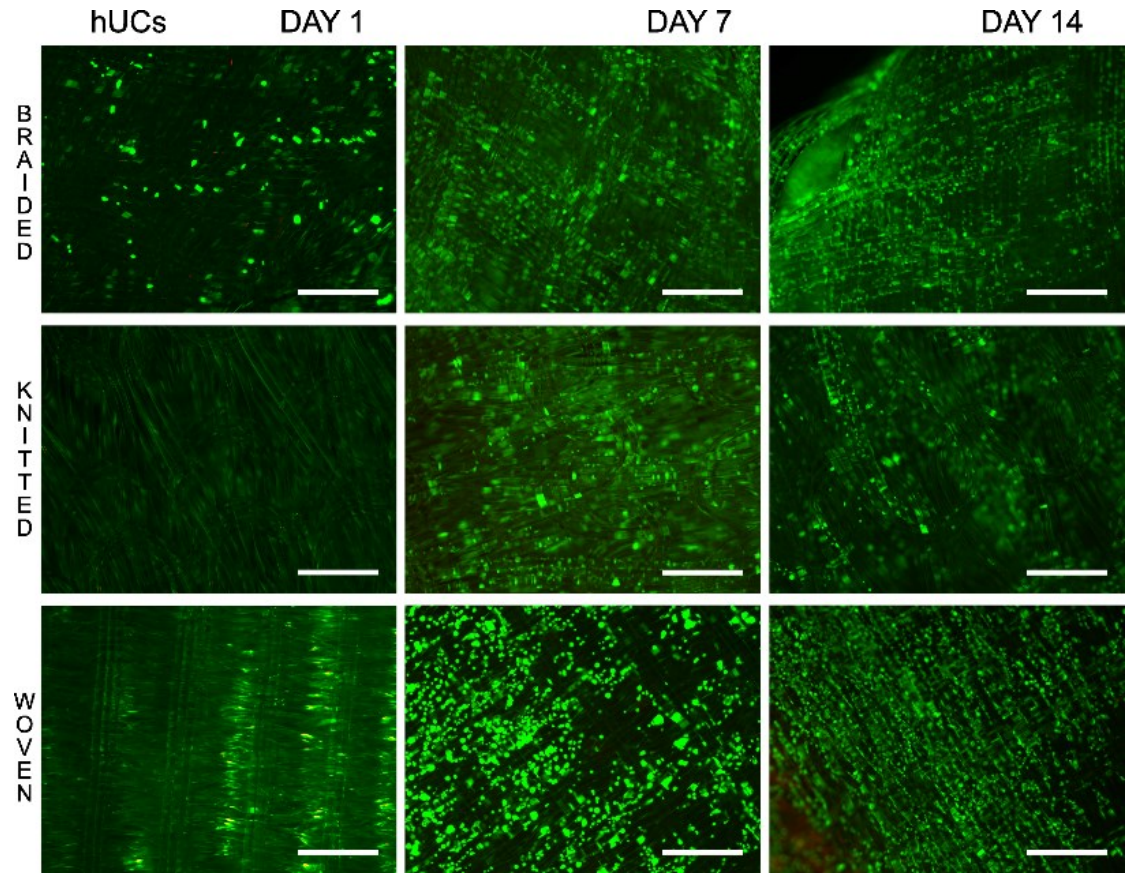

Figure 45. *Viability and distribution analysis of hUCs on PLDLA 96/4 textile scaffolds using fluorescent staining method. Scale bars 500 µm.*

On the top surfaces of the braided and knitted scaffolds, the hUCs seem to prefer the sides of the fibers pointing down inside the scaffold. On the woven scaffolds the cells have attached to all visible sides of the fibers. Because of the large pores in the knitted scaffolds, cells can be seen growing inside the scaffolds on days 7 and 14. On top surfaces braided and knitted scaffolds, hUCs do not prefer any specific sites. On woven scaffolds more cells are attached to the weft yarns than to the warp yarns as can be best seen in the image taken on day 14 (Figure 45). The knitted scaffolds had the smallest number of cells attached to the fibers after 2 weeks. Having significantly larger pores than the other scaffolds seems to be a disadvantage.

The PLDLA 96/4 textile scaffolds supported viability of hFFs as can be seen in the fluorescent images in Figure 46. On the first day, the shape of the attached cells is mostly round on all scaffold types. The area covered by cells increases significantly from day 1 to day 7 for all scaffold types and the cells take a longer shape. On day 14, the cells almost completely covered the top surfaces of the braided and woven scaffolds, while the large pores of the knitted structures remain mostly cell-free. Up to approximately 200 µm long fibroblast bridges were formed in braids and knits. Only four dead cells were found. On braided scaffolds at days 1 and 14 and on a woven scaffold at day 7.

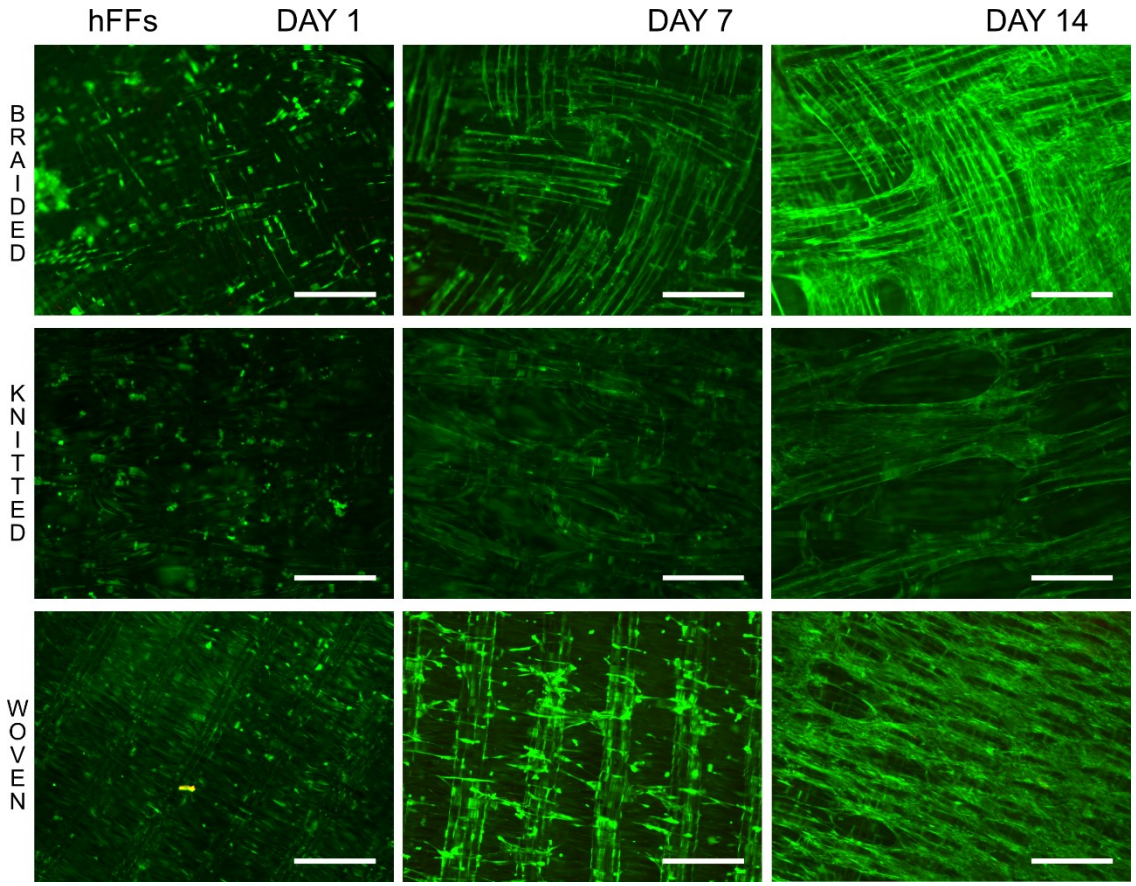

Figure 46. *Viability and distribution analysis of hFFs on PLDLA 96/4 textile scaffolds using fluorescent staining method. Scale bars 500 µm.*

On day 1, the hFFs did not prefer any specific sites on any of the scaffold types. One week after seeding, there were more cells in cavities between the fibers of braided and woven structures than on the outermost surface of the fibers. On day 14, this can be still seen in the woven scaffold in Figure 46 where the highest ridges of the weft yarns are cell-free while the rest of the scaffolds surface is covered in cells. After 2 weeks of cell culture, the braided and knitted scaffolds were almost completely covered in cells and no preference of site for the cells to attach could be seen.

In the crystal violet staining images (Figure 47), hUCs are shown as dark dots on the top surfaces of the scaffolds. A small amount of cells has attached to all scaffold types. In braided and woven scaffolds, the cells did not prefer any sites. The knitted scaffolds had

slightly more cells attached to the long straight parts of the loops than to other parts. The same observation was made from images taken from one layer below the top through the loops.

The hFFs in Figure 47 can be seen as elongated dark areas often spreading over up to several fibers, as best seen in images taken of knitted and woven scaffolds. A small amount of cells was found attached to all scaffold types. No clear preference over attachment site was seen in any of the scaffold types. The dark background and the shadows make observing hFFs on the scaffolds challenging.

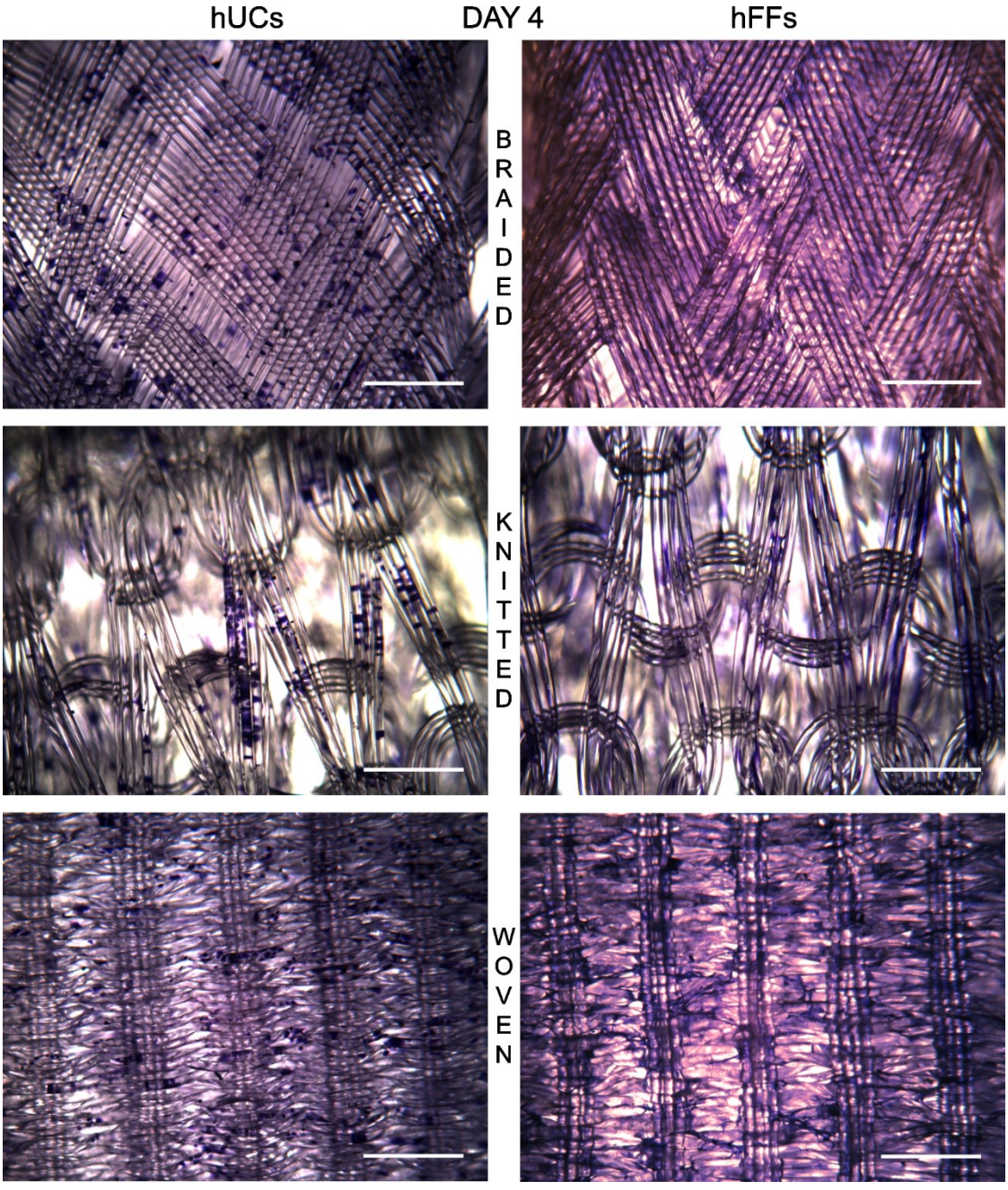

Figure 47. *Viability and distribution analysis of hUCs and hFFs on PLDLA 96/4 textile scaffolds using crystal violet staining method. Scale bars 500 µm.*

Fluorescence and crystal violet staining viability studies showed that PLDLA 96/4 scaffolds supported cell attachment for both hUCs and hFFs. Only a few dead cells were found in the fluorescence images throughout the study. There were no strong implications of the cells preferring any textile type or type-specific site for attachment. The number of attached cells was affected more by the pore sizes. The hUCs did not cover any pores and hFFs did not cover the largest pores in the range of hundreds of micrometers. Both cell types, especially hFFs, preferred pits to ridges. From the two staining techniques used in this experiment, the fluorescence imaging gave a better insight on cell viability and distribution as the images were more suitable for visual analysis. From the crystal violet staining images, it was difficult to separate cells from other dark areas.

6. CONCLUSIONS

The aim of this thesis was to compare cell distribution and viability on textile scaffolds for tissue engineering applications. For the cell culture experiment with hFFs and hUCs, PLDLA 96/4 fibers were manufactured using melt spinning method. The fibers were used as 4- or 8-ply bundles and processed into three types of textile scaffolds: (i) braided, (ii) knitted and (iii) woven. The multi-layered scaffolds were heat treated under compression to have similar thicknesses and sterilized with gamma irradiation.

A 36-week *in vitro* hydrolytic degradation study was conducted for the fibers. DSC was used to observe changes in thermal properties and crystallinity. Tensile testing method was used to evaluate mechanical properties during degradation. A slight increase in melting temperature was observed, which was not expected based on previous studies. The glass transition temperature decreased, similar to previous studies with PLDLA 96/4 fibers. A few percent increase in crystallinity was seen during the degradation study. Decreasing molecular weight increases chain mobility allowing crystals to be formed more easily. Tensile testing experiment showed the ultimate tensile strength of the fibers to decrease during degradation. The changes were rapid during the first three weeks, followed by an overall decreasing trend. The lowest strength values were obtained at the final 36-week time point as expected. Strain at maximum load decreased as well. The changes in mechanical properties are related to the increased crystallinity, which makes the fibers more brittle. Determining molecular weight of the samples at each time point would have been desirable. The molecular weights of polymer chains affect both mechanical and thermal properties of the samples.

To ensure predictable behavior of the scaffolds during the cell culture experiment, the sterilized scaffolds were tested for dimensional stability after heat treatment and in cell culture medium. Both tests showed the scaffolds to retain their shape and dimensions adequately.

The cell culture experiment demonstrated good cell viability for both cell types on all scaffold types. Based on visual inspection from microscopic images, the number of hUCs increased throughout the 2-week test period on braided and woven scaffolds. On knitted scaffolds, the largest number was reached after 1 week of incubation. At the last time point, the knitted scaffolds had the least attached cells. This is due to much larger pores than the other scaffold types had. The number of hFFs increased on all scaffold types during the test period. On day 7, the cells preferred sites between the fibers. On day 14, the fibers on braided and knitted samples were fully covered with cells. Only the pores, especially the largest on knitted scaffolds, remained cell free. On woven scaffolds, only the highest ridges of weft yarn fibers remained uncovered. As a conclusion, both cell

types preferred structures with small pores or no visible pores. In addition, the cells preferred to attach to pits instead of ridges. This was the most evident with hFFs.

The experiments conducted for this thesis demonstrated that PLDLA 96/4 fiber bundles can be processed into biodegradable braided, knitted and woven textile scaffolds. These structures support viability of cells *in vitro*. The number of attached cells was the largest in braided and woven structures that had significantly smaller pores in comparison to knitted scaffolds.

REFERENCES

[1] M.W. King, B.S. Gupta, R. Guidoin, Biotextiles as medical implants, Woodhead Publishing Limited, United Kingdom, 2013, 700 p.

[2] M. Martina, D.W. Hutmacher, Biodegradable polymers applied in tissue engineering research: a review, Polymer International, Vol. 56, No. 2, 2007, pp. 145-157.

[3] S. Ramakrishna, Textile scaffods in tissue engineering, in: T. Xiaoming (ed.), Smart Fibres, Fabrics and Clothing: Fundamentals and Applications, Woodhead Publishing Limited and The Textile Institute, United Kingdom, 2001, pp. 291-313.

[4] B.S. Gupta, Manufacture, types and properties of biotextiles for medical applications, in: M.W. King, B.S. Gupta, R. Guidoin (ed.), Biotextiles as medical implants, Woodhead Publishing Limited, Cambridge, UK, 2013, pp. 3-47.

[5] Z.E. Karamuk, Embroidered Textiles for Medical Applications: New Design Criteria with Respect to Structural Biocompatibility, Doctoral Thesis, Swiss Federal Institute of Technology, Zürich, 2001, 161 p. Available: http://e-collection.library.ethz.ch/eserv/eth:24313/eth-24313-02.pdf.

[6] D. Tessier, Surface modification of biotextiles for medical applications, in: M.W. King, B.S. Gupta, R. Guidoin (ed.), Biotextiles as medical implants, Woodhead Publishing Limited, Cambridge, UK, 2013, pp. 137-156.

[7] K. Torikai, H. Ichikawa, K. Hirakawa, G. Matsumiya, T. Kuratani, S. Iwai, A. Saito, N. Kawaguchi, N. Matsuura, Y. Sawa, A self-renewing, tissue-engineered vascular graft for arterial reconstruction, Journal of Thoracic and Cardiovascular Surgery, Vol. 136, No. 1, 2008, pp. 37-46.

[8] S. Iwai, Y. Sawa, S. Taketani, K. Torikai, K. Hirakawa, H. Matsuda, Novel tissue-engineered biodegradable material for reconstruction of vascular wall, Annals of Thoracic Surgery, Vol. 80, No. 5, 2005, pp. 1821-1827.

[9] S. Farè, P. Torricelli, G. Giavaresi, S. Bertoldi, A. Alessandrino, T. Villa, M. Fini, M.C. Tanzi, G. Freddi, In vitro study on silk fibroin textile structure for Anterior Cruciate Ligament regeneration, Materials Science and Engineering C, Vol. 33, No. 7, 2013, pp. 3601-3608.

[10] A. Hegewald, F. Medved, D. Feng, C. Tsagogiorgas, A. Beierfuss, G. Schindler, M. Trunk, C. Kaps, D. Mern, C. Thome, Enhancing tissue repair in annulus fibrosus defects of the intervertebral disc: analysis of a bio-integrative annulus implant in an in-vivo ovine model, Journal of Tissue Engineering and Regenerative Medicine, Vol. 9, No. 4, 2015, pp. 405-414.

[11] G. Zund, C. Breuer, T. Shinoka, P. Ma, R. Langer, J. Mayer, J. Vacanti, The in vitro construction of a tissue engineered bioprosthetic heart valve, European journal of cardio-thoracic surgery, Vol. 11, No. 3, 1997, pp. 493-497.

[12] H. Fan, H. Liu, S.L. Toh, J.C. Goh, Anterior cruciate ligament regeneration using mesenchymal stem cells and silk scaffold in large animal model, Biomaterials, Vol. 30, No. 28, 2009, pp. 4967-4977.

[13] N. Kawazoe, C. Inoue, T. Tateishi, G. Chen, A cell leakproof PLGA-collagen hybrid scaffold for cartilage tissue engineering, Biotechnology progress, Vol. 26, No. 3, 2010, pp. 819-826.

[14] R. Birla, Introduction to tissue engineering: applications and challenges, Wiley, USA, 2014, 327 p.

[15] W. Wu, X. Feng, X. Feng, T. Mao, H. Ouyang, G. Zhao, F. Chen, Engineering of human tracheal tissue with collagen-enforced poly-lactic-glycolic acid non-woven mesh: A preliminary study in nude mice, British Journal of Oral & Maxillofacial Surgery, Vol. 45, No. 4, 2007, pp. 272-278.

[16] G. Shen, H.C. Tsung, C.F. Wu, X.Y. Liu, X. Wang, W. Liu, L. Cui, Y.L. Cao, Tissue engineering of blood vessels with endothelial cells differentiated from mouse embryonic stem cells, Cell Research, Vol. 13, No. 5, 2003, pp. 335-341.

[17] C.M. Haslauer, A.K. Moghe, J.A. Osborne, B.S. Gupta, E.G. Loboa, Collagen–PCL Sheath–Core Bicomponent Electrospun Scaffolds Increase Osteogenic Differentiation and Calcium Accretion of Human Adipose-Derived Stem Cells, Journal of Biomaterials Science, Vol. 22, No. 13, 2011, pp. 1695-1712.

[18] K. Hemmrich, J. Salber, M. Meersch, U. Wiesemann, T. Gries, N. Pallua, D. Klee, Three-dimensional nonwoven scaffolds from a novel biodegradable poly(ester amide) for tissue engineering applications, Journal of Materials Science: Materials in Medicine, Vol. 19, No. 1, 2008, pp. 257-267.

[19] S. Rajendran, S.C. Anand, Hi-tech textiles for interactive wound therapies, in: V.T. Bartels (ed.), Handbook of Medical Textiles, Woodhead Publishing, Cambridge, United Kingdom, 2011, pp. 38-105.

[20] H. Dabiryan, M.S. Johari, Analysis of the tensile behavior of tubular braids using energy method, part I: theoretical analysis, The Journal of The Textile Institute, Vol. 107, No. 5, 2016, pp. 553-561.

[21] C.T. Laurencin, J.W. Freeman, Ligament tissue engineering: an evolutionary materials science approach, Biomaterials, Vol. 26, No. 36, 2005, pp. 7530-7536.

[22] K. Bilisik, Multiaxis Three Dimensional (3D) Woven Fabric, in: S. Vassiliadis (ed.), Advances in Modern Woven Fabrics Technology, InTech, 2011, pp. 79-106.

[23] E. Karamuk, J. Mayer, Embroidery based vital/avital composites for tissue engineering, 13th International Conference on Composite Materials, Beijing, China, June 2001, pp. 1-7.

[24] B. Selm, B. Bischoff, R. Seidl, Embroidery and smart textiles, in: T. Xiaoming (ed.), Smart Fibers, Fabrics and Clothing: Fundamentals and Applications, Woodhead Publishing, Cambridge, United Kingdom, 2001, pp. 218-225.

[25] C. Rentsch, B. Rentsch, S. Heinemann, R. Bernhardt, B. Bischoff, Y. Förster, D. Scharnweber, S. Rammelt, ECM Inspired Coating of Embroidered 3D Scaffolds Enhances Calvaria Bone Regeneration, BioMed Research International, 2014, pp. 1-15. Available (accessed 31.8.2016): https://www.hindawi.com/journals/bmri/2014/217078/.

[26] L.S. Nair, C.T. Laurencin, Biodegradable polymers as biomaterials, Progress in Polymer Science, Vol. 32, No. 8, 2007, pp. 762-798.

[27] Y. Cao, B. Wang, Biodegradation of silk biomaterials, International journal of molecular sciences, Vol. 10, No. 4, 2009, pp. 1514-1524.

[28] J.J. Alm, J. Frantzén, N. Moritz, P. Lankinen, M. Tukiainen, M. Kellomäki, H.T. Aro, In vivo testing of a biodegradable woven fabric made of bioactive glass fibers and PLGA80—a pilot study in the rabbit, Journal of Biomedical Materials Research Part B: Applied Biomaterials, Vol. 93, No. 2, 2010, pp. 573-580.

[29] S.L. Edwards, J.S. Church, J.A. Werkmeister, J.A. Ramshaw, Tubular micro-scale multiwalled carbon nanotube-based scaffolds for tissue engineering, Biomaterials, Vol. 30, No. 9, 2009, pp. 1725-1731.

[30] E. Ten Hallers, J.A. Jansen, H.A. Marres, G. Rakhorst, G.J. Verkerke, Histological assessment of titanium and polypropylene fiber mesh implantation with and without fibrin tissue glue, Journal of Biomedical Materials Research Part A, Vol. 80, No. 2, 2007, pp. 372-380.

[31] J.C. Middleton, A.J. Tipton, Synthetic biodegradable polymers as orthopedic devices, Biomaterials, Vol. 21, No. 23, 2000, pp. 2335-2346.

[32] P.B. Maurus, C.C. Kaeding, Bioabsorbable implant material review, Operative Techniques in Sports Medicine, Vol. 12, No. 3, 2004, pp. 158-160.

[33] V.R. Sastri, Other Polymers: Styrenics, Silicones, Thermoplastic Elastomers, Biopolymers, and Thermosets, in: V.R. Sastri (ed.), Plastics in Medical Devices - Properties, Requirements, and Applications, 2nd edition ed., Elsevier Inc., Waltham, USA, 2014, pp. 215-261.

[34] J. Nieuwenhuis, Synthesis of polylactides, polyglycolides and their copolymers, Clinical Materials, Vol. 10, No. 1, 1992, pp. 59-67.

[35] P. Gentile, V. Chiono, I. Carmagnola, P.V. Hatton, An overview of poly (lactic-co-glycolic) acid (PLGA)-based biomaterials for bone tissue engineering, International journal of molecular sciences, Vol. 15, No. 3, 2014, pp. 3640-3659.

[36] M.D. Yoon, J.P. Fisher, Polymeric Scaffolds for Tissue Engineering Applications, in: J.P. Fisher, A.G. Mikos, J.D. Bronzino (ed.), Tissue Engineering, CRC Press, Boca Ranton, Florida, USA, 2007, pp. 8:1-8:18.

[37] J.P. Penning, H. Dijkstra, A.J. Pennings, Preparation and properties of absorbable fibres from l-lactide copolymers, Polymer, Vol. 34, No. 5, 1993, pp. 942-951.

[38] A. Gupta, V. Kumar, New emerging trends in synthetic biodegradable polymers–Polylactide: A critique, European polymer journal, Vol. 43, No. 10, 2007, pp. 4053-4074.

[39] J.E. Bergsma, W. De Bruijn, F. Rozema, R. Bos, G. Boering, Late degradation tissue response to poly (L-lactide) bone plates and screws, Biomaterials, Vol. 16, No. 1, 1995, pp. 25-31.

[40] R.P. Brannigan, A.P. Dove, Synthesis, properties and biomedical applications of hydrolytically degradable materials based on aliphatic polyesters and polycarbonates, Biomaterials science, Vol. 5, No. 1, 2017, pp. 9-21.

[41] H.K. Makadia, S.J. Siegel, Poly lactic-co-glycolic acid (PLGA) as biodegradable controlled drug delivery carrier, Polymers, Vol. 3, No. 3, 2011, pp. 1377-1397.

[42] R.A. Miller, J.M. Brady, D.E. Cutright, Degradation rates of oral resorbable implants (polylactates and polyglycolates): rate modification with changes in PLA/PGA copolymer ratios, Journal of Biomedical Materials Research Part A, Vol. 11, No. 5, 1977, pp. 711-719.

[43] P. In Pyo Park, S. Jonnalagadda, Predictors of glass transition in the biodegradable polylactide and polylactide-co-glycolide polymers, Journal of Applied Polymer Science, Vol. 100, No. 3, 2006, pp. 1983-1987.

[44] D. Gilding, A. Reed, Biodegradable polymers for use in surgery: polyglycolic/poly (actic acid) homo-and copolymers, Polymer, Vol. 20, No. 12, 1979, pp. 1459-1464.

[45] M.A. Woodruff, D.W. Hutmacher, The return of a forgotten polymer—Polycaprolactone in the 21st century, Progress in Polymer Science, Vol. 35, No. 10, 2010, pp. 1217-1256.

[46] G.H. Altman, F. Diaz, C. Jakuba, T. Calabro, R.L. Horan, J. Chen, H. Lu, J. Richmond, D.L. Kaplan, Silk-based biomaterials, Biomaterials, Vol. 24, No. 3, 2003, pp. 401-416.

[47] Chemistry of Garments: Animal Fibres, The University of the West Indies, Jamaica, web page. Available (accessed 31.8.2017): http://wwwchem.uwimona.edu.jm/courses/CHEM2402/Textiles/Animal_Fibres.html.

[48] K.C. Dee, D.A. Puleo, R. Bizios, An Introduction To Tissue-Biomaterial Interactions, John Wiley & Sons, Hoboeken, New Jersey, USA, 2002, 228 p.

[49] E.B. Hunziker, From preclinical model to the patient, in: G. Bock, J. Goode (ed.), Tissue engineering of cartilage and bone, Wiley, Chichester, UK, 2003, pp. 70-85.

[50] J.A. Hubbell, Bioactive biomaterials, Current Opinion in Biotechnology, Vol. 10, No. 2, 1999, pp. 123-129.

[51] K.W. Ng, W. Tham, T.C. Lim, D.W. Hutmacher, Assimilating cell sheets and hybrid scaffolds for dermal tissue engineering, Journal of Biomedical Materials Research Part A, Vol. 75, No. 2, 2005, pp. 425-438.

[52] F. Chen, Y. Zhou, S.T. Barnabas, M.A. Woodruff, D.W. Hutmacher, Engineering tubular bone constructs, Journal of Biomechanics, Vol. 40, 2007, pp. 73-79.

[53] J. Swick, Brief Introduction to Preclinical Research, in: T.R. Kucklick (ed.), The Medical Deviec R&D Handbook, CRC Press, Boca Ranton, Florida, USA, 2006, pp. 217-222.

[54] M. Akbari, A. Tamayol, S. Bagherifard, L. Serex, P. Mostafalu, N. Faramarzi, M.H. Mohammadi, A. Khademhosseini, Textile Technologies and Tissue Engineering: A Path Toward Organ Weaving, Advanced Healthcare Materials, Vol. 5, No. 7, 2016, pp. 751-766.

[55] Purasorb PLD 9260, Corbion, Rev. No. 2 / March 2015, 1 p.

[56] R. Sartoneva, S. Haimi, S. Miettinen, B. Mannerstrom, A.M. Haaparanta, G.K. Sandor, M. Kellomaki, R. Suuronen, T. Lahdes-Vasama, Comparison of a poly-L-lactide-co-epsilon-caprolactone and human amniotic membrane for urothelium tissue engineering applications, Journal of the Royal Society, Interface, Vol. 8, No. 58, 2011, pp. 671-677.

[57] V. Ellä, M.E. Gomes, R.L. Reis, P. Törmälä, M. Kellomäki, Studies of P(L/D)LA 96/4 non-woven scaffolds and fibres; properties, wettability and cell spreading before and after intrusive treatment methods, Journal of Materials Science: Materials in Medicine, Vol. 18, No. 6, 2007, pp. 1253-1261.

[58] I.S.V. Lyyra, Optimising polylactide melt spinning using real-time monitoring, Master's thesis, Tampere University of Technology, Faculty of Computing and Electrical Engineering, Tampere, 2015, 110 p. Available: http://urn.fi/URN:NBN:fi:tty-201505201391.

[59] K. Paakinaho, V. Ellä, S. Syrjälä, M. Kellomäki, Melt spinning of poly (l/d) lactide 96/4: Effects of molecular weight and melt processing on hydrolytic degradation, Polymer Degradation and Stability, Vol. 94, No. 3, 2009, pp. 438-442.

[60] E.A. Campo, Selection of Polymeric Materials - How to Select Design Properties from Different Standards, William Andrew Publishing, Norwich, United States, 2008, 253 p.

APPENDIX A: ADDITIONAL REFERENCES FOR THE THEORETICAL PART

Abrahamsson, C.K., Yang, F., Park, H., Brunger, J.M., Valonen, P.K., Langer, R., Welter, J.F., Caplan, A.I., Guilak, F. & Freed, L.E. (2010). Chondrogenesis and mineralization during in vitro culture of human mesenchymal stem cells on three-dimensional woven scaffolds, Tissue Engineering Part A, Vol. 16(12), pp. 3709-3718.

Aigner, J., Tegeler, J., Hutzler, P., Campoccia, D., Pavesio, A., Hammer, C., Kastenbauer, E. & Naumann, A. (1998). Cartilage tissue engineering with novel nonwoven structured biomaterial based on hyaluronic acid benzyl ester, Journal of Biomedical Materials Research Part A, Vol. 42(2), pp. 172-181.

Ajalloueian, F., Zeiai, S., Rojas, R., Fossum, M. & Hilborn, J. (2013). One-stage tissue engineering of bladder wall patches for an easy-to-use approach at the surgical table, Tissue Engineering Part C: Methods, Vol. 19(9), pp. 688-696.

Akbari, M., Tamayol, A., Laforte, V., Annabi, N., Najafabadi, A.H., Khademhosseini, A. & Juncker, D. (2014). Composite living fibers for creating tissue constructs using textile techniques, Advanced functional materials, Vol. 24(26), pp. 4060-4067.

Alm, J.J., Frantzén, J., Moritz, N., Lankinen, P., Tukiainen, M., Kellomäki, M. & Aro, H.T. (2010). In vivo testing of a biodegradable woven fabric made of bioactive glass fibers and PLGA80—a pilot study in the rabbit, Journal of Biomedical Materials Research Part B: Applied Biomaterials, Vol. 93(2), pp. 573-580.

Almarza, A. & Athanasiou, K. (2006). Evaluation of three growth factors in combinations of two for temporomandibular joint disc tissue engineering, Archives of Oral Biology, Vol. 51(3), pp. 215-221.

Almarza, A.J. & Athanasiou, K.A. (2005). Effects of initial cell seeding density for the tissue engineering of the temporomandibular joint disc, Annals of Biomedical Engineering, Vol. 33(7), pp. 943-950.

Almeida, L.R., Martins, A.R., Fernandes, E.M., Oliveira, M.B., Correlo, V.M., Pashkuleva, I., Marques, A.P., Ribeiro, A.S., Durães, N.F. & Silva, C.J. (2013). New biotextiles for tissue engineering: Development, characterization and in vitro cellular viability, Acta biomaterialia, Vol. 9(9), pp. 8167-8181.

Alvarez-Barreto, J.F., Linehan, S.M., Shambaugh, R.L. & Sikavitsas, V.I. (2007). Flow perfusion improves seeding of tissue engineering scaffolds with different architectures, Annals of Biomedical Engineering, Vol. 35(3), pp. 429-442.

Ameer, G., Mahmood, T. & Langer, R. (2002). A biodegradable composite scaffold for cell transplantation, Journal of Orthopaedic Research, Vol. 20(1), pp. 16-19.

Araque-Monrós, M.C., Gamboa-Martínez, T.C., Santos, L.G., Bernabé, S.G., Pradas, M.M. & Estellés, J.M. (2013). New concept for a regenerative and resorbable prosthesis for tendon and ligament: Physicochemical and biological characterization of PLA-braided biomaterial, Journal of Biomedical Materials Research Part A, Vol. 101(11), pp. 3228-3237.

Barber, J.G., Handorf, A.M., Allee, T.J. & Li, W. (2011). Braided nanofibrous scaffold for tendon and ligament tissue engineering, Tissue Engineering Part A, Vol. 19(11-12), pp. 1265-1274.

Bi, F., Shi, Z., Liu, A., Guo, P. & Yan, S. (2015). Anterior cruciate ligament reconstruction in a rabbit model using silk-collagen scaffold and comparison with autograft, PloS one, Vol. 10(5), Available (accessed 1.11.2017): https://doi.org/10.1371/journal.pone.0125900.

Bini, T., Gao, S., Wang, S. & Ramakrishna, S. (2005). Development of fibrous biodegradable polymer conduits for guided nerve regeneration, Journal of Materials Science: Materials in Medicine, Vol. 16(4), pp. 367.

Bini, T., Gao, S., Wang, S. & Ramakrishna, S. (2006). Poly (l-lactide-co-glycolide) biodegradable microfibers and electrospun nanofibers for nerve tissue engineering: an in vitro study, Journal of Materials Science, Vol. 41(19), pp. 6453-6459.

Bini, T., Gao, S., Xu, X., Wang, S., Ramakrishna, S. & Leong, K. (2004). Peripheral nerve regeneration by microbraided poly (L-lactide-co-glycolide) biodegradable polymer fibers, Journal of biomedical materials research Part A, Vol. 68(2), pp. 286-295.

Brennan, M.P., Dardik, A., Hibino, N., Roh, J.D., Nelson, G.N., Papademitris, X., Shinoka, T. & Breuer, C.K. (2008). Tissue-engineered vascular grafts demonstrate evidence of growth and development when implanted in a juvenile animal model, Annals of Surgery, Vol. 248(3), pp. 370-377.

Carrier, R.L., Papadaki, M., Rupnick, M., Schoen, F.J., Bursac, N., Langer, R., Freed, L.E. & Vunjak-Novakovic, G. (1999). Cardiac tissue engineering: cell seeding, cultivation parameters, and tissue construct characterization, Biotechnology and bioengineering, Vol. 64(5), pp. 580-589.

Catapano, G., De Bartolo, L., Vico, V. & Ambrosio, L. (2001). Morphology and metabolism of hepatocytes cultured in Petri dishes on films and in non-woven fabrics of hyaluronic acid esters, Biomaterials, Vol. 22(7), pp. 659-665.

Chen, F., Zhou, Y., Barnabas, S.T., Woodruff, M.A. & Hutmacher, D.W. (2007). Engineering tubular bone constructs, Journal of Biomechanics, Vol. 40pp. 73-79.

Chen, J.L., Yin, Z., Shen, W.L., Chen, X., Heng, B.C., Zou, X.H. & Ouyang, H.W. (2010). Efficacy of hESC-MSCs in knitted silk-collagen scaffold for tendon tissue engineering and their roles, Biomaterials, Vol. 31(36), pp. 9438-9451.

Chen, J. & Chiang, Y. (2006). Surface modification of non-woven fabric by DC pulsed plasma treatment and graft polymerization with acrylic acid, Journal of Membrane Science, Vol. 270(1), pp. 212-220.

Chen, J., Kuo, C. & Lee, W. (2012). Thermo-responsive wound dressings by grafting chitosan and poly (N-isopropylacrylamide) to plasma-induced graft polymerization modified non-woven fabrics, Applied Surface Science, Vol. 262pp. 95-101.

Chen, X., Qi, Y., Wang, L., Yin, Z., Yin, G., Zou, X. & Ouyang, H. (2008). Ligament regeneration using a knitted silk scaffold combined with collagen matrix, Biomaterials, Vol. 29(27), pp. 3683-3692.

Cooper, J.A., Bailey, L.O., Carter, J.N., Castiglioni, C.E., Kofron, M.D., Ko, F.K. & Laurencin, C.T. (2006). Evaluation of the anterior cruciate ligament, medial collateral ligament, achilles tendon and patellar tendon as cell sources for tissue-engineered ligament, Biomaterials, Vol. 27(13), pp. 2747-2754.

Cooper, J.A., Lu, H.H., Ko, F.K., Freeman, J.W. & Laurencin, C.T. (2005). Fiber-based tissue-engineered scaffold for ligament replacement: design considerations and in vitro evaluation, Biomaterials, Vol. 26(13), pp. 1523-1532.

Cooper, J.A.,Jr, Sahota, J.S., Gorum, W.J.,2nd, Carter, J., Doty, S.B. & Laurencin, C.T. (2007). Biomimetic tissue-engineered anterior cruciate ligament replacement, Proceedings of the National Academy of Sciences of the United States of America, Vol. 104(9), pp. 3049-3054.

Correlo, V.M., Costa-Pinto, A.R., Sol, P., Covas, J.A., Bhattacharya, M., Neves, N.M. & Reis, R.L. (2010). Melt Processing of Chitosan-Based Fibers and Fiber-Mesh Scaffolds for the Engineering of Connective Tissues, Macromolecular bioscience, Vol. 10(12), pp. 1495-1504.

Czaplewski, S.K., Tsai, T., Duenwald-Kuehl, S.E., Vanderby, R. & Li, W. (2014). Tenogenic differentiation of human induced pluripotent stem cell-derived mesenchymal stem cells dictated by properties of braided submicron fibrous scaffolds, Biomaterials, Vol. 35(25), pp. 6907-6917.

Dal Pra, I., Chiarini, A., Boschi, A., Freddi, G. & Armato, U. (2006). Novel dermo-epidermal equivalents on silk fibroin-based formic acid-crosslinked three-dimensional nonwoven devices with prospective applications in human tissue engineering/regeneration/repair, International journal of molecular medicine, Vol. 18(2), pp. 241-247.

Dal Pra, I., Freddi, G., Minic, J., Chiarini, A. & Armato, U. (2005). De novo engineering of reticular connective tissue in vivo by silk fibroin nonwoven materials, Biomaterials, Vol. 26(14), pp. 1987-1999.

Day, R.M., Boccaccini, A.R., Shurey, S., Roether, J.A., Forbes, A., Hench, L.L. & Gabe, S.M. (2004). Assessment of polyglycolic acid mesh and bioactive glass for soft-tissue engineering scaffolds, Biomaterials, Vol. 25(27), pp. 5857-5866.

Derwin, K.A., Codsi, M.J., Milks, R.A., Baker, A.R., McCarron, J.A. & Iannotti, J.P. (2009). Rotator cuff repair augmentation in a canine model with use of a woven poly-L-lactide device, The Journal of bone and joint surgery, Vol. 91(5), pp. 1159-1171.

Edwards, S.L., Church, J.S., Werkmeister, J.A. & Ramshaw, J.A. (2009). Tubular micro-scale multiwalled carbon nanotube-based scaffolds for tissue engineering, Biomaterials, Vol. 30(9), pp. 1725-1731.

Edwards, S. & Werkmeister, J. (2012). Mechanical evaluation and cell response of woven polyetheretherketone scaffolds, Journal of Biomedical Materials Research Part A, Vol. 100(12), pp. 3326-3331.

Engelmayr, G.C., Rabkin, E., Sutherland, F.W., Schoen, F.J., Mayer, J.E. & Sacks, M.S. (2005). The independent role of cyclic flexure in the early in vitro development of an engineered heart valve tissue, Biomaterials, Vol. 26(2), pp. 175-187.

Engelmayr, G.C. & Sacks, M.S. (2008). Prediction of extracellular matrix stiffness in engineered heart valve tissues based on nonwoven scaffolds, Biomechanics and modeling in mechanobiology, Vol. 7(4), pp. 309-321.

Engelmayr, G.C., Sales, V.L., Mayer, J.E. & Sacks, M.S. (2006). Cyclic flexure and laminar flow synergistically accelerate mesenchymal stem cell-mediated engineered tissue formation: implications for engineered heart valve tissues, Biomaterials, Vol. 27(36), pp. 6083-6095.

Fan, H., Liu, H., Toh, S.L. & Goh, J.C. (2009). Anterior cruciate ligament regeneration using mesenchymal stem cells and silk scaffold in large animal model, Biomaterials, Vol. 30(28), pp. 4967-4977.

Fan, H., Liu, H., Wong, E.J., Toh, S.L. & Goh, J.C. (2008). In vivo study of anterior cruciate ligament regeneration using mesenchymal stem cells and silk scaffold, Biomaterials, Vol. 29(23), pp. 3324-3337.

Fang, Q., Chen, D., Yang, Z. & Li, M. (2009). In vitro and in vivo research on using Antheraea pernyi silk fibroin as tissue engineering tendon scaffolds, Materials Science and Engineering: C, Vol. 29(5), pp. 1527-1534.

Farè, S., Torricelli, P., Giavaresi, G., Bertoldi, S., Alessandrino, A., Villa, T., Fini, M., Tanzi, M.C. & Freddi, G. (2013). In vitro study on silk fibroin textile structure for Anterior Cruciate Ligament regeneration, Materials Science and Engineering C, Vol. 33(7), pp. 3601-3608.

Freeman, J.W., Woods, M.D., Cromer, D.A., Ekwueme, E.C., Andric, T., Atiemo, E.A., Bijoux, C.H. & Laurencin, C.T. (2011). Evaluation of a hydrogel–fiber composite for ACL tissue engineering, Journal of Biomechanics, Vol. 44(4), pp. 694-699.

Fuchs, S., Motta, A., Migliaresi, C. & Kirkpatrick, C.J. (2006). Outgrowth endothelial cells isolated and expanded from human peripheral blood progenitor cells as a potential source of autologous cells for endothelialization of silk fibroin biomaterials, Biomaterials, Vol. 27(31), pp. 5399-5408.

Funakoshi, T., Majima, T., Iwasaki, N., Suenaga, N., Sawaguchi, N., Shimode, K., Minami, A., Harada, K. & Nishimura, S. (2005). Application of tissue engineering techniques for rotator cuff regeneration using a chitosan-based hyaluronan hybrid fiber scaffold, The American Journal of Sports Medicine, Vol. 33(8), pp. 1193-1201.

Ge, Z., Goh, J.C.H. & Lee, E.H. (2005). The effects of bone marrow-derived mesenchymal stem cells and fascia wrap application to anterior cruciate ligament tissue engineering, Cell transplantation, Vol. 14(10), pp. 763-773.

Ge, Z., Goh, J.C.H. & Lee, E.H. (2005). Selection of cell source for ligament tissue engineering, Cell transplantation, Vol. 14(8), pp. 573-583.

Gellynck, K., Verdonk, P.C., Van Nimmen, E., Almqvist, K.F., Gheysens, T., Schoukens, G., Van Langenhove, L., Kiekens, P., Mertens, J. & Verbruggen, G. (2008). Silkworm and spider silk scaffolds for chondrocyte support, Journal of Materials Science: Materials in Medicine, Vol. 19(11), pp. 3399-3409.

Ghanaati, S., Orth, C., Unger, R.E., Barbeck, M., Webber, M.J., Motta, A., Migliaresi, C. & James Kirkpatrick, C. (2010). Fine-tuning scaffolds for tissue regeneration: effects of formic acid processing on tissue reaction to silk fibroin, Journal of tissue engineering and regenerative medicine, Vol. 4(6), pp. 464-472.

Gloy, Y., Loehrer, M., Lang, B., Rongen, L., Gries, T. & Jockenhoevel, S. (2013). Tubular woven narrow fabrics for replacement of cruciate ligaments, Annals of Biomedical Engineering, Vol. 41(9), pp. 1950-1956.

Gredes, T., Spassov, A., Mai, R., Mack, H., Loster, B.W., Mazurkiewicz-Janik, M., Kubein-Meesenburg, D., Fanghanel, J. & Gedrange, T. (2009). Changes in insulin like growth factors, myostatin and vascular endothelial growth factor in rat musculus latissimus dorsi by poly 3-hydroxybutyrate implants, 6th International Symposium for Young Scientists - Human and Animal Development: Regulatory Mechanisms, Poland, September 9-10, 2008, Polskie Towarzystwo Fizjologiczne, Poland, pp. 77-81.

Gurkan, U.A., Cheng, X., Kishore, V., Uquillas, J.A. & Akkus, O. (2010). Comparison of morphology, orientation, and migration of tendon derived fibroblasts and bone marrow stromal cells on electrochemically aligned collagen constructs, Journal of Biomedical Materials Research Part A, Vol. 94(4), pp. 1070-1079.

Hahner, J., Hoyer, M., Hillig, S., Schulze-Tanzil, G., Meyer, M., Schröpfer, M., Lohan, A., Garbe, L., Heinrich, G. & Breier, A. (2015). Diffusion chamber system for testing of collagen-based cell migration barriers for separation of ligament enthesis zones in tissue-engineered ACL constructs, Journal of Biomaterials Science, Polymer Edition, Vol. 26(16), pp. 1085-1099.

Han, F., Liu, S., Liu, X., Pei, Y., Bai, S., Zhao, H., Lu, Q., Ma, F., Kaplan, D. & Zhu, H. (2014). Woven silk fabric-reinforced silk nanofibrous scaffolds for regenerating load-bearing soft tissues, Acta biomaterialia, Vol. 10(2), pp. 921-930.

Harrington, D.A., Cheng, E.Y., Guler, M.O., Lee, L.K., Donovan, J.L., Claussen, R.C. & Stupp, S.I. (2006). Branched peptide-amphiphiles as self-assembling coatings for tissue engineering scaffolds, Journal of biomedical materials research Part A, Vol. 78(1), pp. 157-167.

Haslauer, C.M., Avery, M.R., Pourdeyhimi, B. & Loboa, E.G. (2015). Translating textiles to tissue engineering: Creation and evaluation of microporous, biocompatible, degradable scaffolds using industry relevant manufacturing approaches and human adipose derived stem cells, Journal of Biomedical Materials Research Part B: Applied Biomaterials, Vol. 103(5), pp. 1050-1058.

He, P., Sahoo, S., Ng, K.S., Chen, K., Toh, S.L. & Goh, J.C.H. (2013). Enhanced osteoinductivity and osteoconductivity through hydroxyapatite coating of silk-based tissue-engineered ligament scaffold, Journal of Biomedical Materials Research Part A, Vol. 101(2), pp. 555-566.

Hegewald, A., Medved, F., Feng, D., Tsagogiorgas, C., Beierfuss, A., Schindler, G., Trunk, M., Kaps, C., Mern, D. & Thome, C. (2015). Enhancing tissue repair in annulus fibrosus defects of the intervertebral disc: analysis of a bio-integrative annulus implant in an in-vivo ovine model, Journal of Tissue Engineering and Regenerative Medicine, Vol. 9(4), pp. 405-414.

Hemmrich, K., Salber, J., Meersch, M., Wiesemann, U., Gries, T., Pallua, N. & Klee, D. (2008). Three-dimensional nonwoven scaffolds from a novel biodegradable poly(ester amide) for tissue engineering applications, Journal of Materials Science: Materials in Medicine, Vol. 19(1), pp. 257-267.

Hess, R., Douglas, T., Myers, K.A., Rentsch, B., Rentsch, C., Worch, H., Shrive, N.G., Hart, D.A. & Scharnweber, D. (2009). Hydrostatic pressure stimulation of human mesenchymal stem cells seeded on collagen-based artificial extracellular matrices, Journal of Biomechanical Engineering, Vol. 132(2), Available (accessed 1.11.2017): http://biomechanical.asmedigitalcollection.asme.org/article.aspx?articleid=1475836.

Hess, R., Jaeschke, A., Neubert, H., Hintze, V., Moeller, S., Schnabelrauch, M., Wiesmann, H., Hart, D.A. & Scharnweber, D. (2012). Synergistic effect of defined artificial extracellular matrices and pulsed electric fields on osteogenic differentiation of human MSCs, Biomaterials, Vol. 33(35), pp. 8975-8985.

Hoerstrup, S.P., Zünd, G., Sodian, R., Schnell, A.M., Grünenfelder, J. & Turina, M.I. (2001). Tissue engineering of small caliber vascular grafts, European journal of cardio-thoracic surgery, Vol. 20(1), pp. 164-169.

Hoerstrup, S.P., Kadner, A., Melnitchouk, S., Trojan, A., Eid, K., Tracy, J., Sodian, R., Visjager, J.F., Kolb, S.A., Grunenfelder, J., Zund, G. & Turina, M.I. (2002). Tissue engineering of functional trileaflet heart valves from human marrow stromal cells, Circulation, Vol. 106(12), pp. 143-50.

Hohlrieder, M., Cicha, K., Teuschl, A., van Griensven, M., Redl, H. & Stampfl, J. (2009). Bioreactor and scaffold design for the mechanical stimulation of silk based anterior cruciate ligament grafts, World Congress on Medical Physics and Biomedical Engineering, September 7-12, 2009, Munich, Germany, Springer, pp. 208-210.

Hoyer, M., Meier, C., Breier, A., Hahner, J., Heinrich, G., Drechsel, N., Meyer, M., Rentsch, C., Garbe, L. & Ertel, W. (2015). In vitro characterization of self-assembled anterior cruciate ligament cell spheroids for ligament tissue engineering, Histochemistry and cell biology, Vol. 143(3), pp. 289-300.

Hoyer, M., Drechsel, N., Meyer, M., Meier, C., Hinüber, C., Breier, A., Hahner, J., Heinrich, G., Rentsch, C., Garbe, L.-., Ertel, W., Schulze-Tanzil, G. & Lohan, A. (2014). Embroidered polymer–collagen hybrid scaffold variants for ligament tissue engineering, Materials Science and Engineering: C, Vol. 43pp. 290-299.

Ichihara, S., Inada, Y., Nakada, A., Endo, K., Azuma, T., Nakai, R., Tsutsumi, S., Kurosawa, H. & Nakamura, T. (2009). Development of new nerve guide tube for repair of long nerve defects, Tissue Engineering Part C: Methods, Vol. 15(3), pp. 387-402.

Ide, A., Sakane, M., Chen, G., Shimojo, H., Ushida, T., Tateishi, T., Wadano, Y. & Miyanaga, Y. (2001). Collagen hybridization with poly (L-lactic acid) braid promotes ligament cell migration, Materials Science and Engineering: C, Vol. 17(1), pp. 95-99.

Inui, A., Kokubu, T., Makino, T., Nagura, I., Toyokawa, N., Sakata, R., Kotera, M., Nishino, T., Fujioka, H. & Kurosaka, M. (2010). Potency of double-layered Poly L-lactic Acid scaffold in tissue engineering of tendon tissue, International orthopaedics, Vol. 34(8), pp. 1327-1332.

Irie, T., Majima, T., Sawaguchi, N., Funakoshi, T., Nishimura, S. & Minami, A. (2011). Biomechanical and histologic evaluation of tissue engineered ligaments using chitosan and hyaluronan hybrid polymer fibers: a rabbit medial collateral ligament reconstruction model, Journal of Biomedical Materials Research Part A, Vol. 97(2), pp. 111-117.

Itoi, Y., Takatori, M., Hyakusoku, H. & Mizuno, H. (2010). Comparison of readily available scaffolds for adipose tissue engineering using adipose-derived stem cells, Journal of Plastic, Reconstructive & Aesthetic Surgery, Vol. 63(5), pp. 858-864.

Iwai, S., Sawa, Y., Taketani, S., Torikai, K., Hirakawa, K. & Matsuda, H. (2005). Novel tissue-engineered biodegradable material for reconstruction of vascular wall, Annals of Thoracic Surgery, Vol. 80(5), pp. 1821-1827.

Iwata, T., Yamato, M., Tsuchioka, H., Takagi, R., Mukobata, S., Washio, K., Okano, T. & Ishikawa, I. (2009). Periodontal regeneration with multi-layered periodontal ligament-derived cell sheets in a canine model, Biomaterials, Vol. 30(14), pp. 2716-2723.

Jockenhoevel, S., Zund, G., Hoerstrup, S.P., Schnell, A. & Turina, M. (2002). Cardiovascular tissue engineering: a new laminar flow chamber for in vitro improvement of mechanical tissue properties, ASAIO journal, Vol. 48(1), pp. 8-11.

Kang, S., Yoo, S.P. & Kim, B. (2007). Effect of chondrocyte passage number on histological aspects of tissue-engineered cartilage, Bio-medical materials and engineering, Vol. 17(5), pp. 269-276.

Karamuk, E., Billia, M., Bischoff, B., Ferrario, R., Wagner, B., Moser, R., Wanner, M. & Mayer, J. (2001). Development of a Textile Wound Dressing Based on Embroidery Technology, European Cells and Materials, Vol. 1(1), pp. 3-4.

Karamuk, E., Mayer, J. & Raeber, G. (2004). Tissue engineered composite of a woven fabric scaffold with tendon cells, response on mechanical simulation in vitro, Composites Science and Technology, Vol. 64(6), pp. 885-891.

Karamuk, E., Mayer, J., Wintermantel, E. & Akaike, T. (1999). Partially degradable film/fabric composites: Textile scaffolds for liver cell culture, Artificial Organs, Vol. 23(9), pp. 881-884.

Kawazoe, N., Inoue, C., Tateishi, T. & Chen, G. (2010). A cell leakproof PLGA-collagen hybrid scaffold for cartilage tissue engineering, Biotechnology progress, Vol. 26(3), pp. 819-826.

Khil, M., Bhattarai, S.R., Kim, H., Kim, S. & Lee, K. (2005). Novel fabricated matrix via electrospinning for tissue engineering, Journal of biomedical materials research part b: applied biomaterials, Vol. 72(1), pp. 117-124.

Kim, B. & Mooney, D.J. (1998). Engineering smooth muscle tissue with a predefined structure, Journal of Biomedical Materials Research, Vol. 41(2), pp. 322-332.

Kreklau, B., Sittinger, M., Mensing, M., Voigt, C., Berger, G., Burmester, G., Rahmanzadeh, R. & Gross, U. (1999). Tissue engineering of biphasic joint cartilage transplants, Biomaterials, Vol. 20(18), pp. 1743-1749.

Kuhbier, J.W., Allmeling, C., Reimers, K., Hillmer, A., Kasper, C., Menger, B., Brandes, G., Guggenheim, M. & Vogt, P.M. (2010). Interactions between spider silk and cells–NIH/3T3 fibroblasts seeded on miniature weaving frames, PloS one, Vol. 5(8), Available (accessed 1.11.2017): https://doi.org/10.1371/journal.pone.0012032.

Laurent, C.P., Vaquette, C., Martin, C., Guedon, E., Wu, X., Delconte, A., Dumas, D., Hupont, S., Isla, N.D. & Rahouadj, R. (2014). Towards a tissue-engineered ligament: Design and preliminary evaluation of a dedicated multi-chamber tension-torsion bioreactor, Processes, Vol. 2(1), pp. 167-179.

Li, Q., Wang, J., Liu, H., Xie, B. & Wei, L. (2013). Tissue-engineered mesh for pelvic floor reconstruction fabricated from silk fibroin scaffold with adipose-derived mesenchymal stem cells, Cell and tissue research, Vol. 354(2), pp. 471-480.

Li, X. & Snedeker, J.G. (2013). Wired silk architectures provide a biomimetic ACL tissue engineering scaffold, Journal of the mechanical behavior of biomedical materials, Vol. 22pp. 30-40.

Li, Y., Ma, T., Yang, S. & Kniss, D.A. (2001). Thermal compression and characterization of three-dimensional nonwoven PET matrices as tissue engineering scaffolds, Biomaterials, Vol. 22(6), pp. 609-618.

Lieshout, M.V., Peters, G., Rutten, M. & Baaijens, F. (2006). A knitted, fibrin-covered polycaprolactone scaffold for tissue engineering of the aortic valve, Tissue engineering, Vol. 12(3), pp. 481-487.

Lin, F., Chen, T., Chen, K., Wu, T. & Chen, C. (2000). An animal study of a novel tri-layer wound dressing material—non-woven fabric grafted with N-isopropyl acrylamide and gelatin, Materials Chemistry and Physics, Vol. 64(3), pp. 189-195.

Lisignoli, G., Fini, M., Giavaresi, G., Aldini, N.N., Toneguzzi, S. & Facchini, A. (2002). Osteogenesis of large segmental radius defects enhanced by basic fibroblast growth factor activated bone marrow stromal cells grown on non-woven hyaluronic acid-based polymer scaffold, Biomaterials, Vol. 23(4), pp. 1043-1051.

Lisignoli, G., Zini, N., Remiddi, G., Piacentini, A., Puggioli, A., Trimarchi, C., Fini, M., Maraldi, N. & Facchini, A. (2001). Basic fibroblast growth factor enhances in vitro mineralization of rat bone marrow stromal cells grown on non-woven hyaluronic acid based polymer scaffold, Biomaterials, Vol. 22(15), pp. 2095-2105.

Liu, H., Fan, H., Wong, E., Toh, S.L. & Goh, J.C. Silk-Based Scaffold for Ligament Tissue Engineering, 14th Nordic-Baltic conference on biomedical engineering and medical physics, Riga, Latvia, June 16–20, 2008, Springer, Berlin, pp. 34-37.

Liu, H., Fan, H., Toh, S.L. & Goh, J.C. (2008). A comparison of rabbit mesenchymal stem cells and anterior cruciate ligament fibroblasts responses on combined silk scaffolds, Biomaterials, Vol. 29(10), pp. 1443-1453.

Lu, H.H., Cooper, J.A., Manuel, S., Freeman, J.W., Attawia, M.A., Ko, F.K. & Laurencin, C.T. (2005). Anterior cruciate ligament regeneration using braided biodegradable scaffolds: in vitro optimization studies, Biomaterials, Vol. 26(23), pp. 4805-4816.

Ma, T., Li, Y., Yang, S. & Kniss, D.A. (2000). Effects of pore size in 3-D fibrous matrix on human trophoblast tissue development, Biotechnology and bioengineering, Vol. 70(6), pp. 606-618.

Ma, T., Li, Y., Yang, S. & Kniss, D.A. (1999). Tissue Engineering Human Placenta Trophoblast Cells in 3-D Fibrous Matrix: Spatial Effects on Cell Proliferation and Function, Biotechnology progress, Vol. 15(4), pp. 715-724.

Mack, H., Mai, R., Lauer, G., Mack, F., Gedrange, T., Franke, R. & Gredes, T. (2008). Adaptation of myosin heavy chain mRNA expression after implantation of poly (3) hydroxybutyrate scaffolds in rat m. latissimus dorsi, J Physiol Pharmacol, Vol. 59(Suppl 5), pp. 95-103.

Majima, T., Irie, T., Sawaguchi, N., Funakoshi, T., Iwasaki, N., Harada, K., Minami, A. & Nishimura, S. (2007). Chitosan-based hyaluronan hybrid polymer fibre scaffold for ligament and tendon tissue engineering, Proceedings of the Institution of Mechanical Engineers, Part H: Journal of Engineering in Medicine, Vol. 221(5), pp. 537-546.

Marijnissen, W.J., van Osch, G.J., Aigner, J., van der Veen, Simone W, Hollander, A.P., Verwoerd-Verhoef, H.L. & Verhaar, J.A. (2002). Alginate as a chondrocyte-delivery substance in combination with a non-woven scaffold for cartilage tissue engineering, Biomaterials, Vol. 23(6), pp. 1511-1517.

Mi, H., Jing, X., Yu, E., McNulty, J., Peng, X. & Turng, L. (2015). Fabrication of triple-layered vascular scaffolds by combining electrospinning, braiding, and thermally induced phase separation, Materials Letters, Vol. 161pp. 305-308.

Min, B., Jeong, L., Nam, Y.S., Kim, J., Kim, J.Y. & Park, W.H. (2004). Formation of silk fibroin matrices with different texture and its cellular response to normal human keratinocytes, International journal of biological macromolecules, Vol. 34(5), pp. 223-230.

Miot, S., Scandiucci de Freitas, P., Wirz, D., Daniels, A., Sims, T., Hollander, A., Mainil-Varlet, P., Heberer, M. & Martin, I. (2006). Cartilage tissue engineering by expanded goat articular chondrocytes, Journal of orthopaedic research, Vol. 24(5), pp. 1078-1085.

Mol, A., Driessen, N.J., Rutten, M.C., Hoerstrup, S.P., Bouten, C.V. & Baaijens, F.P. (2005). Tissue engineering of human heart valve leaflets: a novel bioreactor for a strain-based conditioning approach, Annals of Biomedical Engineering, Vol. 33(12), pp. 1778-1788.

Mol, A., van Lieshout, M.I., Dam-de Veen, C.G., Neuenschwander, S., Hoerstrup, S.P., Baaijens, F.P. & Bouten, C.V. (2005). Fibrin as a cell carrier in cardiovascular tissue engineering applications, Biomaterials, Vol. 26(16), pp. 3113-3121.

Moran, J.M., Pazzano, D. & Bonassar, L.J. (2003). Characterization of polylactic acid–polyglycolic acid composites for cartilage tissue engineering, Tissue engineering, Vol. 9(1), pp. 63-70.

Moreira, R., Gesche, V.N., Hurtado-Aguilar, L.G., Schmitz-Rode, T., Frese, J., Jockenhoevel, S. & Mela, P. (2014). TexMi: development of tissue-engineered textile-reinforced mitral valve prosthesis, Tissue Engineering Part C: Methods, Vol. 20(9), pp. 741-748.

Moutos, F.T., Estes, B.T. & Guilak, F. (2010). Multifunctional hybrid three-dimensionally woven scaffolds for cartilage tissue engineering, Macromolecular bioscience, Vol. 10(11), pp. 1355-1364.

Moutos, F.T. & Guilak, F. (2009). Functional properties of cell-seeded three-dimensionally woven poly (ε-caprolactone) scaffolds for cartilage tissue engineering, Tissue Engineering Part A, Vol. 16(4), pp. 1291-1301.

Müller, F.A., Müller, L., Hofmann, I., Greil, P., Wenzel, M.M. & Staudenmaier, R. (2006). Cellulose-based scaffold materials for cartilage tissue engineering, Biomaterials, Vol. 27(21), pp. 3955-3963.

Nakanishi, Y., Chen, G., Komuro, H., Ushida, T., Kaneko, S., Tateishi, T. & Kaneko, M. (2003). Tissue-engineered urinary bladder wall sing PLGA mesh-collagen hybrid scaffolds: a comparison study of collagen sponge and gel as a caffold, Journal of pediatric surgery, Vol. 38(12), pp. 1781-1784.

Ng, K.W. & Hutmacher, D.W. (2006). Reduced contraction of skin equivalent engineered using cell sheets cultured in 3D matrices, Biomaterials, Vol. 27(26), pp. 4591-4598.

Ng, K.W., Tham, W., Lim, T.C. & Hutmacher, D.W. (2005). Assimilating cell sheets and hybrid scaffolds for dermal tissue engineering, Journal of Biomedical Materials Research Part A, Vol. 75(2), pp. 425-438.

Oliveira, J.T., Crawford, A., Mundy, J., Moreira, A., Gomes, M.E., Hatton, P.V. & Reis, R. (2007). A cartilage tissue engineering approach combining starch-polycaprolactone fibre mesh scaffolds with bovine articular chondrocytes, Journal of Materials Science: Materials in Medicine, Vol. 18(2), pp. 295-302.

Ouyang, H.W., Goh, J.C., Mo, X.M., Teoh, S.H. & Lee, E.H. (2002). The Efficacy of Bone Marrow Stromal Cell-Seeded Knitted PLGA Fiber Scaffold for Achilles Tendon Repair, Annals of the New York Academy of Sciences, Vol. 961(1), pp. 126-129.

Ouyang, H.W., Toh, S.L., Goh, J., Tay, T.E. & Moe, K. (2005). Assembly of bone marrow stromal cell sheets with knitted poly (L-lactide) scaffold for engineering ligament analogs, Journal of Biomedical Materials Research Part B: Applied Biomaterials, Vol. 75(2), pp. 264-271.

Panilaitis, B., Altman, G.H., Chen, J., Jin, H., Karageorgiou, V. & Kaplan, D.L. (2003). Macrophage responses to silk, Biomaterials, Vol. 24(18), pp. 3079-3085.

Pasquinelli, G., Orrico, C., Foroni, L., Bonafe, F., Carboni, M., Guarnieri, C., Raimondo, S., Penna, C., Geuna, S. & Pagliaro, P. (2008). Mesenchymal stem cell interaction with a non-woven hyaluronan-based scaffold suitable for tissue repair, Journal of anatomy, Vol. 213(5), pp. 520-530.

Peh, R., Suthikum, V., Goh, C. & Toh, S. Novel electrospun-knitted silk scaffolds for ligament tissue engineering, World Congress on Medical Physics and Biomedical Engineering, Seoul, Korea, August 27 - September 1, 2006, Springer, Berlin, pp. 3287-3290.

Pelto, J., Björninen, M., Pälli, A., Talvitie, E., Hyttinen, J., Mannerström, B., Suuronen Seppanen, R., Kellomäki, M., Miettinen, S. & Haimi, S. (2013). Novel polypyrrole-coated polylactide scaffolds enhance adipose stem cell proliferation and early osteogenic differentiation, Tissue Engineering Part A, Vol. 19(7-8), pp. 882-892.

Perry, T.E., Kaushal, S., Sutherland, F.W., Guleserian, K.J., Bischoff, J., Sacks, M. & Mayer, J.E. (2003). Bone marrow as a cell source for tissue engineering heart valves, The Annals of Thoracic Surgery, Vol. 75(3), pp. 761-767.

Rentsch, B., Bernhardt, R., Scharnweber, D., Schneiders, W., Rammelt, S. & Rentsch, C. (2012). Embroidered and surface coated polycaprolactone-co-lactide scaffolds: a potential graft for bone tissue engineering, Biomatter, Vol. 2(3), pp. 158-165.

Rentsch, B., Hofmann, A., Breier, A., Rentsch, C. & Scharnweber, D. (2009). Embroidered and surface modified polycaprolactone-co-lactide scaffolds as bone substitute: in vitro characterization, Annals of Biomedical Engineering, Vol. 37(10), pp. 2118-2128.

Rentsch, B., Hofmann, A., Breier, A., Rentsch, C. & Scharnweber, D. (2009). Embroidered and surface modified polycaprolactone-co-lactide scaffolds as bone substitute: in vitro characterization, Annals of Biomedical Engineering, Vol. 37(10), pp. 2118-2128.

Rentsch, C., Rentsch, B., Heinemann, S., Bernhardt, R., Bischoff, B., Förster, Y., Scharnweber, D. & Rammelt, S. (2014). ECM Inspired Coating of Embroidered 3D Scaffolds Enhances Calvaria Bone Regeneration, BioMed Research International, pp. 1-15. Available (accessed 31.8.2016): https://www.hindawi.com/journals/bmri/2014/217078/.

Rentsch, C., Hess, R., Rentsch, B., Hofmann, A., Manthey, S., Scharnweber, D., Biewener, A. & Zwipp, H. (2010). Ovine bone marrow mesenchymal stem cells: isolation and characterization of the cells and their osteogenic differentiation potential on embroidered and surface-modified polycaprolactone-co-lactide scaffolds, In Vitro Cellular & Developmental Biology-Animal, Vol. 46(7), pp. 624-634.

Rentsch, C., Rentsch, B., Breier, A., Hofmann, A., Manthey, S., Scharnweber, D., Biewener, A. & Zwipp, H. (2010). Evaluation of the osteogenic potential and vascularization of 3D poly (3) hydroxybutyrate scaffolds subcutaneously implanted in nude rats, Journal of Biomedical Materials Research Part A, Vol. 92(1), pp. 185-195.

Rentsch, C., Rentsch, B., Breier, A., Spekl, K., Jung, R., Manthey, S., Scharnweber, D., Zwipp, H. & Biewener, A. (2010). Long-bone critical-size defects treated with tissue-engineered polycaprolactone-co-lactide scaffolds: A pilot study on rats, Journal of Biomedical Materials Research Part A, Vol. 95(3), pp. 964-972.

Rentsch, C., Schneiders, W., Hess, R., Rentsch, B., Bernhardt, R., Spekl, K., Schneider, K., Scharnweber, D., Biewener, A. & Rammelt, S. (2014). Healing properties of surface-coated polycaprolactone-co-lactide scaffolds: a pilot study in sheep, Journal of Biomaterials Applications, Vol. 28(5), pp. 654-666.

Roh, J.D., Nelson, G.N., Brennan, M.P., Mirensky, T.L., Yi, T., Hazlett, T.F., Tellides, G., Sinusas, A.J., Pober, J.S. & Saltzman, W.M. (2008). Small-diameter biodegradable scaffolds for functional vascular tissue engineering in the mouse model, Biomaterials, Vol. 29(10), pp. 1454-1463.

Ronald, M., Hagedorn, M.G., Gelinsky, M., Werner, C., Turhani, D., Spaeth, H., Gedrange, T. & Lauer, G. (2006). Ectopic bone formation in nude rats using human osteoblasts seeded poly (3) hydroxybutyrate embroidery and hydroxyapatite-collagen tapes constructs, Journal of Cranio-Maxillofacial Surgery, Vol. 34pp. 101-109.

Rotter, N., Aigner, J., Naumann, A., Planck, H., Hammer, C., Burmester, G. & Sittinger, M. (1998). Cartilage reconstruction in head and neck surgery: comparison of resorbable polymer scaffolds for tissue engineering of human septal cartilage, Journal of Biomedical Materials Research, Vol. 42(3), pp. 347-356.

Sahoo, S., Ouyang, H., Goh, J.C., Tay, T. & Toh, S. (2006). Characterization of a novel polymeric scaffold for potential application in tendon/ligament tissue engineering, Tissue engineering, Vol. 12(1), pp. 91-99.

Sahoo, S., Lok Toh, S., Goh, H. & Cho, J. (2010). PLGA nanofiber-coated silk microfibrous scaffold for connective tissue engineering, Journal of Biomedical Materials Research Part B: Applied Biomaterials, Vol. 95(1), pp. 19-28.

Sahoo, S., Toh, S.L. & Goh, J.C. (2010). A bFGF-releasing silk/PLGA-based biohybrid scaffold for ligament/tendon tissue engineering using mesenchymal progenitor cells, Biomaterials, Vol. 31(11), pp. 2990-2998.

Sahoo, S., Cho-Hong, J.G. & Siew-Lok, T. (2007). Development of hybrid polymer scaffolds for potential applications in ligament and tendon tissue engineering, Biomedical Materials, Vol. 2(3), pp. 169-173.

Sales, V.L., Engelmayr, G.C.,Jr, Mettler, B.A., Johnson, J.A.,Jr, Sacks, M.S. & Mayer, J.E.,Jr (2006). Transforming growth factor-beta1 modulates extracellular matrix production, proliferation, and apoptosis of endothelial progenitor cells in tissue-engineering scaffolds, Circulation, Vol. 114(1), pp. 193-199.

Sartoneva, R., Haaparanta, A.M., Lahdes-Vasama, T., Mannerstrom, B., Kellomaki, M., Salomaki, M., Sandor, G., Seppanen, R., Miettinen, S. & Haimi, S. (2012). Characterizing and optimizing poly-L-lactide-co-epsilon-caprolactone membranes for urothelial tissue engineering, Journal of the Royal Society, Interface, Vol. 9(77), pp. 3444-3454.

Schaefer, D., Martin, I., Shastri, P., Padera, R., Langer, R., Freed, L. & Vunjak-Novakovic, G. (2000). In vitro generation of osteochondral composites, Biomaterials, Vol. 21(24), pp. 2599-2606.

Schmidt, D., Breymann, C., Weber, A., Guenter, C.I., Neuenschwander, S., Zund, G., Turina, M. & Hoerstrup, S.P. (2004). Umbilical cord blood derived endothelial progenitor cells for tissue engineering of vascular grafts, The Annals of Thoracic Surgery, Vol. 78(6), pp. 2094-2098.

Shao, X. & Hunter, C.J. (2007). Developing an alginate/chitosan hybrid fiber scaffold for annulus fibrosus cells, Journal of biomedical materials research Part A, Vol. 82(3), pp. 701-710.

Shen, W., Chen, X., Chen, J., Yin, Z., Heng, B.C., Chen, W. & Ouyang, H. (2010). The effect of incorporation of exogenous stromal cell-derived factor-1 alpha within a knitted silk-collagen sponge scaffold on tendon regeneration, Biomaterials, Vol. 31(28), pp. 7239-7249.

Shen, G., Tsung, H.C., Wu, C.F., Liu, X.Y., Wang, X., Liu, W., Cui, L. & Cao, Y.L. (2003). Tissue engineering of blood vessels with endothelial cells differentiated from mouse embryonic stem cells, Cell Research, Vol. 13(5), pp. 335-341.

Sikavitsas, V.I., Bancroft, G.N., Lemoine, J.J., Liebschner, M.A., Dauner, M. & Mikos, A.G. (2005). Flow perfusion enhances the calcified matrix deposition of marrow stromal cells in biodegradable nonwoven fiber mesh scaffolds, Annals of Biomedical Engineering, Vol. 33(1), pp. 63.

Sittinger, M., Reitzel, D., Dauner, M., Hierlemann, H., Hammer, C., Kastenbauer, E., Planck, H., Burmester, G. & Bujia, J. (1996). Resorbable polyesters in cartilage engineering: affinity and biocompatibility of polymer fiber structures to chondrocytes, Journal of Biomedical Materials Research Part A, Vol. 33(2), pp. 57-63.

Spalazzi, J.P., Dagher, E., Doty, S.B., Guo, X.E., Rodeo, S.A. & Lu, H.H. (2008). In vivo evaluation of a multiphased scaffold designed for orthopaedic interface tissue engineering and soft tissue-to-bone integration, Journal of Biomedical Materials Research Part A, Vol. 86(1), pp. 1-12.

Sun, W., Tiemessen, D.M., Sloff, M., Lammers, R.J., de Mulder, E.L., Hilborn, J., Gupta, B., Feitz, W.F., Daamen, W.F. & van Kuppevelt, T.H. (2012). Improving the cell distribution in collagen-coated poly-caprolactone knittings, Tissue Engineering Part C: Methods, Vol. 18(10), pp. 731-739.

Takashima, K., Hoshino, M., Uesugi, K., Yagi, N., Matsuda, S., Nakahira, A., Osumi, N., Kohzuki, M. & Onodera, H. (2015). X-ray phase-contrast computed tomography visualizes the microstructure and degradation profile of implanted biodegradable scaffolds after spinal cord injury, Journal of synchrotron radiation, Vol. 22(1), pp. 136-142.

Ten Hallers, E., Jansen, J.A., Marres, H.A., Rakhorst, G. & Verkerke, G.J. (2007). Histological assessment of titanium and polypropylene fiber mesh implantation with and without fibrin tissue glue, Journal of Biomedical Materials Research Part A, Vol. 80(2), pp. 372-380.

Tiitu, V., Pulkkinen, H., Valonen, P., Pulliainen, O., Kellomäki, M., Lammi, M. & Kiviranta, I. (2008). Bioreactor improves the growth and viability of chondrocytes in the knitted poly-L, D-lactide scaffold, Biorheology, Vol. 45(3-4), pp. 539-546.

Tognana, E., Chen, F., Padera, R., Leddy, H., Christensen, S., Guilak, F., Vunjak-Novakovic, G. & Freed, L. (2005). Adjacent tissues (cartilage, bone) affect the functional integration of engineered calf cartilage in vitro, Osteoarthritis and cartilage, Vol. 13(2), pp. 129-138.

Tonello, C., Zavan, B., Cortivo, R., Brun, P., Panfilo, S. & Abatangelo, G. (2003). In vitro reconstruction of human dermal equivalent enriched with endothelial cells, Biomaterials, Vol. 24(7), pp. 1205-1211.

Torikai, K., Ichikawa, H., Hirakawa, K., Matsumiya, G., Kuratani, T., Iwai, S., Saito, A., Kawaguchi, N., Matsuura, N. & Sawa, Y. (2008). A self-renewing, tissue-engineered vascular graft for arterial reconstruction, Journal of Thoracic and Cardiovascular Surgery, Vol. 136(1), pp. 37-46.

Tovar, N., Murthy, N.S., Kohn, J., Gatt, C. & Dunn, M. (2012). ACL reconstruction using a novel hybrid scaffold composed of polyarylate fibers and collagen fibers, Journal of Biomedical Materials Research Part A, Vol. 100(11), pp. 2913-2920.

Tschoeke, B., Flanagan, T.C., Cornelissen, A., Koch, S., Roehl, A., Sriharwoko, M., Sachweh, J.S., Gries, T., Schmitz-Rode, T. & Jockenhoevel, S. (2008). Development of a Composite Degradable/Nondegradable Tissue-engineered Vascular Graft, Artificial Organs, Vol. 32(10), pp. 800-809.

Tsumanuma, Y., Iwata, T., Washio, K., Yoshida, T., Yamada, A., Takagi, R., Ohno, T., Lin, K., Yamato, M. & Ishikawa, I. (2011). Comparison of different tissue-derived stem cell sheets for periodontal regeneration in a canine 1-wall defect model, Biomaterials, Vol. 32(25), pp. 5819-5825.

Turner, N.J., Kielty, C.M., Walker, M.G. & Canfield, A.E. (2004). A novel hyaluronan-based biomaterial (Hyaff-11®) as a scaffold for endothelial cells in tissue engineered vascular grafts, Biomaterials, Vol. 25(28), pp. 5955-5964.

Unger, R., Peters, K., Wolf, M., Motta, A., Migliaresi, C. & Kirkpatrick, C. (2004). Endothelialization of a non-woven silk fibroin net for use in tissue engineering: growth and gene regulation of human endothelial cells, Biomaterials, Vol. 25(21), pp. 5137-5146.

Unger, R.E., Wolf, M., Peters, K., Motta, A., Migliaresi, C. & Kirkpatrick, C.J. (2004). Growth of human cells on a non-woven silk fibroin net: a potential for use in tissue engineering, Biomaterials, Vol. 25(6), pp. 1069-1075.

Valonen, P.K., Moutos, F.T., Kusanagi, A., Moretti, M.G., Diekman, B.O., Welter, J.F., Caplan, A.I., Guilak, F. & Freed, L.E. (2010). In vitro generation of mechanically functional cartilage grafts based on adult human stem cells and 3D-woven poly (ε-caprolactone) scaffolds, Biomaterials, Vol. 31(8), pp. 2193-2200.

Van Eijk, F., Saris, D.B., Riesle, J., Willems, W., Van Blitterswijk, C., Verbout, A. & Dhert, W. (2004). Tissue engineering of ligaments: a comparison of bone marrow stromal cells, anterior cruciate ligament, and skin fibroblasts as cell source, Tissue engineering, Vol. 10(5-6), pp. 893-903.

Van Lieshout, M., Vaz, C., Rutten, M., Peters, G. & Baaijens, F. (2006). Electrospinning versus knitting: two scaffolds for tissue engineering of the aortic valve, Journal of Biomaterials Science, Polymer Edition, Vol. 17(1-2), pp. 77-89.

Van Lieshout, M., Vaz, C., Rutten, M., Peters, G. & Baaijens, F. (2006). Electrospinning versus knitting: two scaffolds for tissue engineering of the aortic valve, Journal of Biomaterials Science, Polymer Edition, Vol. 17(1-2), pp. 77-89.

Vaquette, C., Kahn, C., Frochot, C., Nouvel, C., Six, J., De Isla, N., Luo, L., Cooper-White, J., Rahouadj, R. & Wang, X. (2010). Aligned poly (L-lactic-co-e-caprolactone) electrospun microfibers and knitted structure: a novel composite scaffold for ligament tissue engineering, Journal of Biomedical Materials Research Part A, Vol. 94(4), pp. 1270-1282.

Vaquette, C., Viateau, V., Guérard, S., Anagnostou, F., Manassero, M., Castner, D.G. & Migonney, V. (2013). The effect of polystyrene sodium sulfonate grafting on polyethylene terephthalate artificial ligaments on in vitro mineralisation and in vivo bone tissue integration, Biomaterials, Vol. 34(29), pp. 7048-7063.

Walther, A., Hoyer, B., Springer, A., Mrozik, B., Hanke, T., Cherif, C., Pompe, W. & Gelinsky, M. (2012). Novel textile scaffolds generated by flock technology for tissue engineering of bone and cartilage, Materials, Vol. 5(3), pp. 540-557.

Wang, A., Ao, Q., Cao, W., Yu, M., He, Q., Kong, L., Zhang, L., Gong, Y. & Zhang, X. (2006). Porous chitosan tubular scaffolds with knitted outer wall and controllable inner structure for nerve tissue engineering, Journal of Biomedical Materials Research Part A, Vol. 79(1), pp. 36-46.

Wang, A., Ao, Q., Cao, W., Zhao, C., Gong, Y., Zhao, N. & Zhang, X. (2005). Fiber-based chitosan tubular scaffolds for soft tissue engineering: fabrication and in vitro evaluation, Tsinghua Science & Technology, Vol. 10(4), pp. 449-453.

Wang, A., Ao, Q., He, Q., Gong, X., Gong, K., Gong, Y., Zhao, N. & Zhang, X. (2006). Neural stem cell affinity of chitosan and feasibility of chitosan-based porous conduits as scaffolds for nerve tissue engineering, Tsinghua Science & Technology, Vol. 11(4), pp. 415-420.

Wang, A., Ao, Q., Wei, Y., Gong, K., Liu, X., Zhao, N., Gong, Y. & Zhang, X. (2007). Physical properties and biocompatibility of a porous chitosan-based fiber-reinforced conduit for nerve regeneration, Biotechnology Letters, Vol. 29(11), pp. 1697-1702.

Wang, B., Zhang, P., Song, W., Zhao, L. & He, C. (2015). Design and properties of a new braided poly lactic-co-glycolic acid catheter for peripheral nerve regeneration, Textile Research Journal, Vol. 85(1), pp. 51-61.

Wang, J., Wei, Y., Yi, H., Liu, Z., Sun, D. & Zhao, H. (2014). Cytocompatibility of a silk fibroin tubular scaffold, Materials Science and Engineering: C, Vol. 34pp. 429-436.

Wang, X., Li, Q., Hu, X., Ma, L., You, C., Zheng, Y., Sun, H., Han, C. & Gao, C. (2012). Fabrication and characterization of poly (l-lactide-co-glycolide) knitted mesh-reinforced collagen–chitosan hybrid scaffolds for dermal tissue engineering, Journal of the mechanical behavior of biomedical materials, Vol. 8pp. 204-215.

Watanabe, M., Shin'oka, T., Tohyama, S., Hibino, N., Konuma, T., Matsumura, G., Kosaka, Y., Ishida, T., Imai, Y. & Yamakawa, M. (2001). Tissue-engineered vascular autograft: inferior vena cava replacement in a dog model, Tissue engineering, Vol. 7(4), pp. 429-439.

Wendt, H., Hillmer, A., Reimers, K., Kuhbier, J.W., Schäfer-Nolte, F., Allmeling, C., Kasper, C. & Vogt, P.M. (2011). Artificial skin–culturing of different skin cell lines for generating an artificial skin substitute on cross-weaved spider silk fibres, PloS one, Vol. 6(7), Available (accessed 1.11.2017): https://doi.org/10.1371/journal.pone.0021833.

Wolf, F., Candrian, C., Wendt, D., Farhadi, J., Heberer, M., Martin, I. & Barbero, A. (2008). Cartilage tissue engineering using pre-aggregated human articular chondrocytes, European cells & materials, Vol. 16pp. 92-99.

Wu, W., Feng, X., Feng, X., Mao, T., Ouyang, H., Zhao, G. & Chen, F. (2007). Engineering of human tracheal tissue with collagen-enforced poly-lactic-glycolic acid non-woven mesh: A preliminary study in nude mice, British Journal of Oral & Maxillofacial Surgery, Vol. 45(4), pp. 272-278.

Yagi, T., Sato, M., Nakazawa, Y., Tanaka, K., Sata, M., Itoh, K., Takagi, Y. & Asakura, T. (2011). Preparation of double-raschel knitted silk vascular grafts and evaluation of short-term function in a rat abdominal aorta, Journal of Artificial Organs, Vol. 14(2), pp. 89-99.

Yamane, S., Iwasaki, N., Majima, T., Funakoshi, T., Masuko, T., Harada, K., Minami, A., Monde, K. & Nishimura, S. (2005). Feasibility of chitosan-based hyaluronic acid hybrid biomaterial for a novel scaffold in cartilage tissue engineering, Biomaterials, Vol. 26(6), pp. 611-619.

Yokota, T., Ichikawa, H., Matsumiya, G., Kuratani, T., Sakaguchi, T., Iwai, S., Shirakawa, Y., Torikai, K., Saito, A. & Uchimura, E. (2008). In situ tissue regeneration using a novel tissue-engineered, small-caliber vascular graft without cell seeding, The Journal of thoracic and cardiovascular surgery, Vol. 136(4), pp. 900-907.

Yuan, J., Nie, W., Qiang, F., Lian, X., Hou, T. & Tan, Z. (2009). Novel three-dimensional nerve tissue engineering scaffolds and its biocompatibility with Schwann cells, Chinese Journal of Traumatology (English Edition), Vol. 12(3), pp. 133-137.

Zavan, B., Brun, P., Vindigni, V., Amadori, A., Habeler, W., Pontisso, P., Montemurro, D., Abatangelo, G. & Cortivo, R. (2005). Extracellular matrix-enriched polymeric scaffolds as a substrate for hepatocyte cultures: in vitro and in vivo studies, Biomaterials, Vol. 26(34), pp. 7038-7045.

Zhang, L., Ao, Q., Wang, A., Lu, G., Kong, L., Gong, Y., Zhao, N. & Zhang, X. (2006). A sandwich tubular scaffold derived from chitosan for blood vessel tissue engineering, Journal of biomedical materials research Part A, Vol. 77(2), pp. 277-284.

Zhang, X., Hua, H., Shen, X. & Yang, Q. (2007). In vitro degradation and biocompatibility of poly (L-lactic acid)/chitosan fiber composites, Polymer, Vol. 48(4), pp. 1005-1011.

Zhao, F. & Ma, T. (2005). Perfusion bioreactor system for human mesenchymal stem cell tissue engineering: dynamic cell seeding and construct development, Biotechnology and bioengineering, Vol. 91(4), pp. 482-493.

Zou, X.H., Zhi, Y.L., Chen, X., Jin, H.M., Wang, L.L., Jiang, Y.Z., Yin, Z. & Ouyang, H.W. (2010). Mesenchymal stem cell seeded knitted silk sling for the treatment of stress urinary incontinence, Biomaterials, Vol. 31(18), pp. 4872-4879.

Zund, G., Breuer, C., Shinoka, T., Ma, P., Langer, R., Mayer, J. & Vacanti, J. (1997). The in vitro construction of a tissue engineered bioprosthetic heart valve, European journal of cardio-thoracic surgery, Vol. 11(3), pp. 493-497.

Zund, G., Ye, Q., Hoerstrup, S.P., Schoeberlein, A., Schmid, A.C., Grunenfelder, J., Vogt, P. & Turina, M. (1999). Tissue engineering in cardiovascular surgery: MTT, a rapid and reliable quantitative method to assess the optimal human cell seeding on polymeric meshes, European journal of cardio-thoracic surgery, Vol. 15(4), pp. 519-524.

APPENDIX B: FIBER MATERIALS USED IN TE TEXTILES

Material	Number of research articles
PGA	36
Silk	36
PLGA	28
PLA	25
PCL	14
PET	13
Hyaluronic acid	11
P(LA-CL)	10
Chitosan	8
PHAs	4
PP	4
PGA+PLLA BLEND	3
Chitosan + Hyaluronic acid BLEND	2
Collagen	2
PA	2
PDS	2
PTFE	2
Alginate	1
BioGlass	1
Carbon nanotube	1
Cellulose	1
Chitosan + PBS BLEND	1
Chitosan + PBTA BLEND	1
P(DTD DD)	1
PBS	1
PE	1
PEA	1
PEEK	1
PLLA + PCL BLEND	1
PS	1
PVDF	1
Starch + PCL BLEND	1
Titanium	1

APPENDIX C: DSC RESULTS

Hydrolysis week	Dry/Wet	T_m (°C)	S.D.	T_g (°C)	S.D.	X_c (%)	S.D.	n
0	Dry	154.5	0.56	60.2	0.10	42.4	0.19	2
1	Wet	155.1	0.40	59.9	0.02	43.0	0.52	2
8	Wet	154.7	0.18	60.0	0.00	44.6	0.19	2
16	Wet	155.3	0.36	59.7	0.05	45.7	0.38	2
24	Wet	155.6	0.36	59.4	0.02	46.0	0.98	2
28	Wet	156.0	0.07	59.6	0.17	49.5	17.71	2
36	Wet	156.5	0.28	59.3	0.01	44.1	0.13	2

APPENDIX D: TENSILE TESTING RESULTS

Hydrolysis week	Dry/Wet	Stress at max. Load (MPa)	S.D.	Load at max. Load (N)	S.D.	Strain at max. Load (%)	S.D.	n
0	Dry	308.6	29.9	2.0	0.1	79.8	11.4	6
0	Wet	298.5	45.1	2.0	0.1	81.3	7.2	6
1	Wet	280.2	24.2	1.9	0.1	76.6	12.2	6
2	Wet	257.3	27.3	1.9	0.2	78.7	17.1	6
3	Wet	237.5	25.7	1.8	0.2	85.0	7.7	6
4	Wet	257.0	6.6	1.9	0.1	80.8	4.4	6
8	Wet	272.2	21.1	2.0	0.2	77.3	15.2	6
12	Wet	213.6	10.3	1.5	0.1	85.7	8.0	6
16	Wet	240.0	13.5	1.7	0.1	78.2	7.8	6
20	Wet	235.9	13.7	1.7	0.1	86.6	9.5	6
24	Wet	240.6	12.7	1.7	0.1	82.7	11.9	6
28	Wet	227.7	17.9	1.6	0.1	78.3	10.2	5
32	Wet	213.9	10.5	1.5	0.1	78.6	9.4	6
36	Wet	201.2	16.1	1.5	0.1	74.2	8.9	6